2019-05-05

Design of Bioluminescent Protein-Conjugates with Bioorthogonal Chemistry for Applications in Biomedicine

Angeliki Moutsiopoulou
University of Miami, a.moutsiopoulou@gmail.com

UNIVERSITY OF MIAMI

DESIGN OF BIOLUMINESCENT PROTEIN-CONJUGATES WITH BIOORTHOGONAL CHEMISTRY FOR APPLICATIONS IN BIOMEDICINE

By

Angeliki Moutsiopoulou

A DISSERTATION

Submitted to the Faculty
of the University of Miami
in partial fulfillment of the requirements for
the degree of Doctor of Philosophy

Coral Gables, Florida

May 2019

UNIVERSITY OF MIAMI

A dissertation submitted in partial fulfillment of
the requirements for the degree of
Doctor of Philosophy

DESIGN OF BIOLUMINESCENT PROTEIN-CONJUGATES WITH BIOORTHOGONAL CHEMISTRY FOR APPLICATIONS IN BIOMEDICINE

Angeliki Moutsiopoulou

Approved:

_____ Angel Kaifer, Ph.D. Professor of Chemistry	_____ Roger Leblanc, Ph.D. Professor of Chemistry
_____ James Wilson, Ph.D. Assosiate Professor of Chemistry	_____ Guillermo Prado, Ph.D. Dean of the Graduate School
_____ Sapna K. Deo, Ph.D Professor of Biochemistry and Molecular Biology	

MOUTSIOPOULOU, ANGELIKI (Ph.D., Chemistry)
Design of Bioluminescent Protein-Conjugates (May 2019)
with Bioorthogonal Chemistry for Applications in Biomedicine;

Abstract of a dissertation at the University of Miami.

Dissertation supervised by Professor Angel Kaifer.
No. of pages in text. (117)

Bioconjugation is one of the common ways of modifying biomolecules with reporters and other moieties for applications in the development of various sensing systems. However, achieving specific and efficient bioconjugation is challenging. Bioorthogonal chemistry can overcome these challenges as these reactions are designed to work under physiological conditions and target a specific functionality on the target biomolecule. Different functional groups can be introduced genetically or chemically on biomolecules to have a unique reactive group in order to perform bioorthogonal reactions. Herein, work relating to the development of bioluminescent biosensing systems by applying bioorthogonal chemistry between the bioluminescent proteins and other biomolecules is discussed. In particular, antibodies for the development of immunoassays that are labeled bioorthogonally with a bioluminescent protein, *Gaussia* luciferase were prepared and an immunoassay for the detection of interferon-γ was developed. Also, bioluminescent molecular aptamer beacons utilizing *Gaussia* luciferase as a reporter is described. In this work, an inhibitor molecule was attached on the beacon to reduce the signal-to-noise ratio and improve the sensitivity. Finally, the prospective research is highlighted as new biosensors can be designed with different bioorthogonal reactions and techniques.

This thesis is dedicated to my family
for their support and love.

Acknowledgments

I would like to acknowledge those who guided, inspired, and supported my doctoral journey.

First and foremost, I owe my deepest gratitude to my two advisors, Professor Sapna Deo and Professor Angel Kaifer. Thank you for your mentorship and confidence in me. I would like to extend my special thanks to Sapna because besides the guidance that she gave me these four years, she encouraged me and supported me in different aspects of my life. I feel myself blessed that I had such a great mentor.

Also special thanks to Emre, our lab director and my friend. He supported me, helped with my research and he made me a better scientist. I admire you. You are such a kind, generous, and knowledgeable person.

Furthermore, I would like to thank my parents, Sofia and Theodoros, my brother, Nikos, my grandmother, Katerina and my uncle, Leonidas. I know without their support, their love, and their trust I wouldn't be the person that I am today, and I couldn't finish with this chapter of my life. Thank you so much and I love you (*Ευχαριστώ πολύ και σας αγαπάω*).

In my quest for the Ph.D degree, I was fortunate to be surrounded by a loving family away from home that I can call my friends. Special thanks to Anna, Pepy, Christos, Alexia, Anastasia, Marita, and Devon.

Contents

List of Figures

List of Acronyms

β-ME 2-mercaptoethanol,

BCA Bicinchoninic acid.

CuAAC Cu-catalyzed azide alkyne cycloaddition.

4-DBCO 4-dibenzocyclooctynol- cyclooctyne for the copper-free click reaction.

NHS-DBCO Dibenzocyclooctyne-*N*-hydroxysuccinimidyl ester.

DABCYL 4-(4-dimethylaminophenylazo)-benzoic acid- black quencher.

DTT dithiothreitol.

EDC 1-Ethyl-3-(3-dimethylaminopropyl)carbodiimide– Heterobifunctional linker that conjugates carboxyls to primary amines.

ELISA Enzyme-Linked Immunosorbent Assay.

FAM 6-carboxyfluorescein.

FRET Fluorescence Resonance Energy Transfer– Non-radiative energy transfer from donor to acceptor molecules.

FBDP Formylbenzene Diazonium Hexafluorophosphate- Bifunctional crosslinker that conjugates aldehydes and hydrazine functional groups.

Hynic Hydrazinonicotinic acid- crosslinker for hydrazine introduction

sulfo-S-Hynic sulfo-succinimidyl-6-hydrazino-nicotinamide- soluble in aqueous buffers

GLuc Gaussia Luciferase- bioluminescent protein.

GLucY Gaussia Luciferase with a tyrosine mutation.

IFN-γ Interferon-γ- cytokine- activator of the immune system.

IMAC Immobilized-Metal Affinity Chromatography.

IPTG isopropyl β-D-1-thiogalactopyranoside– Non-metabolizable analog of a lactose metabolic product used to induce expression of a protein under control of the Lac operon.

LOD Limit of Detection.

MAB Molecular aptamer beacon

MWCO Molecular Weight Cutoff**.**

NP-40 nonyl phenoxyethoxyethanol.

NHS N-hydroxysuccinimidyl ester- amine reactive crosslinker

PEG polyethylene glycol.

PVDF polyvinylidene fluoride.

SDS-PAGE sodium dodecyl sulfate– polyacrylamide gel electrophoresis.

SPAAC Strain Promoted Azide-Alkyne Click reaction

Tween 20 sorbital monolaurate.

Chapter 1

Introduction: Bioorthogonal Reactions in Biomolecule Conjugation and their Applications

Overview

The chemical conjugation between biomolecules and more specifically, between proteins or with other biomolecules, is challenging because of the complex structure of the biomolecules as they have several reactive sites. Unfortunately, bioconjugation techniques cannot solve this problem, and hence bioorthogonal reactions were introduced and these improved the conjugation between biomolecules. These reactions take advantage of unique reactive sites located on the biomolecule, which have been genetically or chemically introduced. The resulting conjugation products are typically reproducible, and maintain the structure and the function of the biomolecule. This chapter introduces the different bioorthogonal reactions which have been developed as well as these applications.

1.1 Perspective

Bioconjugate techniques to connect biomolecules and to combine the properties of each one is useful for designing new (bio) components for biomedical applications. The need to study the interactions between protein-protein or protein-oligonucleotide, to develop assays for detection purposes or to research general binding studies, has led to the development of various bioconjugation techniques between biomolecules.[2,3] This can usually be achieved by performing specific chemical reactions between proteins and other biomolecules, including, but not limited to nucleic acids, antibodies, enzymes. However, this chemical modification, through these bioconjugate techniques, is challenging. One important criteria for the chemical conjugation strategy is the chemical modification of proteins which should maintain the protein function, as well as structural integrity. Generally, biomolecules are large in size and can contain different functional groups. For example, proteins consist of amino acids with side chains, including carboxylic acids, amines, thiols, etc. Therefore, conjugating these biomolecules may lead to problems with regioselectivity and stoichiometry. This means the conjugation site should be controlled so that the conjugates can be reproducible.[4] The improvement of the bioconjugate reactions occurred with the development of the bioorthogonal reactions, which are selective, and the conjugation of biomolecules into a specific reactive position. Therefore, these bioconjugates are reproducible, and they maintain the properties of each biomolecule.

1.1.1 Crosslinking methods

For decades, amino acids of proteins have been modified through different processes in order to synthesize a bioconjugate. The crosslinking of two biomolecules in a classical

sense, involves using a method where one creates an intermediate complex with the first biomolecule, using the crosslinking reagent, and then allowing the second biomolecule to react with the complex. The crosslinking method includes two categories: one-step and two-step reactions. The crosslinking may also be performed as a one-step reaction in which all the reagents are added into one pot at the same time. The problem with this method is that the reaction cannot be controlled, and the size and the stoichiometry of products may vary. On the other hand, the two-step reaction is when one biomolecule is activated with the crosslinker, and the by-products are removed, as well as the excess of the crosslinker, before the addition of the second biomolecule (Figure 1.1).[5]

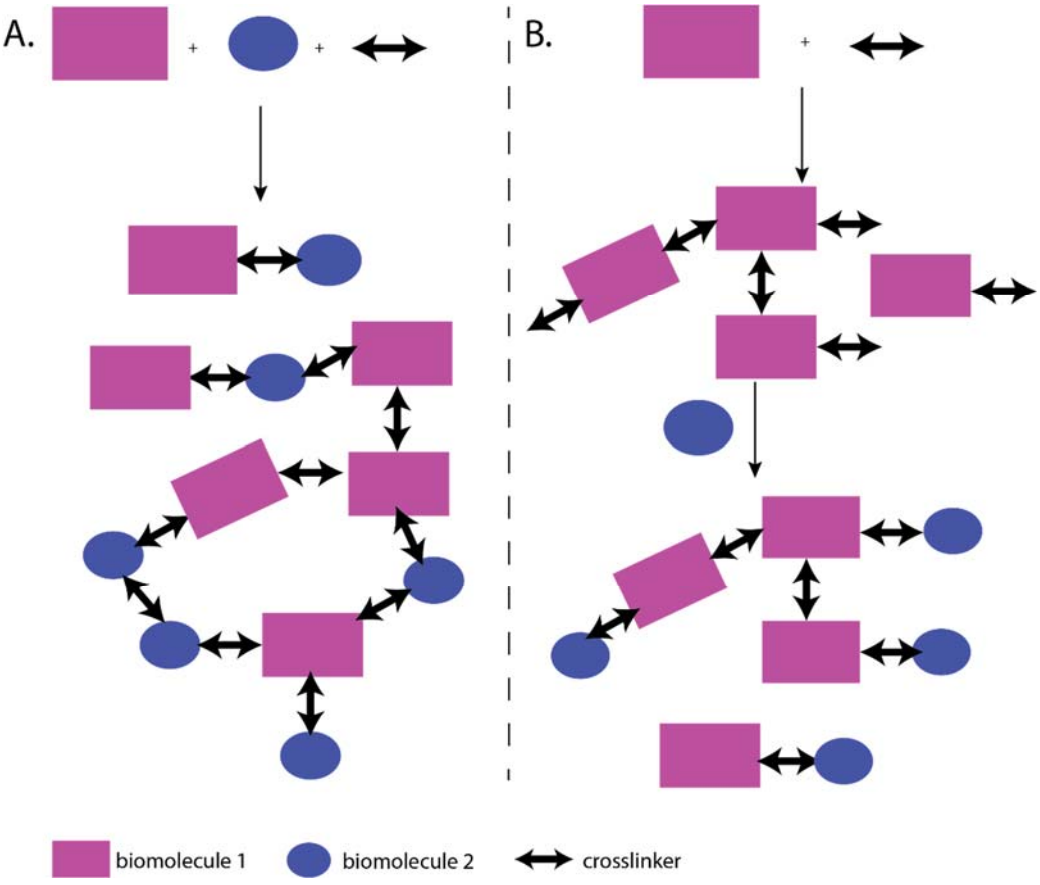

Figure 1.1. A. A one-step crosslinking results in a polymeric complex and B. a two-step reaction results to a more controllable product.

The crosslinker reagents can be classified into two broad categories: the homobifunctional and the heterobifunctional crosslinkers (Figure 1.2). Homobifunctional crosslinkers contain the same functionality at both ends. For example, the most common homobifunctional compound is the N-hydroxysuccinimidyl (NHS) esters, which modify the amines of the biological molecules. However, the main disadvantage of this type of crosslinker is that the final products might include different bioconjugates, because the active intermediated- biomolecule may react with itself. Also, in the case of proteins that have many amines, the crosslinker can activate different amines in the same molecule, resulting in further polymerization and even precipitation of the product. However, if the reaction conditions are controlled, the disadvantages may be avoided.[6,7] Heterobifunctional crosslinkers consist of different end group functionality, so they may react with different groups of each biological molecule. For example, the most common heterobifunctional reagent includes one end which reacts with amines, and the other end reacts with sulfhydryl groups.[8,9] This reagent overcomes the disadvantage of the homobifunctional crosslinkers and the crosslinking reactions usually occur in two or more steps.

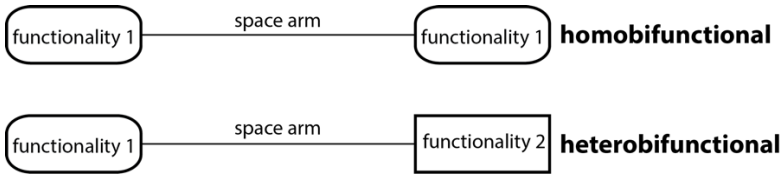

Figure 1.2. Schematic design of homobifunctional and heterobifunctional crosslinkers.

1.1.2 Common protein bioconjugation methods

The protein bioconjugation is dependent on the amino acid accessibility and the conditions of the environment (pH, temperature). The primary amines in a protein are categorized by the α-amines which are the N-terminal amines of the protein, and the ε-amines of the lysine residues (Figure 1.3). The deprotonated form of the amines are strong nucleophiles and

readily react with amine-reactive reagents, most common the sulfo-NHS esters which are soluble in aqueous buffers.[10]

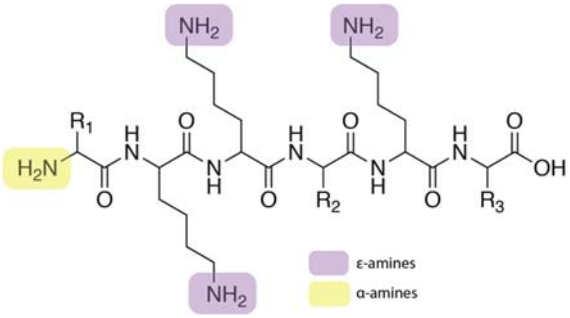

Figure 1.3. A peptide structure indicating the position of α and ε-amines.

Since the lysine residue is one of the most common amino acid on a polypeptide, but the disadvantage is that the bioconjugation reactions cannot be controlled, and the products will vary. Also, if the protein is derivatized with an excess of the crosslinker, this may affect either the functionality of the protein by blocking important sites, such as the enzymatic pocket of an enzyme, or by affecting its solubility. The bioconjugation on the lysine residues can be controlled by exploring the reactivity under different conjugation conditions, and the topological location of each amine group.

The other most common amino acid for bioconjugation purposes is the cysteine residue. Cysteine residue is a less abundant amino acid in an average protein structure, and is also a nucleophile. It is a structurally important residue since the formation of disulfide bridges is crucial in the tertiary structure of a protein. Therefore, these sulfur bridges need to be reduced in order to free the sulfhydryl groups, and to make them available for the bioconjugation reactions. Dithiothreitol (DTT), β-mercaptoethanol (β-Me) and tris(2-carboxyethyl)phosphine (TCEP) are the most common reagents used to reduce the disulfide bridges,[11] and these reagents need to be removed after the reduction step because they may affect the second biomolecule which, next, will be conjugated. The drawback of

this method is the possible air oxidation of the sulfhydryl groups along with the restoration of the bridges.[12] Therefore, the reduction is usually performed immediately before the conjugation reaction. As mentioned above, the cysteine residues play an important role in the protein structure. The reduction of the disulfide bridges, for the purpose of subsequent conjugation might affect the tertiary structure of the protein, and hence, the protein functionality. This is why, most of the time, novel cysteine residues are introduced into the protein structure through site-directed mutagenesis, which do not form disulfide bonds but retain the protein functionality.

1.1.3 Bioorthogonal reactions

Bioorthogonal chemistry was introduced to overcome the limitation of the biomolecules which have similar reactive sites and where the results of classical bioconjugation are complex (Figure 1.4). In 2003, Carolyn Bertozzi referred and coined the term "bioorthogonal chemistry"[13] which describes as the reactions that can occur in a living system without interfering with the biological pathways.[14] The reagents of this chemistry are soluble in aqueous environments, are non-toxic, react rapidly with the preferred biomolecules and do not affect any other cellular processes *in vivo*.[15] So, under physiological conditions, the reactions have very high, if not quantitative yields, and the product is stable under these conditions.

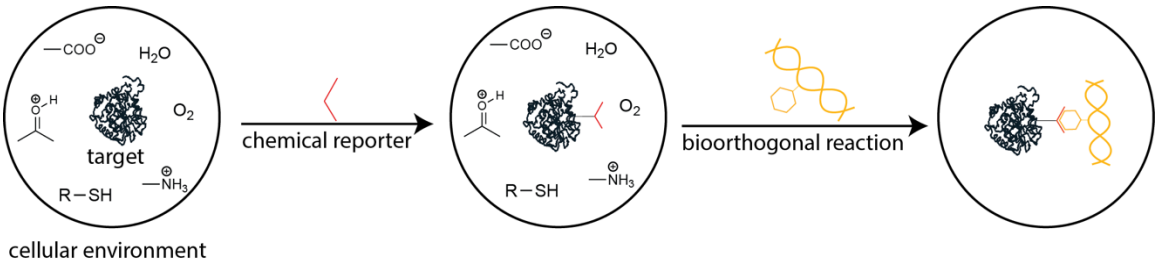

Figure 1.4. Bioorthogonal scheme reaction in a cellular environment. The "red" represents the chemical reporter that reacts with a specific molecule, and the "yellow" represents the bioorthogonal reaction that happens with the specific molecule.

Ketones and aldehydes are found mainly in glycans and in genetically modified proteins such as when unnatural amino acids are introduced. These are strong electrophiles and react with hydrazides and alkoxyamines, to synthesize hydrazone and oxime products, respectively.[16] However, these reactions proceed under acidic conditions, pH 5~6, where the reaction kinetics are relatively slow. To overcome these drawbacks, aniline is usually introduced as the catalyst so the reactions may proceed under neutral pH.[17,18] The aniline accelerates both reactions by creating a protonated aniline Schiff base, and because this is a strong electrophile, it undergoes immediately the synthesis of the hydrazone or oxime products (Figure 1.5).

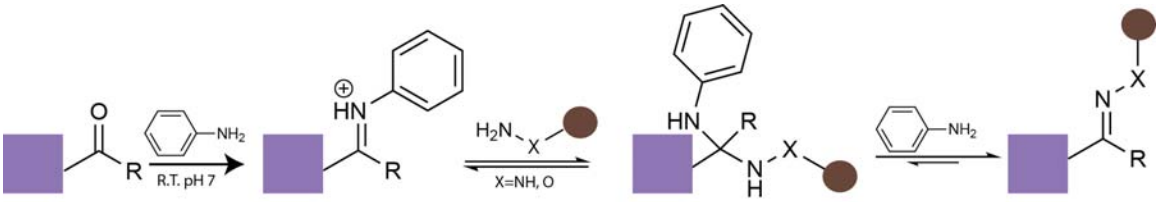

Figure 1.5. The mechanism of the bioorthogonal reaction between a carbonyl compound and hydrazides or alkoxyamines using aniline as catalyst.

Another chemical compound that can undergo bioorthogonal reactions, is the 1,2,4,5-tetrazines which react with the alkenes through Diels-Alder cycloaddition. In 2008, for the first time two research groups developed the tetrazine cycloadditions through bioorthogonal chemistry. Fox et al. applied bioorthogonal chemistry through reverse Diels-Alder reaction between tetrazine and cyclooctene molecules. The reaction was studied for

its rates and yield, using different substituted tetrazines in different medias: water, cell media or lysate, and organic solvents. To apply this chemistry in biomolecule conjugation, the protein thioredoxin, modified with *trans*-cyclooctene through sulfur-maleimide chemistry, reacted faster with a tetrazine derivative under physiological conditions that had no catalyst.[19] During the same period, another group, Devaraj et al. applied the tetrazine bioorthogonal chemistry to cell imaging, though norbornene-modified antibodies and a tetrazine molecule conjugated with fluorophore.[20] Overall, the advantages of this cycloaddition reaction are the rapid kinetics under physiological conditions, include the use of no catalyst, the stability of the compounds in biological fluids, and the ability of the tetrazines to quench some fluorophores.[21] The main disadvantage of this bioorthogonal reaction is the synthesis of the tetrazine molecule, which requires hydrazine as the starting material. Hydrazine is hazardous in nature and is banned by many countries.

1.1.4 Bioorthogonal reactions with amino acids

Although the bioorthogonal reactions, identified above, existed for specific functional group, - such as carbonyl and an alkene -, it was necessary to develop methods that are compatible with the 20 natural amino acids. Lysine and cysteines residues are two of the most common amino acids to conjugate through different reagents, but they cannot undergo bioorthogonal reactions. Few research studies have developed bioorthogonal reactions with arginine, tryptophan, and methionine residues.[22] Under physiological conditions, arginine is protonated, since it has a pKa of 10.76 and it reacts with α,β-dicarbonyl compounds to form a Schiff-based product. For example, methylglyoxal reacts with the arginine residues through Maillard reaction (Figure 1.6).[23] Unfortunately, this type of reaction is very slow

and the dicarbonyl compounds can potentially react with lysine residues which can result in unwanted side reactions.

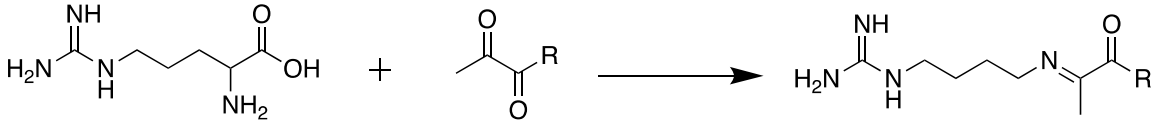

Figure 1.6. Arginine residue reacts with a methylglyoxal derivative through Maillard reaction.

Methionine residues are rare in the protein structure and can be highly selective for bioorthogonal reactions. Alkylation, in the sulfur of methionine, has been introduced by Kramer and Deming, resulting in producing sulfonium ions, which are stable for further conjugations with other biomolecules.[24,25] Recently, a redox approach to conjugate methionine was developed by Lin et al.[26] Methionine residue is a weak nucleophile under physiological pH, but at low pH, it changes to sulfonium salts, and reacts with electrophilic compounds. Lin et al. managed to conjugate the methionine residue under neutral pH, which was called redox-activated chemical tagging (ReACT). The methionine residue underwent a sulfur imidation reaction using oxaziridine as the reagent which is a strong electrophile (Figure 1.7). This reaction had rapid kinetics, which happened in less than 5 min, and had 100% yield.

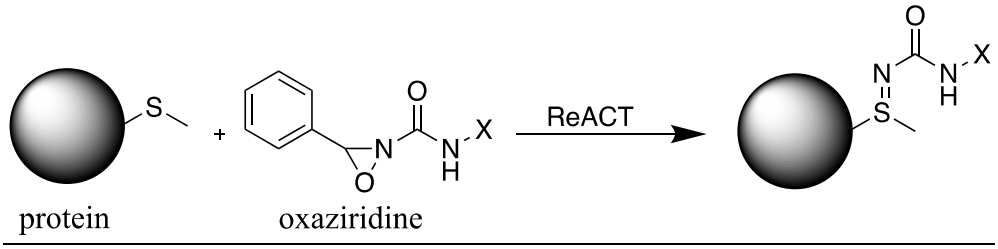

Figure 1.7. The redox-activated chemical tagging (ReACT) between the methionine residue of a protein and the oxaziridine molecule under physiological conditions.

The amino acid that has one of the lowest abundance in proteins, tryptophan, has not been studied in detail for its bioorthogonality. In 2000, Li et al. took advantage of the Pictet-Spengler reaction, and consequently N-terminal tryptophan residue reacted with an

aldehyde-modified peptide (Figure 1.8).[27] The drawback of this reaction is the use of glacial acetic acid which may affect histidine residues, as well as several other N-terminal residues.[28]

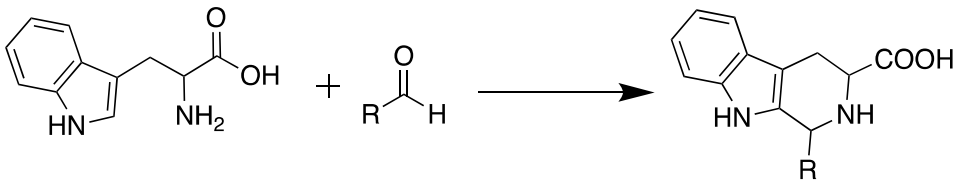

Figure 1.8. Pictet-Spengler reaction where a tryptophan residue reacts with an aldehyde.

1.1.5 Tyrosine bioorthogonal chemistry

Tyrosine residues have been considered ideal candidates for bioorthogonal reactions because they are usually buried within the hydrophobic core of protein structure (amphiphilic properties of the phenol ring). Thus, tyrosine residue may be introduced using site-directed mutagenesis on the protein surface, for the ease of access for the bioorthogonal reactions. Two main sites of tyrosine residue that are amenable to be modified, are the ortho position of the phenolic ring, and the hydroxyl group. The direct alkylation of the phenolic group of the tyrosine can occur in aqueous buffer under basic conditions through Pd-catalyzed alkylation.[29] Because of the basic reaction conditions to create the phenolic anion, only proteins that are stable at higher pH can be used. Another reaction that was developed was a chemoselective Mannich-type reaction with aniline analogues and aldehydes which modify the ortho position of the phenol ring.[30] Under physiological conditions, many different groups or biomolecules may be introduced on tyrosine residues using this approach. The disadvantages of this method are the possible side reactions with the tryptophan residues and with the reduced sulfur groups of the cysteine residue.[31]

Barbas group from the Scripps Research Institute has made a lot of progress in tyrosine bioorthogonal chemistry. In 2009, the group developed an orthogonal method for specific labeling the ortho position of tyrosine residues using cyclic diazodicarboxamides like 4-phenyl-3*H*-1,2,4-triazole-3.5(4*H*)-dione (PTAD). These cyclic diazodicarboxamides analogues are stable, in aqueous buffers and a broad range of pH, whereas, the acyclic ones are not stable, and they decompose faster than the reaction with the tyrosine molecule. Also, the chemoselectivity of PTAD was studied, showing that the aqueous conditions activated only the phenol ring of the tyrosine.[32,33]

First, Francis and his group introduced the diazonium-coupling reagents for the ortho position modification of the tyrosine residues.[34,35] Different viruses were exposed to the diazonium reagents which were synthesized from aniline analogues. Under acidic conditions, the aniline analogues are converted to their diazonium salts, which further react with the tyrosine residues *in situ*. Also, following the same procedure, another group attached polyethylene glycol (PEG) analogues onto the tyrosine residues through the functionalization of the polymer with aniline for further diazonium coupling (Figure 1.9).[36]

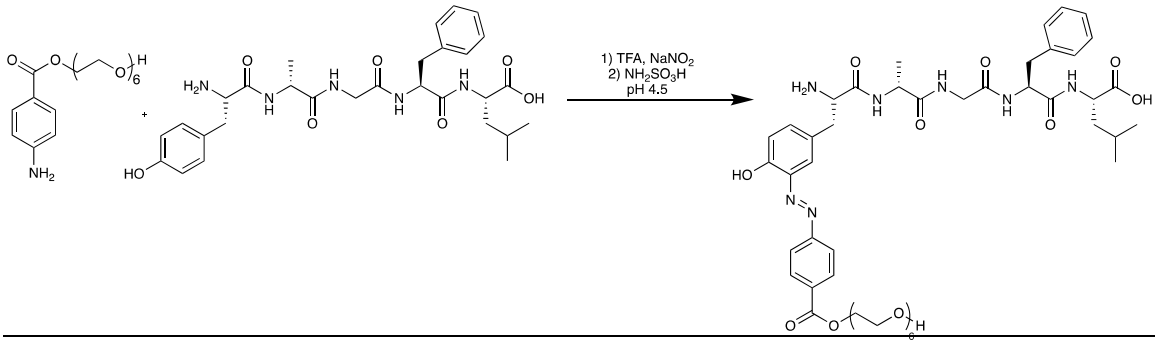

Figure 1.9. Bioorthogonal reaction of a tyrosine residue with aniline analogues under acidic conditions. The conversion of the aniline to the diazonium salt happens in-situ.

Unfortunately, the low pH for the reaction may affect the tertiary structure of the protein and thus, its functionality and furthermore, the diazonium coupling reaction is usually

performed under slightly basic conditions. Therefore, Barbas and his group synthesized diazonium salts that provide bifunctional properties and are bench-stable. The advantages of these diazonium salts are the stability and the reactivity in the aqueous buffers, and because of their bifunctionality, they provide further bioorthogonality into the protein.[37] 4-formyl benzene diazonium hexafluorophosphate (FBDP) provides an aldehyde functionality on the protein (Figure 1.10) for further conjugation with hydrazine- or aminooxy-modified molecules.[38] Reacting the FBDP with the biomolecules in mildly basic pH gives a yield ~100%. But, the most important characteristic of the FBDP diazonium salt is its stability, the high reactivity after 3 months stored at 4 °C, and the selectivity against the tyrosine residues.

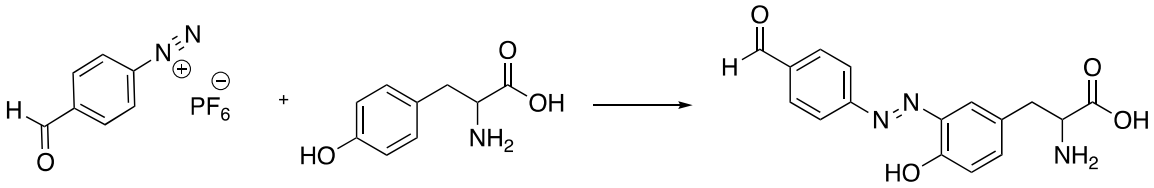

Figure 1.10. The reaction on ortho position of tyrosine with FBDP provides aldehyde functionality on the protein.

1.1.6 Click chemistry

Click chemistry is the most characteristic category of the bioorthogonal reactions, which was introduced for the first time in 2001 by Sharpless.[39] The name "click" means the direct attachment of two specific chemical groups in high yield without intermediate reactions or byproducts, using reagents that are stable in water and oxygen. The [3+2] cycloaddition between azide and alkyne is the most common click reaction to produce 1,2,3-triazoles. The azides are considered ideal candidates for bioorthogonal reactions because they are not present in the biomolecules so they can be introduced with classic chemistry or genetic modification. These are small molecules, stable in the metabolic procedures, selective electrophile, and have minimum reactivity with the natural functionalities. Generally,

several biomolecules have been functionalized with the azide moiety such as proteins,[40] glycans,[41] and lipids,[42] using the Staudinger ligation between azides and phosphines. The Staudinger ligation was the first bioorthogonal reaction that was used in living systems, but the reaction was slow, when compared to the rapid biological pathways.[43] The first 1,3-dipolar cycloaddition to produce five-membered ring was examined thoroughly by Huisgen.[44] The numbers that characterize a cycloaddition, are the numbers of the new σ-bonds at the expense of the π- bonds. The problem with these 1,3-dipolar cycloaddition reactions, is that they could only occur in elevated temperatures and at pressures which is against the bioorthogonality. To overcome this disadvantage, two different groups introduced the Cu as the catalyst of the [3+2] cycloaddition between azides and terminal alkynes.[45,46] The Cu-catalyzed azide-alkyne cycloaddition (CuAAC) reaction occurs rapidly at room temperature. The first mechanism of the CuAAC was proposed by Sharpless (Figure 1.11).[46]

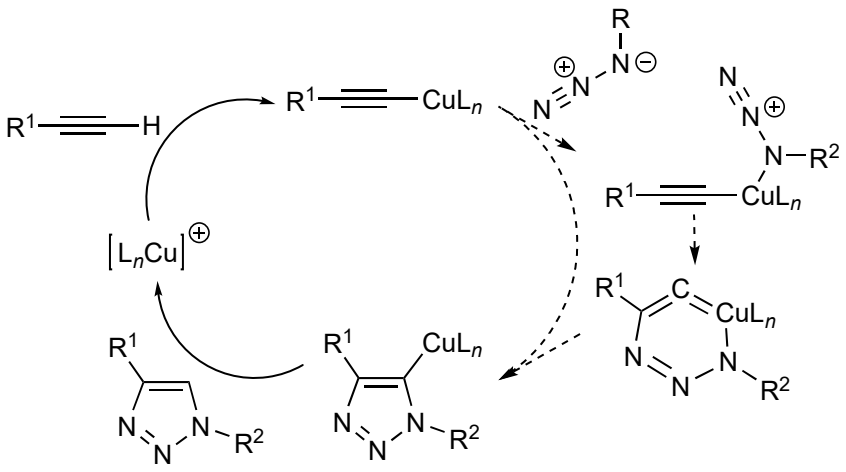

Figure 1.11. The suggested mechanism by Sharpless for the Cu-catalyzed azide alkyne cycloaddition (CuAAC).

Unfortunately, the copper ions are toxic to many organisms, so it was necessary to find another method. Cyclooctynes are the smallest stable cycloalkynes that can exist and in 1961, Wittig and Krebs observed that these react with the azides, "like an explosion", to

give the triazole product.[47] The "explosion" happens because the cyclooctyne has 18 kcal/mol of ring-strain energy.[48] After almost 40 years, Bertozzi's group took advantage of this "explosion", and proceeded with copper-free click reaction *in vivo* under physiological conditions, introducing the Strain Promoted Azide-Alkyne Click (SPAAC) reaction (Figure 1.12).[49]

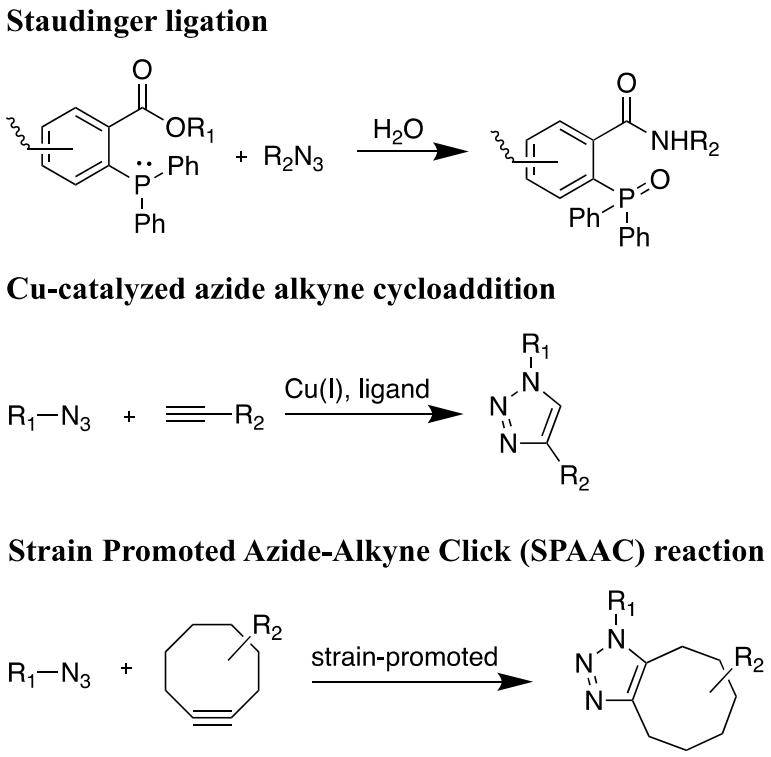

Figure 1.12. Different reactions that azides can undergo.

To improve the reaction capability of the cyclooctynes, as well as the reaction rates, the same group attached the difluoromethylene moiety as the electron withdrawing molecule, to the already existed high-strain-energy cyclooctyne, synthesizing Difluorinated Cyclooctyne (DIFO).[50] The fluorescent DIFO was directly labeled with the azide-conjugated glycans in a living system. The main disadvantage of DIFO was the semi-solubility in water, which is one of the requirements of the bioorthogonal reactions.

A year later, Boons and his group introduced a new cyclooctyne for the copper-free click reactions.[1] 4-dibenzocyclooctynols (4-DBCO) (Figure 1.13) includes two aromatic rings that enforce higher ring strain energy, and therefore, they react faster with the azides. Also, this compound is stable against nucleophilic attacks, because the *ortho* protons of the aromatic rings shield the triple bond.

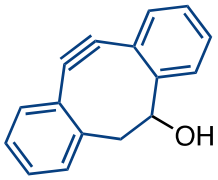

Figure 1.13. The structure of the 4-DBCO according to the reference[1]. The blue color is the structure of the DBCO. The 4-DBCO can be modified with different functional groups besides hydroxyl group.

Boons group took advantage of the hydroxyl group which was conjugated with biotin, and which further interacted with a fluorophore (FITC)-avidin. The imaging studies in the cells showed that the fluorescence intensity from the SPAAC reaction was higher than the Staudinger reaction.

Different applications have been designed using bioorthogonal reactions. Molecules such as antibodies are complicated, since they are high-molecular weight molecules and consist of different amino acids. Antibodies are mainly used in immunoassays to detect analytes of interest. Applying bioorthogonal chemistry on the antibodies, and conjugating them with different labels, may be useful for the improvement of sensitivity and specificity in biomedical measurements.

1.2 Bioorthogonal reactions on antibodies

As mentioned above, bioorthogonal reactions are very useful to conjugate protein or antibodies with different molecules, as desired. These reactions are very selective and maintain the functionality of the biomolecule. Fischer-Durand et al. synthesized a

bioorthogonal bifunctional crosslinker for antibodies, which includes a hydrazide function at one end, and an azide at the other end.[51] The hydrazide end formed a hydrazone bond with aldehyde groups, which formed from the oxidized sugar moieties of the antibody, and the azide end participated to CuAAC reaction, with a coumarine-derivative fluorophore (Figure 1.14). The group performed an immunoassay to prove that the fluorophore-antibody was still functional.

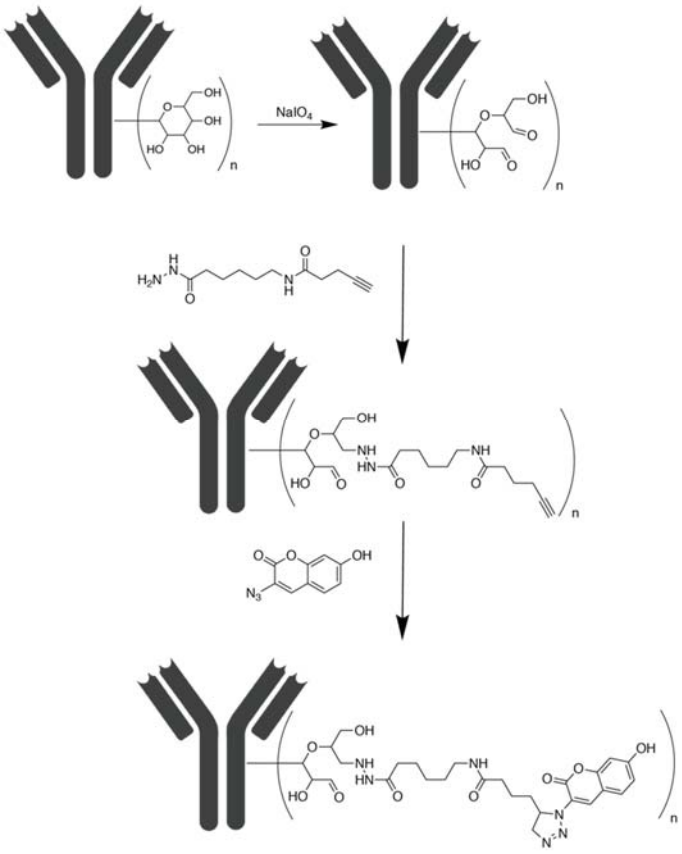

Figure 1.14. Conjugation of the antibody with the fluorophore coumarine with bioorthogonal linker.

Recently, another group developed a sandwich-type immunoassay which involved the binding of the antigen with two different antibodies. The first antibody or "capture antibody" was coated onto the solid phase (96-well microplate), and the label was attached to the secondary antibody or the "detection antibody", where the signal was correlated with

the concentration of the analyte. This sandwich-type immunoassay was a point-of-care immunoassay for morphine and two biomarkers (interleukin-6 and HIV capsid antigen 24), using peroxide test strips (PTS).[52] The secondary antibody was labeled through bioorthogonal reaction with glucose oxidase. The detection antibody was conjugated with trans-cyclooctene, which reacted with the modified 1,2,4,5-tetrazine-glucose oxidase through SPAAC chemistry. Performing two SPAAC reactions, the secondary antibody had two layers of glucose oxidase, because the researchers proved that the limit of detection was much lower than with one reaction. The labeled secondary antibody with the two layers enhanced the signal, and this immunoassay was more sensitive than horseradish peroxide (HRP)-based immunoassay (Figure 1.15).

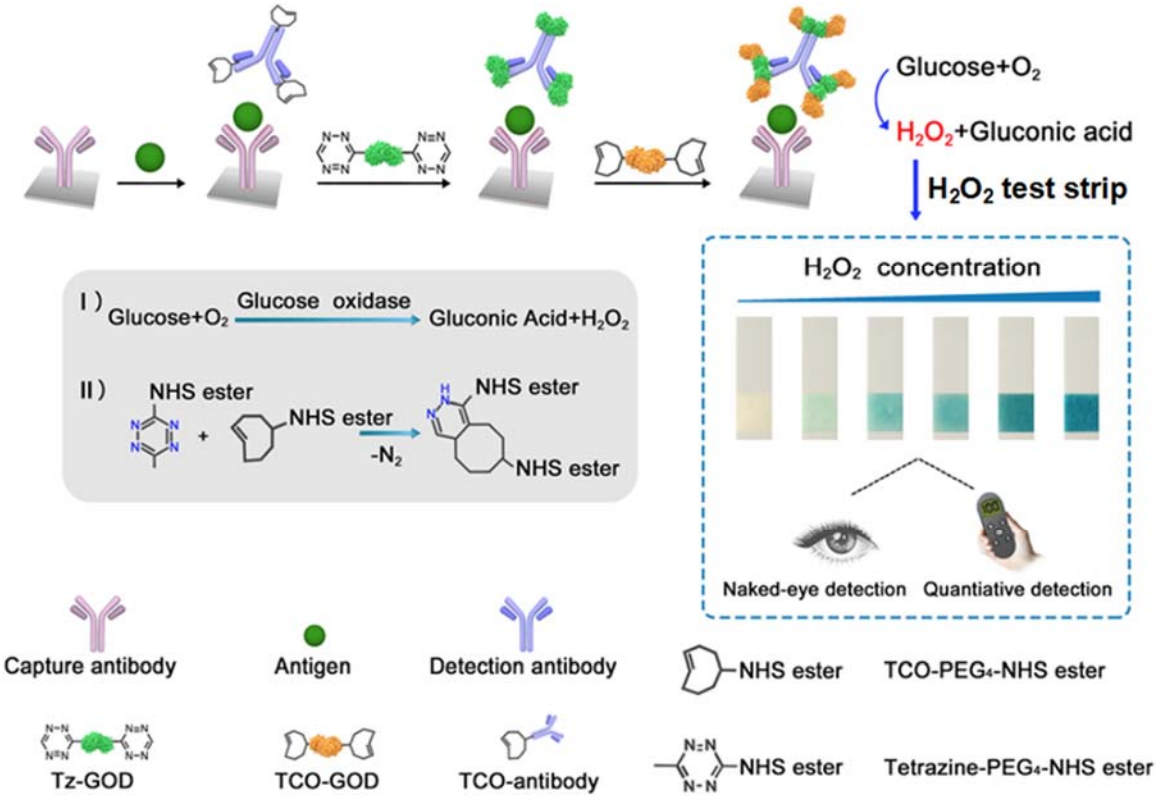

Figure 1.15. Schematic diagram of bioorthogonal reactions between tetrazine and cyclooctyne to develop an immunoassay using peroxide strips as detector. Reprinted with permission from {*Anal. Chem.*, 2017, *89* (11), pp 6113–6119}. Copyright {2017} American Chemical Society."

1.3 Bioorthogonal reactions on nucleic acids

Bioorthogonal reactions on nucleic acids for imaging and diagnostics are important for specific labeling especially with proteins. Nucleic acids are less complicated than the other biomolecules because they have very few reactive sites, and it is much easier to introduce a desirable site. There are several research groups that have studied the bioorthogonal reactions on the nucleic acids, and they showed promising labeling *in vitro* and *in vivo*.[53] Different modification approaches will be reported in this section.

The alkyne or azide group has been introduced in several positions of the aromatic rings of the nucleotides, such as in position 5 of the pyrimidine system (Figure 1.16A & B),[54,55] and in position 7 of the deazapurine system (Figure 1.16C).[56] Introducing these groups, the nucleic acids can be modified further with labels such as fluorophores, chromophores through CuAAC labeling.

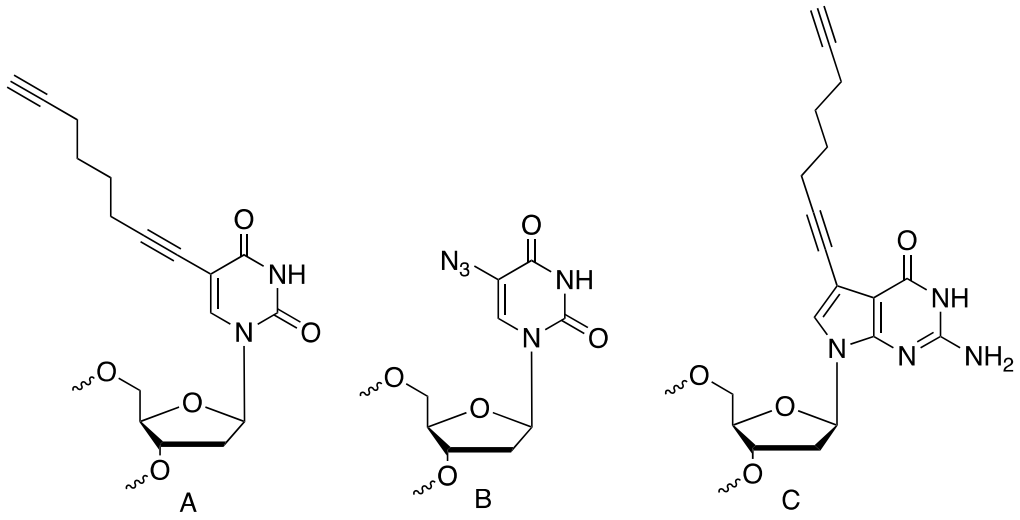

Figure 1.16. Examples of alkyne or azide-modified nucleotides.

Besides CuAAC, other bioorthogonal reactions have been applied on the nucleic acids to avoid the copper ions which have strong cytotoxicity. Singh et al. developed for the first time, a solid-state oligonucleotide conjugation at 5' end through SPAAC, between

monocyclic octyne and several azide-modified molecules at room temperature for possible future application in biomedicine.[57] Another research group took advantage of the Diels-Alder cycloaddition between dienophile and maleimide molecule.[58] The dienophile was introduced in the position 5 of the pyrimidine ring, whereas, the fluorophores were modified with maleimides molecules.

To conclude, conjugating the detection antibody with a label can be challenging since antibody is a large biomolecule with many reactive sites. Bioorthogonal reactions can solve this problem through the introduction of a unique functional group on both protein and antibody. Similarly, conjugation of nucleic acid or oligonucleotides to other biomolecules can be performed using biorthogonal reactions. In this dissertation work, we took advantage of the specificity of conjugation afforded by the biorthogonal reaction, and developed a variety of novel assays as described in subsequent chapters.

Assays which can be applied *in vivo* detection, are valuable for discerning spontaneous or transitory abnormalities that indicate an underlying disease state using minimally- or non-invasive procedures.[59-61] Although labeled antibodies for real-time protein detection have been in use since 1985, this method only provides information on the location of the antibodies, but the presence of target must be inferred or estimated *in vitro*. Therefore, new real-time detection techniques are required to address deficiencies in target specificity, signal detection, and cellular delivery.[62] The following section is a brief analysis of the diagnostic applications based on molecular aptamer beacons, which provide advantages like high selectivity and sensitivity, a switchable signal, and a simple design.

1.4 Development of molecular aptamer beacon

Since the development of the first MB by Tyagi and Kramer[63] in 1996, many studies have demonstrated their use as sensors, imaging constructs, and therapeutics.[64,65] Much of the inherent utility of MBs derives from their self-contained signaling system derived from a loop region and a terminal stem that forms a closed, hairpin structure. The loop region contains an antisense recognition domain against a nucleic acid target, and the absence of target allows the molecular beacon to self-hybridize at the stem (Figure 1.17). By labeling the MB sequence termini independently with an energy donor and a complementary acceptor, a closed hairpin results in resonance energy transfer (RET) upon donor excitation. Hybridization at the loop applies tensile stress at the stem, leading to eventual separation of the donor and acceptor for generation of a dose-dependent signal (Figure 1.17). In general, the mechanism of target detection in MBs is oligonucleotide hybridization, and it has been demonstrated that they have better nucleotide mismatch selectivity than linear nucleic acids.[66,67]

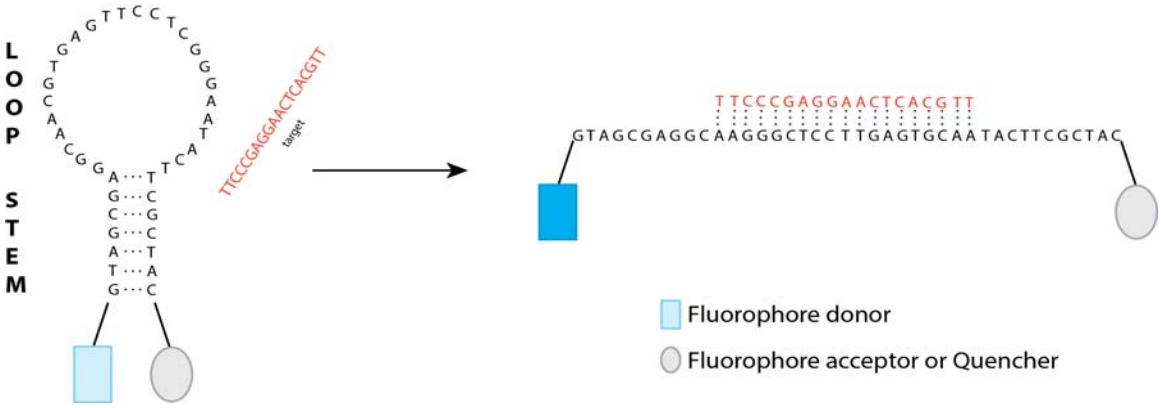

Figure 1.17. Working principle of a typical fluorescent molecular beacon upon target binding.

Before the term "aptamers" existed, Kramer et al.[68] identified RNA molecules that would specifically bind ethidium bromide. Almost 15 years later, a process called SELEX (Systematic Evolution of Ligands by EXponential enrichment) was developed

independently by two research groups for the purpose of generating *de novo* aptamer sequences against specific ligand molecules such as proteins, small molecules and cells.[69-71] The aptamers that are selected using SELEX are isolated from library of 10^{14}-10^{15} random oligonucleotide strands and are selected based on affinity to a specific target of interest (Figure 1.18). After repeated cycles of higher stringency and a final PCR enrichment step, the "best" oligonucleotide sequence against the analyte is isolated. Initial targets for SELEX included DNA polymerase (gp43) and dyes that were acting as mimics of metabolic cofactors. These developments spurred significant interest in aptamer development, as they provided similar functionality to antibodies without the expensive and cumbersome selection process. Compared to antibodies, aptamers can tolerate non-physiological conditions, high temperatures, extreme pH, and organic solvents,[72] Aptamers can efficiently bind a diverse size range of molecules, due largely to binding constants (K_d) ranging from picomolar to nanomolar,[73] and are easily functionalized with binding moieties for further conjugation reactions with reporters. As a result of high specificity, low binding constants, and easy manipulation, aptamers have found significant application in imaging, diagnostics, and therapy.[74,75]

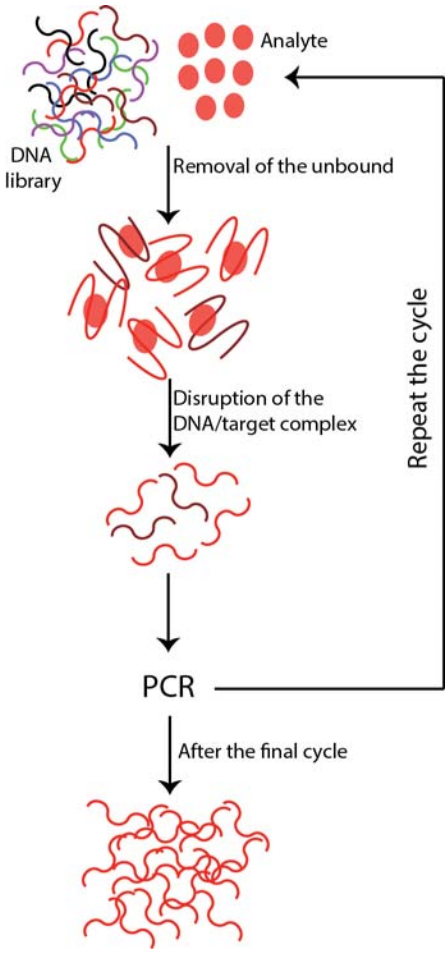

Figure 1.18. Schematic steps of SELEX.

Molecular beacons and aptamers have been used extensively, as both can be labeled with different molecules and emit signal in different wavelengths. Given their highly similar structure, molecular beacons can recognize proteins as well as antisense oligonucleotides; however, most MB/protein interactions are non-specific and interfere with selective target binding.[65] Conversely, aptamers are rationally designed for binding proteins or other small and large molecules with high specificity but are incapable of generating a switchable, dose-dependent signal. In order to merge these attributes, a molecular aptamer beacon (MAB)[65] was designed to consist of a self-hybridizing stem functionalized with one or multiple signaling moieties joined by an internal aptamer domain for target recognition.

1.5 Working Principle of Molecular Aptamer Beacon

MABs can be broadly classified by the size of their targets, where small molecules are typically sequestered within the interior of the recognition domain and larger targets such as proteins are recognized by interfacial binding with the aptamer secondary structure. Although aptamers have a similar structure to molecular beacons, the single-stranded loop sequences that correspond to the target hybridization domain of MBs have very definitive three-dimensional conformations that can selectively bind a vast array of structured ligands (Figure 1.19). These stable, three-dimensional structures increase overall selectivity by allowing a variety of forces including Van Der Waals, dipole-dipole, electrostatic, etc. to influence target recognition.[76] In that sense, they can act similar to antibodies. In general, MABs rely on a "closed" configuration in the absence of target that enables the standard stem-loop conformation and allows interaction of the functionalized termini. Target binding denatures the stem and either activates or changes the signal. This method of action has been referred to as "target-induced structure switching" due to the conformational change that accompanies molecular recognition.[75] The necessity of structural change can be visualized from Figure 1.19, where the similarity between MBs and MABs is unmistakable.

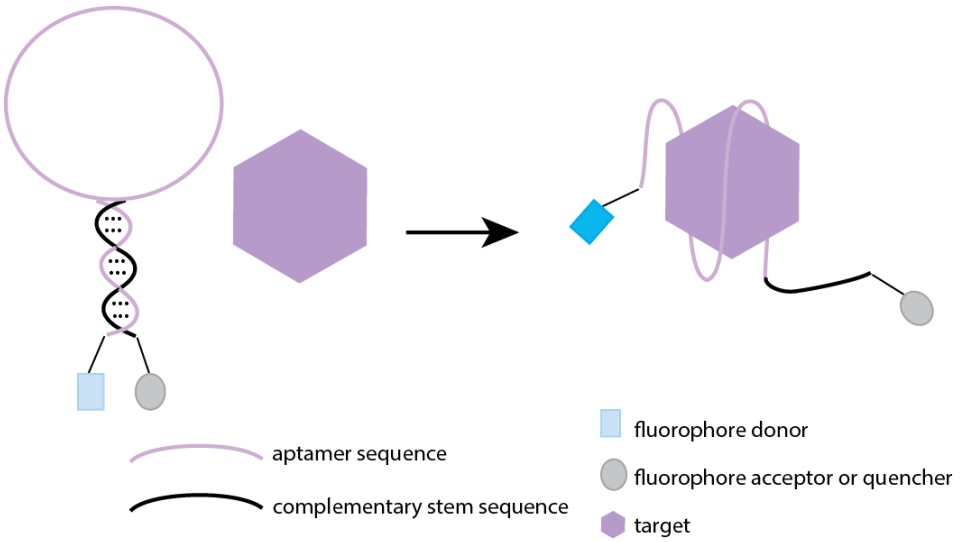

Figure 1.19. Working principle of the molecular aptamer beacon (MAB).

As with MBs, terminal signaling for MABs is often provided by RET interactions that provide distance-dependent signal attenuation or wavelength shifting in the absence of target. Common fluorophores comprise the standard optical sensors, with donors and acceptors designed as complementary pairs. As a RET technique, fluorescence RET (FRET) relies on the non-radiative transfer of energy from a fluorophore donor to an acceptor that typically re-emits most of the energy at a longer wavelength. The intensity of the emission is dependent on the distance and the dipole orientation between the fluorophores, the overlap of the emission and absorbance spectra, and the refractive index of the solvent; optimization of these variables leads to improved sensitivity.[77] Fluorescence acceptors are small molecules with an absorption energy that overlaps the emission energy of a complementary donor, leading to non-radiative transfer of excitation energy from the donor fluorophore. Acceptors can be divided into fluorescence acceptors and dark quenchers. Where fluorescence acceptors re-emit a portion of the transferred energy, dark quenchers absorb the energy and transmit it to the surroundings as heat.[78] Besides a fluorophore-quencher arrangement, other energy donors and acceptors as well as

intercalating dyes within the stem can be used for signaling (Figure 1.20). A variety of MABs incorporating diverse target recognition domains have been designed, and besides the small molecule fluorophores, optical signaling moieties can include quantum dots, intercalating dyes, or bioluminescent proteins as energy donors combined with dark quenchers, graphene oxide, carbon nanostructures, or gold nanoparticles as energy acceptors. Additionally, electrochemical techniques have seen the development of many variants including enzymes and redox-active mediators. In this section, we focus on the optical labeling variants that have been applied to *in vitro* and *in vivo* MAB detection/imaging assays.

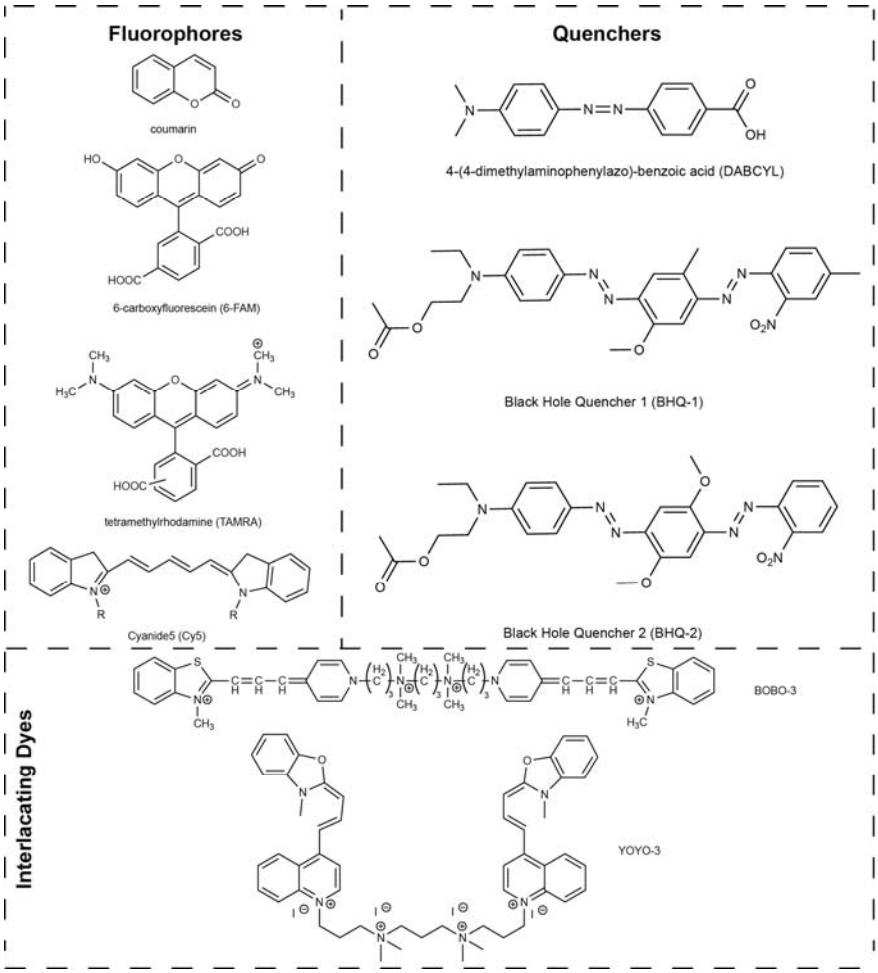

Figure 1.20. Chemical structures of fluorophores, quenchers and intercalating dyes that are mentioned in the text.

1.6 Imaging constructs

1.6.1 Fluorophore-quencher pairs

Possibly as a combination of their MB heritage and rapid development, MABs have often retained the fluorescence donor/acceptor reporter arrangement that is common for so many detection platforms. For *in vitro* assay design, fluorescence has many desirable characteristics including fixed quantum yield, decent intensity, and a wide variety of available labels. Additionally, the small size and site-specific coupling of fluorescent dyes generates low-molecular weight probes with high reproducibility. Although not as significant of a concern, fluorescence probes are very cost-effective and can be discarded in solution-phase assays or reused by immobilizing on a solid support.

The first group to demonstrate the utility of an aptamer sequence within a fluorescent MB platform provided evidence that analytical characterization of protein/DNA interactions were possible using aptamer beacon technology.[79] Previously, MBs had demonstrated non-specific protein interactions; therefore, Weihong Tan's group initially showed that single-strand binding protein (SSB) produced only a slightly lower fluorescence enhancement than cDNA while binding at a significantly faster rate. Based on this observation, the researchers replaced the cDNA detection domain of the MB with an aptamer for the detection of the model protein thrombin. Upon target recognition, this aptamer forms a G-quadruplex structure, bringing the fluorophore in close proximity to the quencher and attenuating the fluorescence intensity. To prove that this signal decrease was due specifically to the recognition of thrombin by the aptamer, they heat-denatured thrombin and observed no change in the fluorescence signal intensity – proving that the change was

due to three-dimensional recognition of the thrombin tertiary structure. This was the first time an aptamer-based molecular beacon was used to detect a protein in solution.

Shortly after, Hamaguchi et al[80] used the same G15 thrombin-binding aptamer as the Tan group but produced several variants that had additional nucleotides at the 5′ end. Because signal-off assay formats can be problematic *in vivo*, they attempted to shift the conformational equilibrium away from G-quadruplex formation by using the extra nucleotides to form a true stem – enabling fluorescence quenching in the unbound state. This also allowed a fluorophore-quencher pair consisting of fluorescein and 4-(4-dimethylaminophenylazo)-benzoic acid (DABCYL) to separate sufficiently upon thrombin binding to generate a dose-dependent fluorescence signal. After selecting the variant with the highest fluorescence, they discovered that this aptamer sequence was very selective and did not respond to other serine proteases or SSB. As part of their findings, this group suggested that MAB technology cannot be used for proteins that bind nonspecifically to ssDNA sequences due to the risk false positives. Also, they found that the assay buffer must be optimized due to the effect that certain ions such as K^+ and Mg^{2+} have on aptamer conformation and the resulting fluorescence intensity.

It was well-known prior to this that non-specific and targeted metal ion/nucleic acid interactions were natural parts of biological systems; however, the realization that MABs could be applied to selective ionic recognition spurred the selection and development of beacons against elemental ions. For instance, Kim et al.[81] designed a MAB for the detection of potassium ions (K^+) to address the need for more sensitive and selective assay designs. Their method combined MAB with conjugated polyelectrolytes (CPEs) through electrostatic and hydrophobic interactions to increase the optical sensitivity of the system.

Upon target binding, the K^+-aptamer formed a G-quadruplex, bringing the fluorophore (6-FAM) and the quencher DABCYL in close proximity and quenching the fluorescence signal. In the absence of target, CPEs that were electrostatically attached to the MAB linearized the beacon and served as FRET acceptors from the 6-FAM fluorophore (Figure 1.21). Moreover, the system was highly selective for K^+ over Na^+, with an LOD calculated to be ~1.5 nM. As evident from the detection of adenosine triphosphate (ATP) using an identical system with an ATP-binding aptamer, this system is capable of detecting a diverse range of analytes under the assumption that an appropriate G-quadruplex-forming aptamer has been identified. However, utility in more complex matrices was limited by the off-type design.

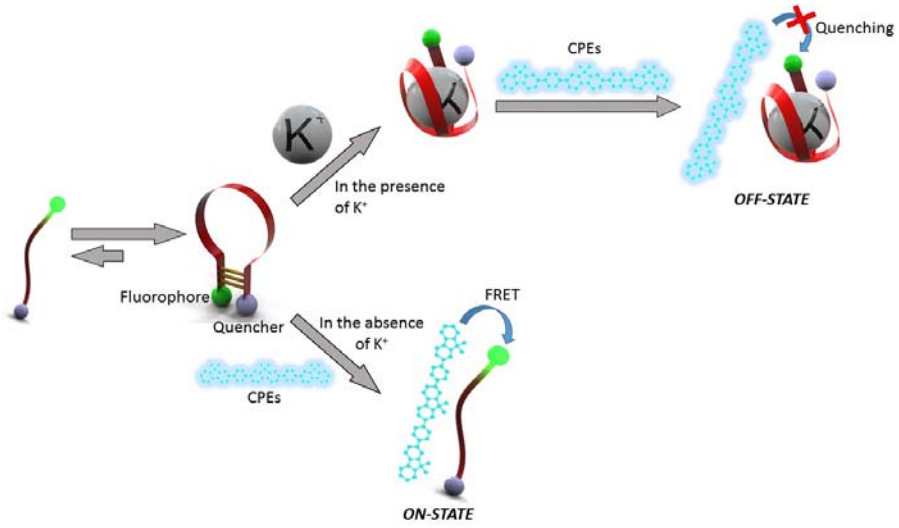

Figure 1.21. The working principle of MAB against potassium ions with or without the conjugated polyelectrolytes (CPEs).

The Tan group[82] realized this limitation as they developed two divergent types of *in situ*, thrombin-specific MABs for use in living cells. The first, similar to their original, relied on off-type quenching of 6-carboxyfluorescein (6-FAM) emission with DABCYL upon target binding. In this case, thrombin recognition resulted in approximately 60% decrease in the fluorescence signal. This study indicated that the G-quadruplex form of the aptamer was

both the recognition structure for thrombin binding and the mechanism for bringing the two ends of the aptamer in close proximity (Figure 1.22). Because of the signal-off format, this MAB was not ideal for a complex matrix, so the second MAB was designed with 6-FAM as a fluorescence acceptor of FRET signaling from the energy donor coumarin. In the presence of the target, coumarin fluorescence decreased as the fluorescence of 6-FAM increased. This enabled them to use ratiometric FRET signal amplification, improving their signal intensity 14-fold. By using this approach, the signal-to-noise ratio and sensitivity were dramatically enhanced. This was the first study to demonstrate the promise of MABs for real-time, *in situ* monitoring of proteins.

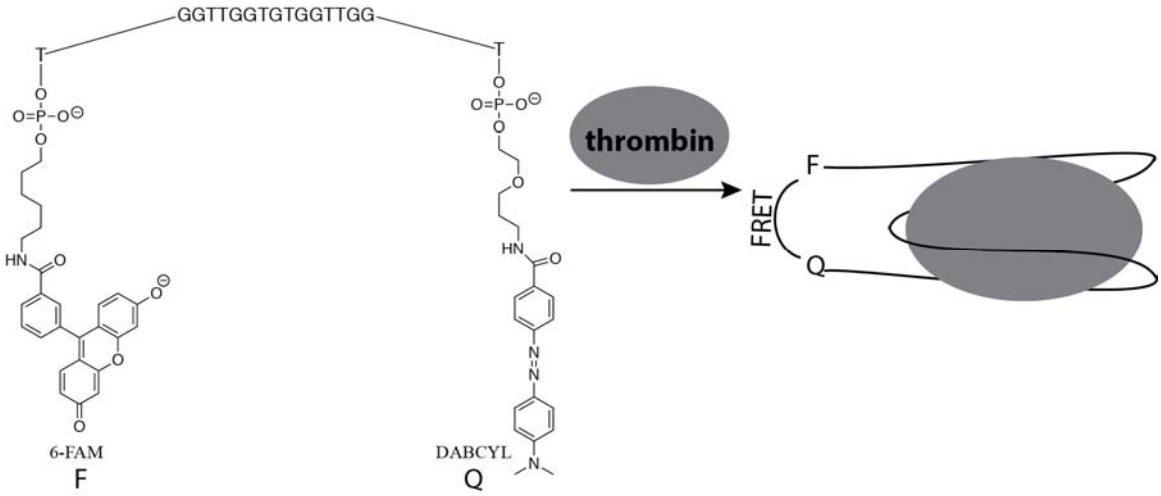

Figure 1.22. The working principle of an off-type thrombin-binding MAB.

As more aptamers were redesigned for use as beacons, the variety of potential targets expanded as well. For example, Tok et al.[83] designed a MAB for myotonic dystrophy kinase-related Cdc42-binding kinase α (MRCKα) by conjugating a 5′ FAM fluorophore and a 3′ DABCYL to the ends of the stem. As opposed to conventional antibodies, this aptamer could distinguish the active form of MRCKα from the inactive form. Moreover, the aptamer was highly selective and did not detect a similar Rho-associated serine/threonine kinase, PAK. One of the first MABs that was reported for HIV-1[84] was

against the trans-activator of transcription (Tat-1) protein, a regulatory protein that increases the efficiency of HIV-1 viral transcription. This assay was designed around the use of a fluorescent beacon containing fluorescein and DABCYL and a non-functionalized duplex aptamer sequence (Figure 1.23). They demonstrated that in the presence of full-length Tat-1, the functionalized aptamer beacon and MAB-complementary oligonucleotide sequence formed a stabilized ternary complex around Tat-1. The full-length Tat-1 sequence was also compared with its truncated CQ form and shown to provide a higher signal-to-noise ratio than the truncated peptide. Additionally, there was no change in the fluorescence intensity in the presence of other RNA binding proteins.

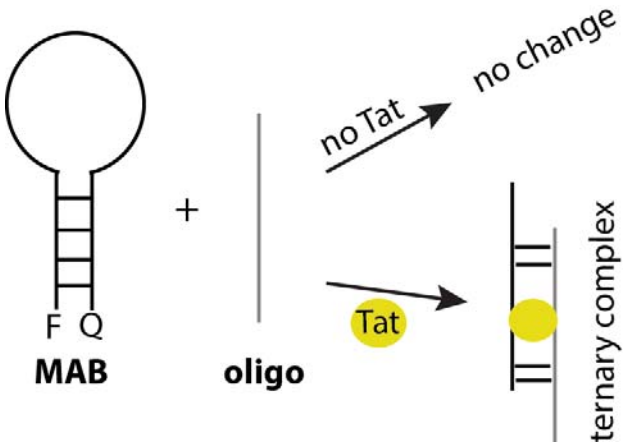

Figure 1.23. Working principle of Tat-1 MAB with and without analyte.

Further, due to the importance of HIV-1 reverse transcriptase (RT) as a target for diagnosis, a MAB was designed by Liang et al.[85] for the real-time detection of HIV-1 in living cells. The synthetic aptamer 93del, a truncated form of the HIV-1 RT aptamer, generates a stable G-quadruplex form upon HIV-1 RT binding. In a similar approach to that used by Hamaguchi et al.,[80] several stem-length variants were developed to optimize aptamer binding and fluorescence intensity. Using a carboxytetramethylrhodamine (TAMRA) fluorophore and a DABCYL quencher, an increase of fluorescence signal for each variant was measured against different concentrations of HIV-1 RT, demonstrating that the 5-

nucleotide stem generated the highest fluorescence intensity. This MAB was used for *in vitro* imaging of HIV-1 integrated into live U1 cells, where it associated with HIV-1 RT in the cytoplasm (Figure 1.24). Although imaging in living cells with MAB is challenging, this MAB was able to selectively recognize target and produce a fluorescence signal bright enough to visually track native, non-functionalized protein.

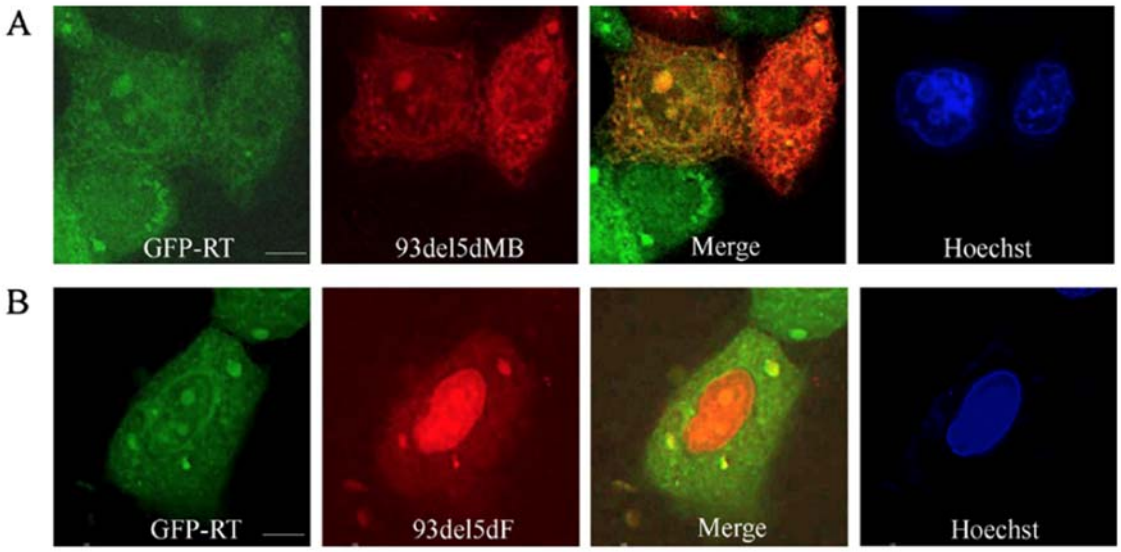

Figure 1.24. Fluorescence intensity of HIV-1 RT in HeLa cells. (A) Co-localization of aptamer 93del and green fluorescence protein (GFP) tagged-RT in non-fixed HeLa cells. (B) Identical experiment as panel A using a control 93del aptamer without quencher and demonstrating that 93del did, indeed, interact with GFP-RT in the cytoplasm. The intensity of signal in the nucleus was attributed to the presence of excess probes that tend to accumulate in the nucleus irrespective of target.

As the benefits of *in situ* imaging using aptamer beacons became more apparent, many oligonucleotide variants have been investigated for their fluorescence intensity and quenching efficiency to select the ideal sequence. For example, Tuleuova et al. monitored the release of interferon-γ (IFN-γ) by immobilizing MABs with spacer variants on a glass slide via avidin-biotin interactions.[86] Specifically, the aptamer sequences incorporated a 3′ biotin for immobilization on an avidin-coated glass slide and a 5′ 6-FAM fluorescence label. The paired quencher (BHQ-1) was placed at the 3′ end of a complementary oligonucleotide against the aptamer sequence. Recognition of IFN-γ by the aptamer

sequence was more kinetically favorable than hybridization between the complementary nucleotides, thereby releasing the quencher sequence and generating a concentration-dependent increase in fluorescence intensity. After identifying the ideal sequence, they also characterized target hybridization using surface plasmon resonance (SPR) and calculated the binding constant (K_d) while demonstrating that interleukin-6 did not generate a detectable signal – proving the specificity of the MAB. Performing the same studies in serum-containing media, however, resulted in a fluorescence signal loss of 20-30% due to a matrix effect. Lastly, they applied this design to detection of IFN-γ using a neutravidin-coated microfluidic device. This was the first aptamer-based, electrochemical detection of IFN-γ using a microfluidic device. Aside from the matrix effect, this study was promising because it was reproducible and did not require additional manipulations such as wash steps.

Continuing the development of *in situ* MAB approaches, an engineered, switchable aptamer micelle flare (SAMF) nanostructure was developed by Wu et al.[87] for imaging of ATP. The core of the nanostructure consisted of terminal diacyllipid molecules conjugated between a 5′-DABCYL and TAMRA-functionalized MAB (Figure 1.25). Having characteristic stem-loop architecture, the MAB was quenched in the absence of target but would open upon ATP binding to generate a dose-responsive fluorescence signal. Confirmation of selectivity was obtained using other triphosphates and indicated that the system only recognized ATP. For demonstration of utility, they delivered the MAB into the HeLa cells. When the SAMF was in close proximity to a cell membrane, it disintegrated into individual molecules and allowed the diacyllipid tails to embed into the cell membrane. Intracellular ATP expression was then detected and imaged using confocal

microscopy. Therefore, this construct was able to non-specifically deliver an anti-ATP MAB into living cells and measure target concentrations changes in real time.

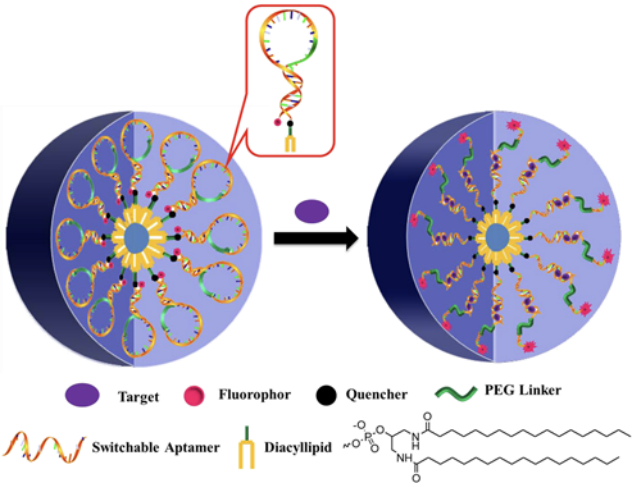

Figure 1.25. Working principle of an aptamer micelle flare in the presence of ATP. {Reprinted with permission from ACS Nano 2013, 7, 7, 5724-5731}. Copyright {2013} American Chemical Society.

A significant difficulty in the development of aptamer beacons for *in vivo* imaging has been the rapid nuclease-mediated degradation of the aptamer in serum and in the cytosol.[88,89] Aptamers with inherent stability can be selected during the SELEX process, but this can still potentially select against optimal binding affinity. For this reason, there are few studies that explore the development of *in vivo* imaging constructs using MAB designs. However, the few that exist show promising results. Based on recognition of the overexpressed receptor protein tyrosine kinase-7 (PTK7) found in certain cancer cells,[90] Shi et al. designed a MAB that was comprised of three segments: the aptamer sequence (sgc8), a linker section, and a stem section complementary to part of the aptamer sequence. Binding of the extracellular domain of PTK7 resulted in increased fluorescence intensity as the FAM fluorophore was separated from the BHQ-1 (Figure 1.26).

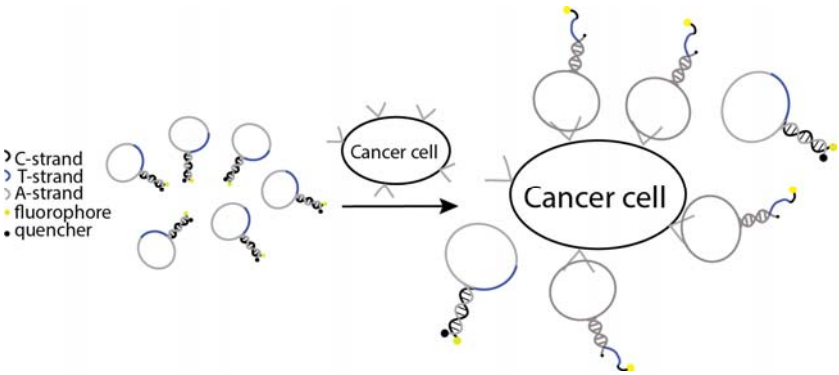

Figure 1.26. Working principle of anti-kinase 7 MAB in the presence of cancer cells.

Following *in vitro* optimization, flow cytometry assays were performed against human acute lymphoblastic leukemia CCRF-CEM cells, in which they discovered that the use of Cy5 and BHQ-2 resulted in a higher signal-to-noise ratio. As shown in Figure 1.27, a fluorescent signal was evident in the tumor site within 15 min. On the other hand, the "always on" aptamer was non-specific, and the fluorescent signal was observed throughout the whole body of the animal. The authors indicated that the large fluorescence background was evidence of some MAB degradation, but the heat map still indicated preferential localization at the tumor site.

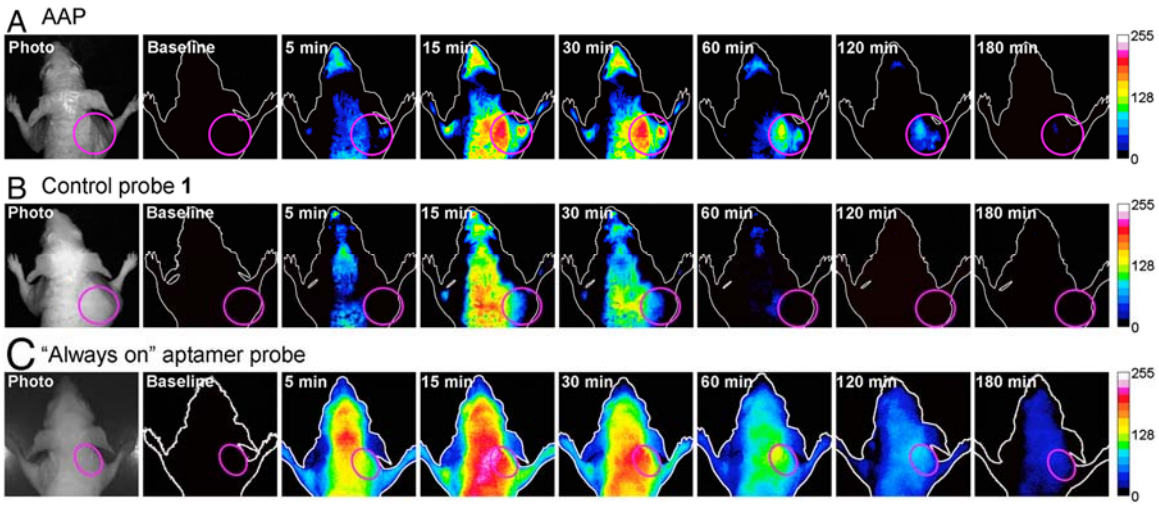

Figure 1.27. In vivo, time-dependent fluorescence imaging of CCRF-CEM tumors. Nude mice subcutaneously injected with CCRF-CEM tumor cells (pink circle) were injected with (A) anti-PTK1 MAB, (B) nonsense aptamer beacon as negative control, and (C) unquenched fluorophore-conjugated aptamer probe, respectively. Reprinted with permission from PNAS March 8, 2011 108 (10) 3900-3905. Copyright (2011) National Academy of Sciences.

With the successful delivery of therapeutic agents using cell- or tissue-specific constructs, the next logical step was selectable or inducible tracking of these delivery vehicles using beacons. This was achieved in an aptamer beacon-conjugated liposome delivery vehicle containing the anti-cancer drug doxorubicin, gold nanocages for generating infrared-induced heat, and sodium bicarbonate for generating CO_2.[91] This scheme relied on cellular recognition via an anti-Mucin-1 (MUC1) aptamer that signaled delivery to the target cell by a conformationally-induced change in FRET between terminal FITC and Cy3 fluorophores. In addition, recognition of MUC1 by the aptamer led to endocytosis of the delivery complex. Given the utility of real-time imaging and selective recognition of delivery complexes, platforms such as this should become more common as aptamers against other overexpressed surface markers are developed.

1.6.2 Quantum dot/quencher pairs

With the advent of new nanomaterials, quantum dots (QDs)[92] have been gaining significant interest and, as such, they have been studied as great candidates for labels in MABs instead of the classic fluorophores. Despite their larger size and potential toxicity, they have certain advantages over fluorescent dyes such as broad absorbance and narrow emission spectra, higher quantum yields, and photochemical stability.[93] However, they are often difficult to quench efficiently due to their large size in relation to the effective Förster radius.[94]

The first QD-aptamer beacon was developed by Levy et al[94] as part of a thrombin sensor. The impetus for this design derived from the incorporation of quantum dots on molecular beacons[95] and a protein-based biosensor against maltose.[96] In a precursor to the method used by Tuleuova et al. for IFN-γ detection, the terminal end of the beacon was immobilized to the QD through biotin-streptavidin interactions, while two Eclipse

quenchers were conjugated to a complementary sequence against the aptamer. This method enabled adequate quenching as a result of the large number of quenching moieties present around a single QD donor. Without target present, the quencher-conjugated anti-aptamer sequence remained hybridized (Figure 1.28). Addition of target resulted in formation of the standard G-quadruplex, loss of the complementary sequence, and a 19-fold increase in fluorescence intensity. Selectivity of the anti-thrombin aptamer was determined against lysozyme, another commonly encountered enzyme in biological systems.

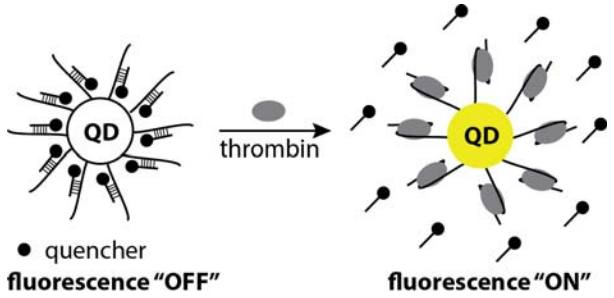

Figure 1.28. The targeting principle of the first quantum dot thrombin MAB.

Despite the significant brightness of QDs, typical detection limits for MABs hover in the nanomolar range. An approach to improve sensitivity includes the introduction of reflective photonic crystals that enhance signal intensity within a certain engineered wavelength range. Photonic crystals are materials that change the optical properties of incident light and create a forbidden gap in the photonic band structure.[97] Generally, photonic crystals have been applied to inks, paints, and coatings on mirrors and lenses. Wang et al. designed a QD-aptamer sensor for thrombin by combining the technology of photonic crystals with a quenched QD-MAB.[98] Their strategy depended on the recovery fluorescence signal in comparison to maximum and minimum values that were measured before and after the addition of an aptamer-specific quencher probe. Briefly, QD 605-aptamer was immobilized onto a photonic crystal surface through amine/diisothiocynate chemistry (maximum signal). Then, a complementary sequence functionalized with a terminal Iowa black

quencher was allowed to hybridize to the aptamer, resulting in FRET quenching (minimum signal). In the presence of thrombin, the fluorescent signal was recovered due to displacement of the quencher probe under equilibrium conditions (Figure 1.29). The resulting detection limit of 3.8 pM was dramatically lower than previous attempts without photonic crystal enhancement and was mainly the result of an improved signal-to-noise ratio.

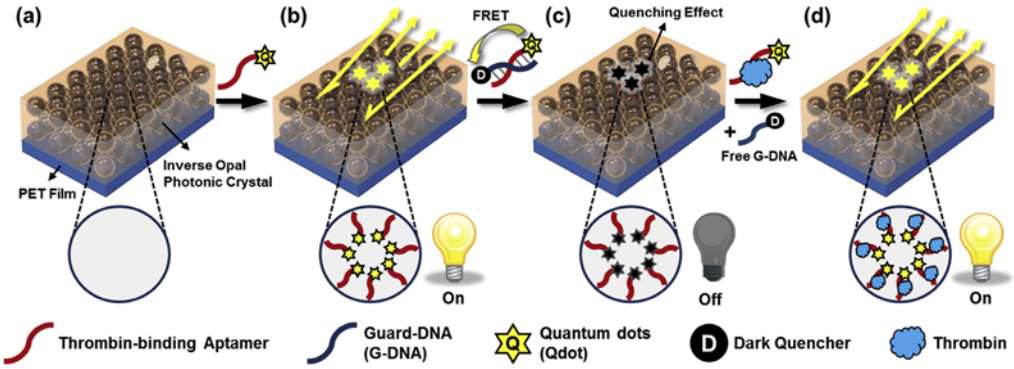

Figure 1.29. The incorporation of an anti-thrombin MAB in photonic crystals to increase sensitivity.

Disadvantages to the use of anti-aptamer complementary sequences containing signaling moieties include the need for removing excess, non-hybridized label as well as the possibility of false-positive signals in the presence of endogenous complementary sequence. These drawbacks can be eliminated through the use of one-piece MABs that incorporate intercalating dyes. For example, Chi et al. developed a thrombin detection platform using the DNA intercalating dye 1,1′-(4,4,7,7-tetramethyl-4,7-diazaundecamethylene)-bis-4-[3-methyl-2,3-dihydro-(benzo-1,3-thiazole)-2-methylidene]-pyridinium tetraiodide (BOBO-3) and an anti-thrombin aptamer attached to a carboxyl-functionalized QD 565 using a primary amine and EDC/NHS chemistry.[99] BOBO-3 intercalated into the double-stranded stem portion of the beacon and became a FRET acceptor of the QD emission in the absence of target. When thrombin was present, the quadruplex form of the aptamer resulted in release of BOBO-3 and direct QD emission,

with a corresponding detection limit of around 1 nM. After comparing three thrombin-binding aptamers on the same platform, the final version incorporated the aptamer sequence that was shown to select against BSA while providing the most rapid response to analyte.

Mucin 1 (Muc1), an overexpressed glycoprotein on the surface of cancer cells, was another target of an almost identical system subsequently developed by the Hah lab.[100] As demonstrated previously by Chi et al., BOBO-3 was intercalated into the intact stem of an aptamer beacon directly immobilized on QD 565. This anti-Muc1 aptamer allowed FRET from the QD to BOBO-3 in the absence of target, while target binding led to release of BOBO-3 and loss of FRET signaling (Figure 1.30). Quantitation of the Muc1 protein could be obtained to a detection limit of 50 nM over three orders of magnitude. However, the overall decrease in FRET signal upon target binding only ranged from 10-60%, with a FRET efficiency of only approximately 40%. This likely resulted from the significant distance between FRET partners and highlighted the need for an approach that reduced this gap.

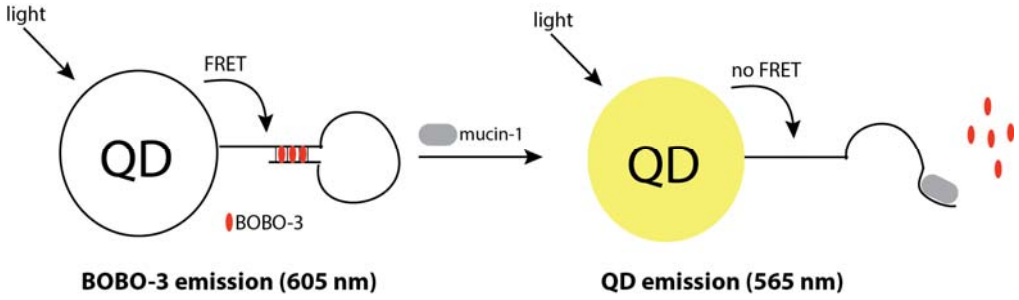

Figure 1.30. Development of a QD-MAB using the intercalating dye BOBO-3.

The solution came in the form of a biaptameric detection system for thrombin developed by Lao et al.[101] that used two of the aptamer sequences vetted by Chi et al.[99] For this, a non-signaling aptamer beacon was attached directly to QD 565 while a second aptamer beacon containing the intercalating dye YOYO-3 in its stem was free in solution. This

design improved overall sensitivity compared to the previous design[99] that incorporated FRET emission in the absence of target. As these two aptamer sequences were designed to bind different epitopes of thrombin, a binding event generated a sandwich structure at the QD surface, causing translocation of positively-charged YOYO-3 to the surface of the negatively-charged QD (Figure 1.31). QD emission was then transferred via FRET to YOYO-3. Because this system uses FRET signaling rather than direct measurements of a fluorescent molecule, this design needs no optimization and is therefore very modular. A drawback to this method is the requirement for multiple aptamer sequences against a single target – restricting its use to proteins or other large molecules.

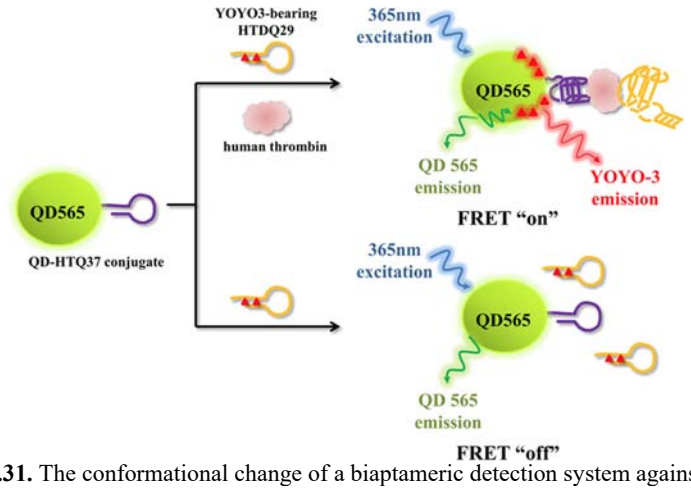

Figure 1.31. The conformational change of a biaptameric detection system against thrombin, using the intercalating dye YOYO-3. {Reprinted with permission from ACS Appl. Mater. Interfaces 2016, 8, 19, 12048-12055}. Copyright {2016} American Chemical Society.

Another approach to mitigate concern about quenching efficiency is the use of QD-aptamer beacon conjugates as combination imaging/delivery constructs. For example, Bagalkot et al. designed a MAB against prostate-specific membrane antigen PSMA[102] that also served as a carrier for the anti-cancer drug doxorubicin (Dox). Because of the inherent fluorescence of Dox, a natural intercalating agent, uptake of the delivery/signaling complex resulted in intracellular release of Dox, which could be visualized through confocal microscopy. Prior to release, Dox acted as both a quencher of QD 490 emission as well as

a self-quencher when intercalated into the A10 RNA aptamer, rendering the entire construct "dark" until cargo release (Figure 1.32). As a dual-function construct, simultaneous prostate cancer cell imaging and therapy were possible. Selectivity of this conjugate was tested against PSMA-negative PC3 prostate adenocarcinoma cells, and after a 90 min incubation period, fluorescence was shown to increase only in PSMA-expressing LNCaP cells. Moreover, cytoxicity testing indicated that inclusion of Dox within the imaging construct led to selective cell death among PSMA-positive cells even though free Dox was highly toxic regardless of PSMA expression. This work was the first demonstration of a "theranostic" device incorporating a MAB.

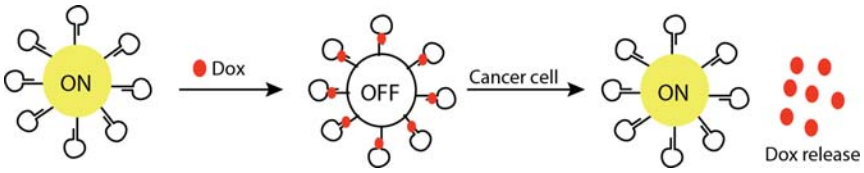

Figure 1.32. Schematic of an anti-PSMA MAB construct. The fluorescence intensity increased when Dox intercalated into the GC section of the MAB while increasing upon binding of the cancer cells, with subsequent release of Dox.

1.6.3 Carbon nanostructures, graphene oxide, and carbon nanotubes

Some of the most commonly used carbon nanostructures for analytical methods consist of single-walled carbon nanotubes (SWCNs), graphene oxide (GO), and carbon quantum dots (CQDs). Carbon nanostructures have been shown to be efficient fluorescent quenchers and can be attached to oligonucleotides with relative ease. Due to π-π interactions between individual oligonucleotides and the graphene rings of the carbon nanostructures, oligonucleotides can be non-covalently attached to the carbon nanostructures in order to act as energy acceptors. There are several groups that have leveraged this interaction to develop carbon-quenched beacon structures, and GO is a common example that demonstrates a high quenching efficiency stemming from relatively strong absorption of single-stranded nucleic acid. This strategy relies on adsorption of the single-stranded loop

region of a beacon onto the GO surface. Target binding interrupts the GO/nucleic acid intermolecular associations and releases the aptamer beacon to the solution – restoring the fluorescence signal (Figure 1.33).

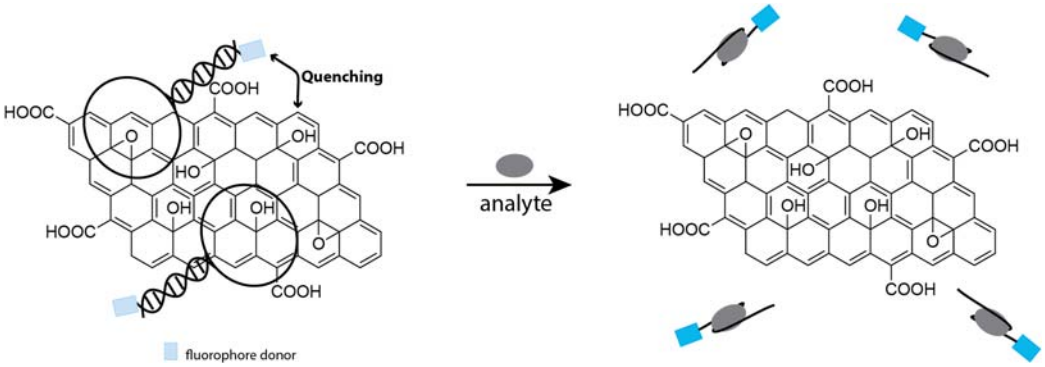

Figure 1.33. The working principle of MAB when GO is used as quencher.

As a proof of concept, Dong et al.[103] repurposed a QD-graphene oxide MB as an aptamer probe to detect thrombin. For this, the QDs were coupled with the anti-thrombin MAB using mercaptoacetic acid-capped CdTe QDs and EDC reagent. After addition of GO suspension to the QDs-MAB solution, the fluorescence intensity decreased more than 90% and was recovered in a dose-dependent manner upon addition of thrombin. Additionally, the fluorescence intensity exhibited a linear increase upon increasing the target concentration that demonstrated the high quenching efficiency of this construct.

Simultaneously, another group designed a MAB/GO platform for real-time detection in living cells. Wang et al. took advantage of the several studies that have analyzed the sequence and conformation of anti-ATP aptamers[104] to develop an anti-ATP MAB. Labeling with 6-FAM demonstrated that high fluorescence quenching efficiency was possible in the absence of ATP molecules. The fluorescence recovery was almost 90% in the presence of ATP, and the detection system was shown to be highly selective. Subsequently, this system was tested in murine epithelial cells, with results that mirrored the *in vitro* work. Additionally, it was demonstrated that the GO was not only the vehicle

for cellular entry of the MAB but also protected the MAB from intracellular enzymatic cleavage.

On the other hand, Chen et al.[105] has argued that although graphene oxide is a good luminescence quencher, it still suffers in real-world systems from drawbacks such as relatively long assay times, synthetic complexity, and poor detection limits. They reasoned that these drawbacks can be caused by either the insulating nature of GO that limits electron transfer efficiency or non-specific fouling of the GO surface in complex matrices. To address these issues, they doped the GO with nitrogen and sulfur to enhance electron transfer and generate more negative surface charge. With this strategy, they improved the existing MAB/GO quencher design and applied this system to the simultaneous detection of thrombin and IgE using QD 525 and QD 623 as fluorescence donors. The introduction of heteroatoms into the GO structure improved quenching efficiency to less than 10% of the fluorescence maximum and reduced the assay time to less than 1 min.

Another method that has been investigated to help address the aforementioned disadvantages is termed long-range resonance energy transfer (LrRET), a phenomenon that sees a change in the distance dependence of resonance transfer and can lead to reduced background signal and improved sensitivity. The Huang lab reported a comparison between a standard fluorophore/quencher-labeled MAB and a MAB labeled only with a fluorescence dye but suspended in solution with multi-walled carbon nanotubes (MWCNT).[106] In this system, both aptamers required a non-functionalized, antisense aptamer sequence for intercalation of ATP (Figure 1.34). Prior to target exposure, both aptamers were quenched by surface associations with the MWCNT, but the presence of ATP resulted in the formation of an aptamer/complement duplex structure that was

released from the wall of MWCNTs to allow recovery of the fluorescence emission. There was no fluorescence enhancement in the presence of other nucleoside triphosphates. The quenching efficiency of the MWCNTs was 99% with a 10-fold increase in signal-to-noise ratio over a standard aptamer beacon using a terminal fluorophore/quencher system. Additionally, the limit of detection, at 0.5 μM, was slightly better than existing methods. The main advantages of this platform were the enhanced signal-to-noise ratio and quenching efficiency that resulted from the use of LrRET quenching by MWCNTs – demonstrating the potential for these unique RET acceptors in other aptamer beacons systems.

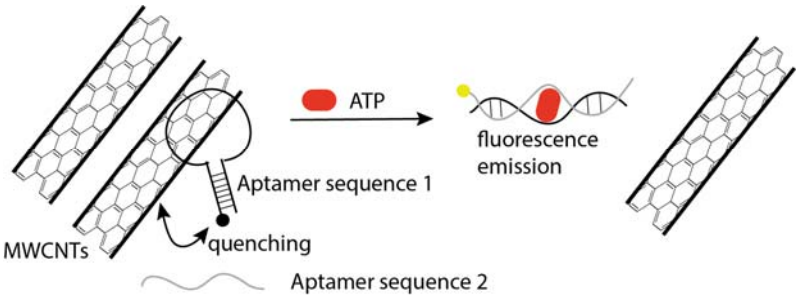

Figure 1.34. LrRET-based MAB. Fluorescence intensity of the anti-ATP MAB increased when the beacon was released from the MWCNTs.

A similar strategy was employed by He et al.,[107] where the quenching efficiency of DABCYL in a traditional aptamer beacon format was directly compared with graphene oxide quenching of an identical aptamer sequence without direct quencher attachment. As with MWCNTs, the quenching efficiency was robust (98%) and generated almost 100-fold improvements in detection limit and dynamic range when compared to the standard MAB configuration. Besides its high specificity against other ATP analogues, this probe could detect ATP in cancer cell lysate with high sensitivity and a showed a detection limit of 2 μM in buffer. This and Wang et al's studies[104] demonstrated that GO/MAB systems can

successfully be used in homogeneous plate assays as well as for real-time, *in vitro* cell analysis of ATP concentrations.

An essentially identical strategy was employed for the detection of cellular prion protein (PrP).[108] This study used an anti-PrP aptamer sequence functionalized with a TAMRA fluorophore and showed ~97% quenching efficiency GO. Upon PrP binding, the MAB showed increase in the fluorescence intensity, with a detection limit of 309 ng/mL and an approximately equivalent signal-to-noise ratio as seen with MWCNTs.

1.6.4 Metallic nanoparticles

Gold nanoparticles (AuNPs) are the subject of substantial research, with many potential applications being developed for use in imaging, diagnostics, therapeutics, etc. Their properties are governed by their size and shape – attributes that can be controlled during synthesis to generate highly precise, tuned structures for a specific application. By careful tuning, they can exhibit extremely high quenching efficiencies, with some studies demonstrating better than 100X the quenching efficiency of DABCYL under certain conditions.[109]

As bare AuNPs precipitate rapidly in high-salt environments, they are typically coated completely with nucleic acid to avoid interaction. This can be advantageous for assay development, as the functionalized AuNPs appear to form a unique environment within the interstitial space of the oligonucleotide monolayer that can enhance hybridization efficiency and reduce nuclease cleavage within the monolayer.[110] A novel adaptation of aptamer-functionalized AuNPs, developed by Chad Mirkin's lab, capitalized on these advantages in the form of a "nano-flare" composed of a AuNP core and decorated with anti-ATP switchable aptamer sequences.[111] This probe consisted of a central 13 nm AuNP

that was densely coated with thiolated aptamers. The aptamer was hybridized with an antisense reporter sequence containing a Cy5 fluorophore that, in the absence of target, remained hybridized to the aptamer and quenched by the AuNP. Conversely, ATP binding disrupted hybridization of the reporter strand due to conformational switching of the aptamer sequence, leading to a dose-dependent increase in fluorescence emission as the reporter strand diffused away (Figure 1.35). Following *in vitro* studies of sensitivity and specificity, the aptamer gold nanoflares were applied *in situ* using Hela cells to demonstrate cell permeability of the construct and subsequent detection using flow cytometry.

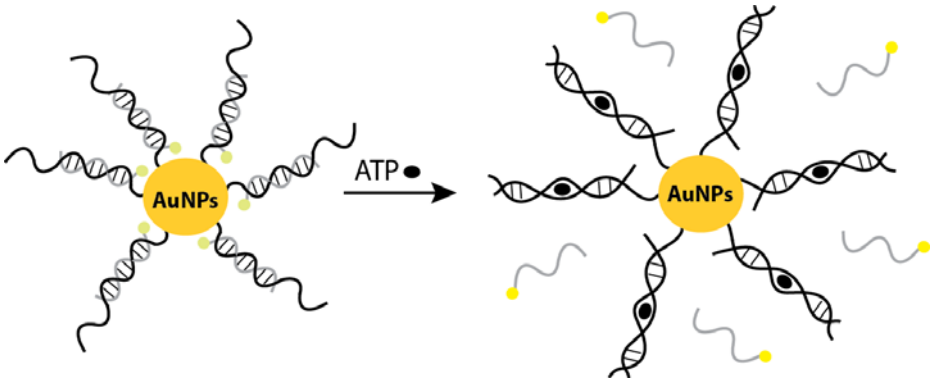

Figure 1.35. Aptamer gold nano-flares decorated with thiol-terminated aptamer sequences hybridized to Cy5-complementary sequence. ATP target changes the conformation of the aptamer and releases the fluorescent complementary sequence.

Given the utility of a self-contained signaling system, a similar approach was followed by Zhang et al. for the detection of urinary adenosine (Ade).[112] In this method, the respective roles of the aptamer and antisense reporter were reshuffled, and the aptamer sequence became both the recognition domain and the reporter. For this, a short, thiolated antisense sequence to the aptamer was immobilized on the AuNP, while the 6-FAM-labeled aptamer sequence was hybridized to the antisense sequence and quenched by FRET with the gold surface. The presence of Ade led to conformational change of the MAB sequence for release of the aptamer and restoration of fluorescence intensity (Figure 1.36). In addition, this platform had almost 10-fold selectivity for adenosine over the remaining nucleobases,

and the AuNPs were shown to provide a 10% higher quenching efficiency over the universal quencher, DABCYL. This method was applied to human urine samples from patients with lung cancer and showed comparable results to an HPLC method.

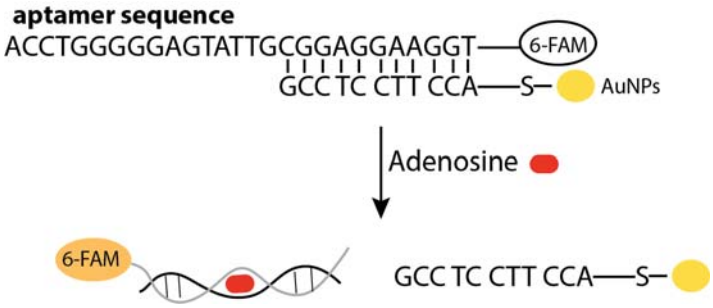

Figure 1.36. Schematic of a MAB against urinary adenosine. Upon adenosine binding, the MAB changed its conformation, resulting in the release of the fluorescent oligonucleotide sequence and increased fluorescence intensity.

A significant difficulty in using nanoparticle (or really any) MAB is tailoring the stem region to provide the optimum balance between retention of closed-loop structure in the absence of target while maintaining sufficient sensitivity and selectivity when operational. An additional optimization was identified by Armstrong and Strouse when questioning the placement of the aptamer sequence within the beacon.[113] Using 3′ AuNPs to quench the fluorescence of a 5′ 6-FAM, they evaluated how the target binding affinity of identical aptamer beacon sequences was affected by their relative positions. They evaluated five aptamer locations within the beacon, ranging from completely single-stranded as part of the loop to mostly double-stranded, and found that binding affinity decreased with increasing double-stranded character. This would indicate that competition between target binding and hybridization allows a more dynamic response to the presence of target and, while not necessarily intuitive, actually provided substantial improvements in dynamic range. Their primary goal, however, was to demonstrate the ability to tailor MABs for an ideal target concentration range without changing the aptamer or stem sequence. When comparing the detection range for the single-stranded and double-stranded aptamers, they

demonstrated that the aptamer with exclusively single-stranded character had a detection range that was shifted by approximately five orders of magnitude lower than the almost exclusively double-stranded aptamer. The other three aptamer locations showed varying dynamic ranges that were framed by these extremes. This indicated that MAB designs using identical aptamers could be applied to a diverse range of target environments without requiring T_m-altering changes to the MAB sequence or affecting the aptamer selectivity.

Although commonly employed as quenchers due to their electronic properties, metal nanoparticles also can be tuned to act as luminescence donors. While the synthetic tolerances are more demanding, success in generating nanoparticles with diameters approximating Fermi wavelengths generates metal nanoparticles that exhibit discrete energy levels mirroring molecular orbital transitions.[114] By relying on sequence-dependent assembly of small-scale nanoclusters, Liu et al. developed the first "activatable silver nanoclusters beacon (ASNCB)" probe that contained variations of a 5′ DNA scaffold sequence, allowing assembly of silver nanoparticles into three discrete nanocrystals (Ag NCs) with unique emission properties.[115] In the case of the aptamer complexes, ATP and thrombin were the proof-of-concept targets. They were designed with an aptamer sequence against either ATP or thrombin and a terminal stem region containing a BHQ-1 or BHQ-2 at the 3′ end. In the presence of target, the MAB stem was forced open to separate the NCs from the quencher and generate a fluorescence signal. The authors also imaged ATP in real time using MCF-7 cancer cells and confocal microscopy. These novel AgNC MABs demonstrated the capability of real-time, multiplexed detection using a synthetically-simplistic beacon design that avoided covalent conjugation of a fluorescence reporter.

Despite their derivation as specialized molecular beacons, aptamer beacons have proven capable of filling a wide range of applications that include the traditional duties of real-time detection and imaging that were pioneered by MBs as well as a completely new role that merges a self-contained signaling construct with antibody-like selective recognition of an immense variety of stationary or mobile target molecules. The assay formats to which these aptamer beacons can be applied is almost as diverse as their targets, and the choice of terminal signaling moieties can be assay, target, or matrix dependent. We have seen the variety of signaling constructs that have been developed to address specific conditions or requirements, and the continuing improvement of existing nanomaterials along with the development of new ones will likely open frontiers that had been previously inaccessible to traditional beacons. Repurposing existing technology for use in beacons is also ongoing, with reporters such as bioluminescence proteins providing higher sensitivity and better signal-to-noise ratios than fluorescent dyes in a standard MB.[116,117] Although the most significant challenge to the broad incorporation of MAB technology is the tendency for *in vivo* aptamer beacon degradation in circulation, new aptamers that incorporate synthetic mimics of nucleic acids such as peptide nucleic acids (PNAs)[118] and locked nucleic acids (LNAs)[119] can be constructed. Continued development of more robust MABs should lead to significant improvements in the early detection of severe diseases, and further incorporation of these beacons into "theranostic" platforms could provide new ways to target specific cell types, real-time tracking of therapeutic efficacy, and better outcomes during the treatment of aggressive diseases.

Chapter 2

Bioorthogonal Protein Conjugation: Application to the Development of a Highly Sensitive Bioluminescent Immunoassay for the Detection of Interferon-γ[1,2]

Overview

Bioorthogonal conjugation eliminates the shortcomings of classical conjugation methods. The conjugation of antibodies to reporter proteins, such as bioluminescent protein, can be controlled with orthogonal conjugation methods. Here we report a bioluminescent immunoassay for the sensitive detection of interferon-γ (IFN-γ) that utilizes orthogonal conjugation of bioluminescent protein, *Gaussia* luciferase to anti-IFN-γ antibody. The IFN-γ is produced by the immune system and the detection of the IFN-γ is pivotal for the detection of persistent viral and bacterial infections. A bioorthogonal conjugation approach is used to conjugate an anti-IFN-γ antibody with a GLuc mutant containing the N-terminal tyrosine using formylbenzene diazonium hexafluorophosphate reagent (FBDP) in hydrophilic mild pH environment yielding high conjugation efficiency (60%). This reagent is shown to be specific for tyrosine (Tyr) residues. Therefore, conjugation through Tyr was orthogonal and not detrimental to the bioluminescence activity of GLuc. The immunoassay described in this paper is a sandwich type assay and involves a capture and a detection antibody. The assay was validated for its robustness, precision, accuracy, limit of detection, and recovery.

[1] A. Moutsiopoulou et al. Bioconjugate Chem., 2017, 28, 1749–1757
[2] The original Supplementary Information to the article has been included as Methods on page 65

2.1 Preface

Reporter-labeled antibodies are commonly prepared for use in a variety of applications including immunoassays,[120] in-situ binding assays,[121] imaging,[122] diagnosis,[123] targeted therapy,[124] and drug delivery.[125] Reporters that are most commonly conjugated to antibodies are fluorescent dyes,[126] and proteins, such as enzymes,[127] fluorescent proteins,[128] and bioluminescent proteins.[129] Although the fluorescent dyes are commonly employed as reporters, they usually lack the required sensitivity. In order to achieve high sensitivity, labels such as enzymes or bioluminescent proteins are commonly employed.[130] Bioluminescence-based immunoassays have shown exquisite sensitivity and ease of use in complex matrices since the background associated with the bioluminescent detection is very low.[131] This makes bioluminescent protein an attractive reporter for conjugating to antibodies.[132]

Thus far, bioluminescent proteins are conjugated to antibodies using specific and non-specific chemical methods and genetic fusion, if the gene sequence for the antibody is available.[133-135] Non-specific chemical conjugation can result in heterogeneous conjugates that can lead to loss of the functional property of the antibody as well as the bioluminescent reporter. In general specific conjugation of bioluminescent proteins to antibodies is also a significant challenge due to the unavailability of unique amino acids with appropriate chemical functionality necessary for conjugation, which necessitates protein engineering to introduce unique cysteines if not detrimental to protein activity.[129,136,137] Further, a few important criteria to be considered while designing protein reporter-antibody conjugation include maintaining the structural and functional integrity of the biomolecules involved, reproducibility of the conjugation, control of biomolecule conjugation ratio, stability of the

conjugates, ability to perform reaction in hydrophilic environments, etc. Many different orthogonal bioconjugation methods with superior performance over the traditional conjugation method have been developed that involve the use of less common amino acid residues.[138,139] However, these methods have not been used for conjugating bioluminescent proteins to antibodies. Among the orthogonal conjugation methodologies, modification of the tyrosine (Tyr) residue is gaining popularity among researchers since they appear with intermediate frequency in a protein, and chemical reactivity of the Tyr phenol ring provides for several diverse reactions. The types of reactions performed with the Tyr residue can be varied according to the reaction conditions. For example, under basic conditions, the phenol ring provides a proton for the O-acylation of the Tyr.[32] On the other hand, an ene-type reaction at an aromatic carbon can occur under acidic conditions.[32] Several groups have performed a Mannich-type reaction modifying the *ortho* position of the phenol of the Tyr[140] in a peptide for the purpose of the bioconjugation of the peptide to poly(ethylene glycol).[36] The Barbas group developed an orthogonal method for specific labeling of Tyr residues.[32,33] Additionally, the Barbas group introduced a stable diazonium salt, the formylbenzene diazonium hexafluorophosphate (FBDP) for the modification of the Tyr residues. This diazonium salt provides bioorthogonal aldehyde functionality and reacts specifically with the *ortho* position of the phenol group of the Tyr residue.[37] Francis and co-workers also used the diazonium-coupling reactions with the most accessible Tyr residue to modify the interior of a bacteriophage.[35] The most outstanding feature for the diazonium-coupling reaction is that it occurs in an aqueous solution, near neutral pH and at room temperature.[37]

We have employed the orthogonal Tyr labeling strategy described above for the conjugation of a mutant of the bioluminescent protein, *Gaussia* luciferase (GLuc) to an interferon-γ (IFN-γ) antibody and employed this reporter-labeled antibody in the development of a highly sensitive bioluminescent immunoassay. GLuc, originally isolated from copepod, *Gaussia princeps,* has been used by many groups as the bioluminescent reporter of choice.[141,142] In general, GLuc is one of the smallest known bioluminescent proteins consisting of 185 amino acids with a molecular weight of 19.9 kDa.[143] Upon addition of its substrate, coelenterazine, GLuc emits a blue light with an emission maximum at 480 nm and is one of the brightest coelenterazine-dependent bioluminescent proteins.[144] Bright bioluminescence emission and high sensitivity that can be achieved using GLuc as a label in an antibody-based sensing has not been exploited to the fullest yet. Additionally, the chemical reaction between GLuc and its substrate does not require any cofactors such as ATP or calcium ions. Lastly, this protein has four cysteine residues that improve its thermostability and hence conjugation through the cysteine could be detrimental to its stability.[144,145] In previous work, we have introduced a Tyr residue on GLuc creating a mutant termed GLucY containing Tyr at an easily accessible location which can be chemically modified to develop bioanalytical applications.[146] This GLuc mutant contains only one other Tyr that is embedded inside the protein structure and hence not easily accessible for conjugation. Therefore, this GLuc mutant is an ideal candidate to study bioorthogonal conjugation through Tyr for selective conjugation to an antibody. In order to perform the chemical conjugation through the N-terminal Tyr residue of the GLuc mutant, the stable diazonium salt, FBDP, was synthesized as per the literature reported method.[37] FBDP provides aldehyde functionality on the Tyr residue of GLuc, which under

slightly acidic conditions reacts with a hydrazine group introduced on the antibody through the sulfo-succinimidyl-6-hydrazino-nicotinamide (sulfo-S-Hynic) and amine reaction.

Here, as a proof of concept for the applicability of the Tyr-based bioconjugation methodology, we have developed a bioluminescent immunoassay to detect the antigen, IFN- γ. The IFN-γ is produced by the immune system as a response to a bacterial and viral infection. A continuous production of the IFN-γ along with other inflammatory cytokines is triggered in order to activate the immune system when challenged by an infecting virus, such as HIV[147]. As such IFN-γ is an important biomarker for monitoring infections.

2.2 Discussion

In this chapter, we demonstrate the applicability of the Tyr-based bioconjugation methodology and show that the orthogonal conjugation method provides for a facile conjugation of bioluminescent protein to antibody. The conjugate prepared was employed in the development of a bioluminescent sandwich-type immunoassay to detect the antigen, IFN- γ.

2.2.1 Reporter, GLucY Protein Expression and Purification

For our work, we use GLucY, a mutant of GLuc, containing a Tyr residue at the N-terminus, which was previously prepared in our laboratory.[146] The Tyr residue on GLucY provides a phenol moiety that can be used specifically for bioconjugation. The most important consideration for conjugation through the Tyr residues is that they are much less common than lysine residues. Therefore, if we introduce Tyr at a site away from the active site of the protein its modification is less likely to cause a detrimental effect on the activity of the protein. The protein GLucY was expressed and purified, in high concentration, from

the soluble fraction of an *E. coli* culture (Origami™ 2 strain).[146] This method yielded about 15–20 mg purified protein per liter of culture, using immobilized-metal affinity chromatography (IMAC) following cell lysis. The calculated molecular weight for GLucY was ~22.1 kDa when analyzed by SDS-PAGE (Figure 2.1).

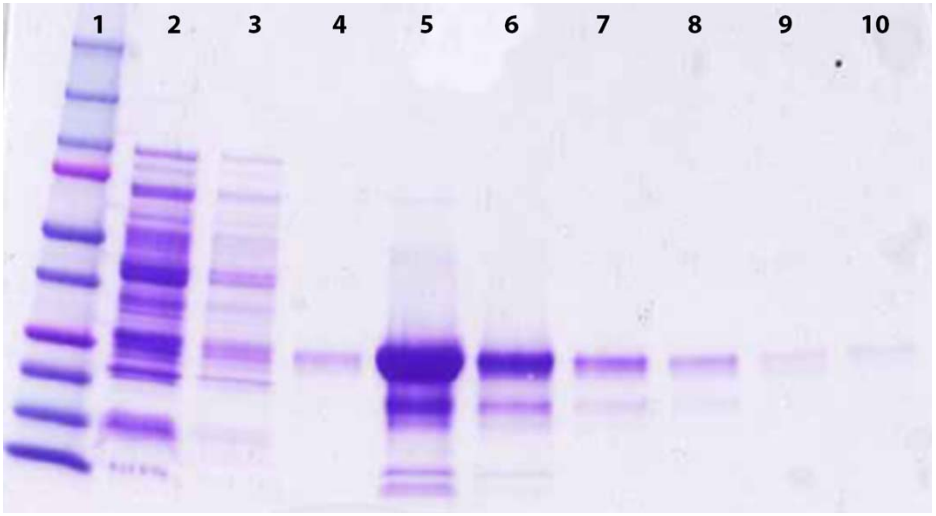

Figure 2.1. Purification of GLucY from Origami™ 2 Express E. coli. Lanes 1) Precision Plus Protein™ Dual Color Standard; 2) flowthrough; 3) lysis buffer wash; 4) wash buffer wash; 5–10) elution fractions. The purified band was calculated to have a molecular weight of 22.1 kDa.

2.2.2 Conjugation of GLucY to Antibody Using Conventional method

As a comparison, we performed chemical conjugation of GLucY to antibody using a commonly used glutaraldehyde-based method. For that, we followed a standard published protocol used for antibody conjugation without optimizing it.[134] The GLucY-antibody conjugation was confirmed using Western blot (Figure 2.2). However, the conjugate did not retain any bioluminescence activity of GLucY and hence we did not employ this conjugate for immunoassay development. This loss of activity potentially could be due to the overconjugation of GLucY or the steric crowding of the GLucY active sites by the IFN-γ antibody. This could be avoided by further optimizing the protocol; nevertheless, this study points to the difficulty when conjugation is performed through non-specific methods.

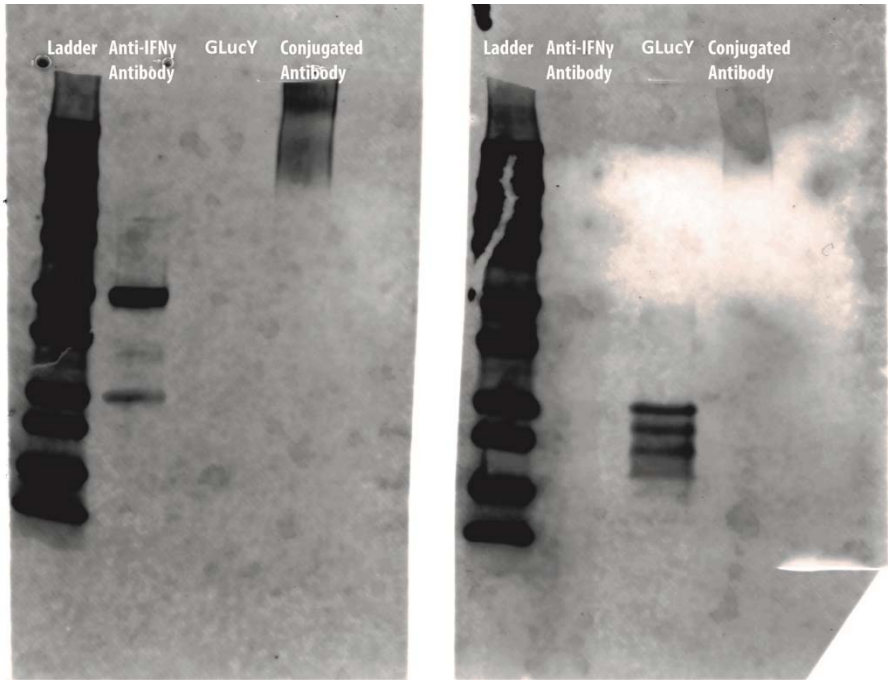

Figure 2.2. Western blot analysis of the conventional bioconjugation of the anti-human IFN-γ with the GLucY using two different antibodies. A) Membrane is probed with anti-mouse secondary antibody reactive towards anti-human IFN-γ antibody B) Membrane is probed with primary antibody against GLuc.

2.2.3 Modification of GLucY Using FBDP

To perform conjugation through Tyr on GLucY, we chose the diazonium salt chemistry because it provides a more controllable conjugation reaction with the biomolecule. The diazonium salt, formylbenzene diazonium hexafluorophosphate (FBDP), has two major advantages; it can be easily synthesized and is stable. FBDP was synthesized according to the literature method[37] (Figure 2.3A) and the product was characterized with ^{1}H-NMR spectroscopy (data not shown). The diazonium salt, FBDP, provides a bioorthogonal aldehyde functionality that is at the *ortho position* to the phenol group on the Tyr residue, since the phenol moiety activates the *ortho* and the *para* positions for the electrophilic substitution reaction (Figure 2.3B). A secondary reaction can be performed with the aldehyde using the sulfo-S-Hynic modified biomolecule. Furthermore, the modification of the Tyr residue with the FBDP can be monitored based on a change in the electronic

absorption spectrum. The absorption spectrum between 250-450 nm shows a broad band around 350 nm (Figure 2.3C), which is absent in the spectra of unreacted GLucY and FBDP. Also, mass spectroscopy data (not shown) indicated a molecular weight increase that is consistent with the molecular weight of FBDP. After FBDP labeling, the protein was subjected to tryptic digestion followed by the mass spectroscopy analysis of the resulting peptides. This analysis showed that the diazonium salt reacts only with the Tyr residues and not with the amines of the lysine residues or the amino terminus. The extent of conjugation was calculated using an Aldehyde Quantification Assay Kit (Abcam, Cambridge, Massachusetts) according to the manufacturer's instructions. The results showed that approximately 60% of the GLucY was modified with FBDP. This is an efficient coupling reaction especially considering its regioselectivity, in which only one of the Tyr residue is preferentially modified with the FBDP. In order to check if the modification of the protein with FBDP has any detrimental effect on the bioluminescence activity of GLucY, several aliquots of GLucY were reacted with different mole ratios of FBDP. The results showed that the protein can be successfully modified with 1 equivalent of FBDP without detriment to its bioluminescence. For convenience, FBDP-modified GLucY will be referred to as GLucYFBDP in this manuscript.

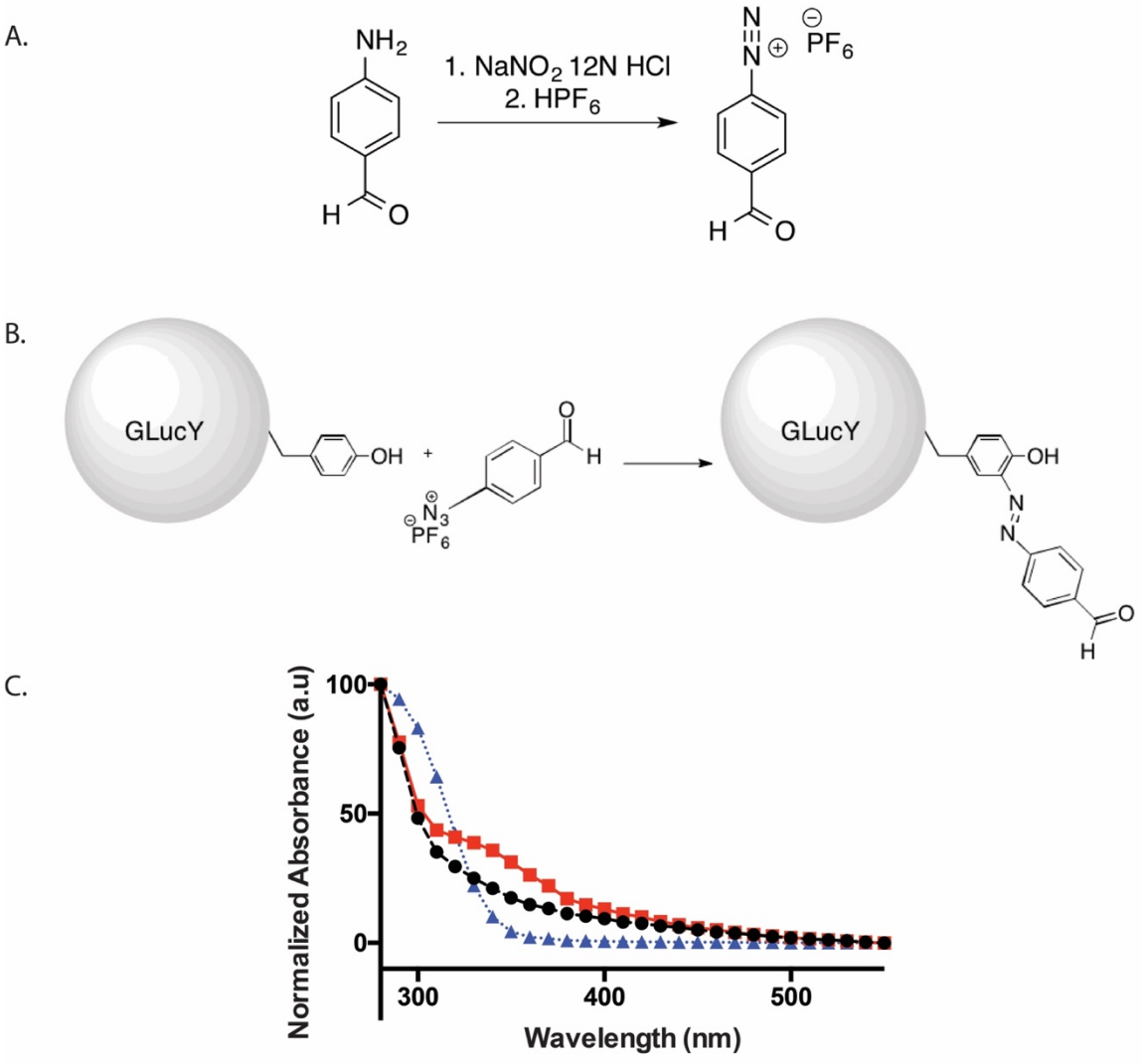

Figure 2.3. A) Synthesis of FBDP according to literature, B) Schematic of the chemical reaction of modification of the GLucY with FBDP (GLucYFBDP) and C) The absorbance spectra of GLucY, (●)GLucYFBDP (■), and FBDP (▲).

2.2.4 Conjugation of Anti-human Interferon-γ Antibody with GLucYFBDP

There are many chemicals, such as glutaraldehyde, that can be used to modify antibodies. Sulfo succinimidyl-6-hydrazino-nicotinamide (sulfo-S-Hynic) is a crosslinker that reacts with the amines of lysines present on the antibodies at physiological pH (Figure 2.4). By optimizing the stoichiometry, the reaction between the mouse anti-human interferon-γ antibody with the sulfo-S-Hynic can be controlled so that about 2-3 lysines would be

modified with hydrazinonicotinic acid (Hynic) moieties. This ratio allowed us to preserve the function of the antibody. Also, by controlling the number of Hynic moieties, we can control the number of GLucY that are conjugated to the antibody in order to optimize the sensitivity of the system.

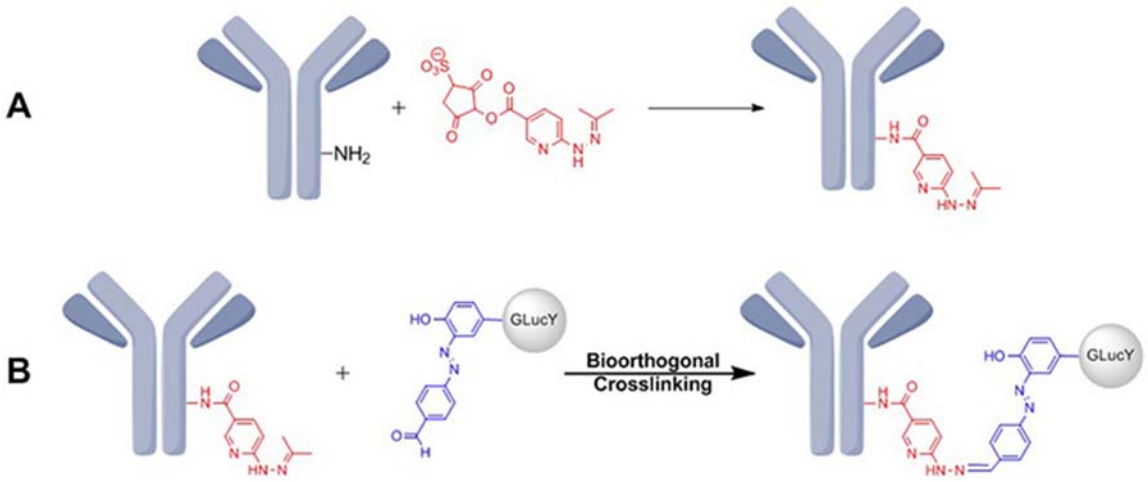

Figure 2.4. A) Modification of anti-IFN-γ antibody with sulfo succinimidyl-6-hydrazino-nicotinamide (sulfo-S-Hynic), B) Bioorthogonal conjugation of anti-IFN-γ antibody with GLucY.

The commercially available mouse anti-human IFN-γ antibody was modified with sulfo-S-Hynic according to the manufacturer's instructions. The stoichiometry of the reaction was adjusted so that the final product would have about 2-3 Hynic moieties per antibody. Then, Hynic-modified antibody and the GLucYFBDP were mixed in the conjugation buffer and allowed to react overnight at 4 °C to give the GLuc-labeled antibody. This GLucY-anti-IFN-γ antibody conjugate is referred to as the detection antibody (dAb) for the remainder of the text. The final bioconjugation was confirmed by Western Blot analysis (Figure 3). We used two different antibodies to visualize the bands. A primary antibody that targets GLuc and an anti-mouse secondary antibody that binds modified mouse anti-human-IFN-γ primary antibody were employed. Both blots confirmed that the dAb was successfully synthesized, as there is a bright broad band higher than 100 kDa that can be

detected with both antibodies, indicating the presence of the GLucY as well as the anti-human-IFN-γ antibody (Figure 2.5). The presence of a broad smear is an indication of multiple different products of the conjugation of the detection antibody with the bioluminescent protein.

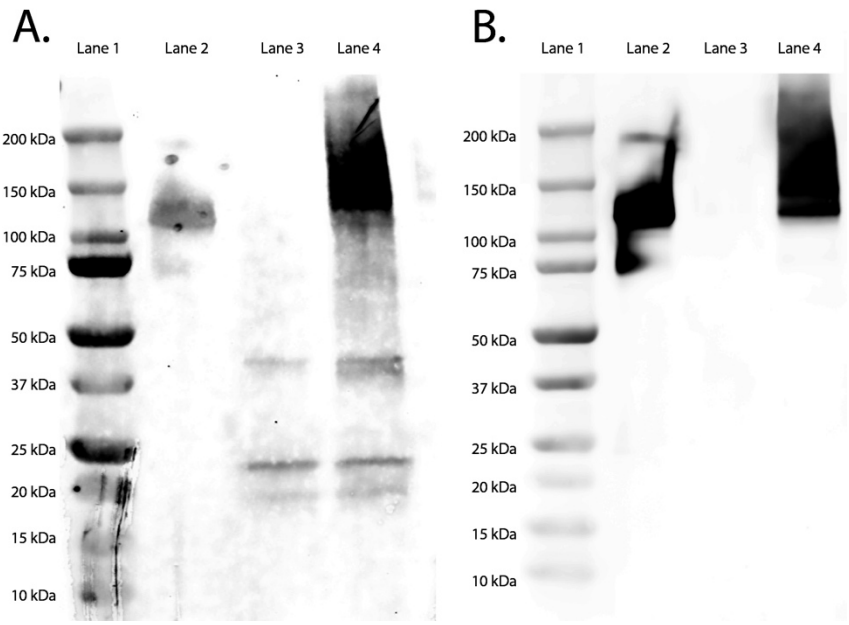

Figure 2.5. Western blot analysis of the bioconjugation of the anti-human IFN-γ with the GLucYFBDP using two different antibodies. A) Membrane is probed with primary antibody against GLuc B) Membrane is probed with anti-mouse secondary antibody reactive towards anti-human IFN-γ antibody. Lanes 1) Precision Plus Protein™ Dual Color Standard; 2) Commercial anti-human-IFN-γ primary antibody; 3) GLucYFBDP; 4) Detection antibody.

2.2.5 Development of the Immunoassay

The next step was to develop a bioluminescent immunoassay for the detection of IFN-γ. Our immunoassay is a sandwich type immunoassay and involves a capture antibody that binds human IFN-γ as well as a detection antibody against a different epitope of the IFN-γ. The immunoassay was developed in a Maxisorb polystyrene 96-well black plate. Each assay step was carefully studied under different conditions (Figure 2.6). Many variables were optimized to achieve the lowest limit of detection (LOD) of the antigen. The

parameters that were optimized are the incubation time, incubation temperature, concentration of the capture antibody, concentration of the detection antibody, the incubation time of the antigen, and the effect of several commercially available blocking buffers for an efficient blocking step (Figure 2.6).

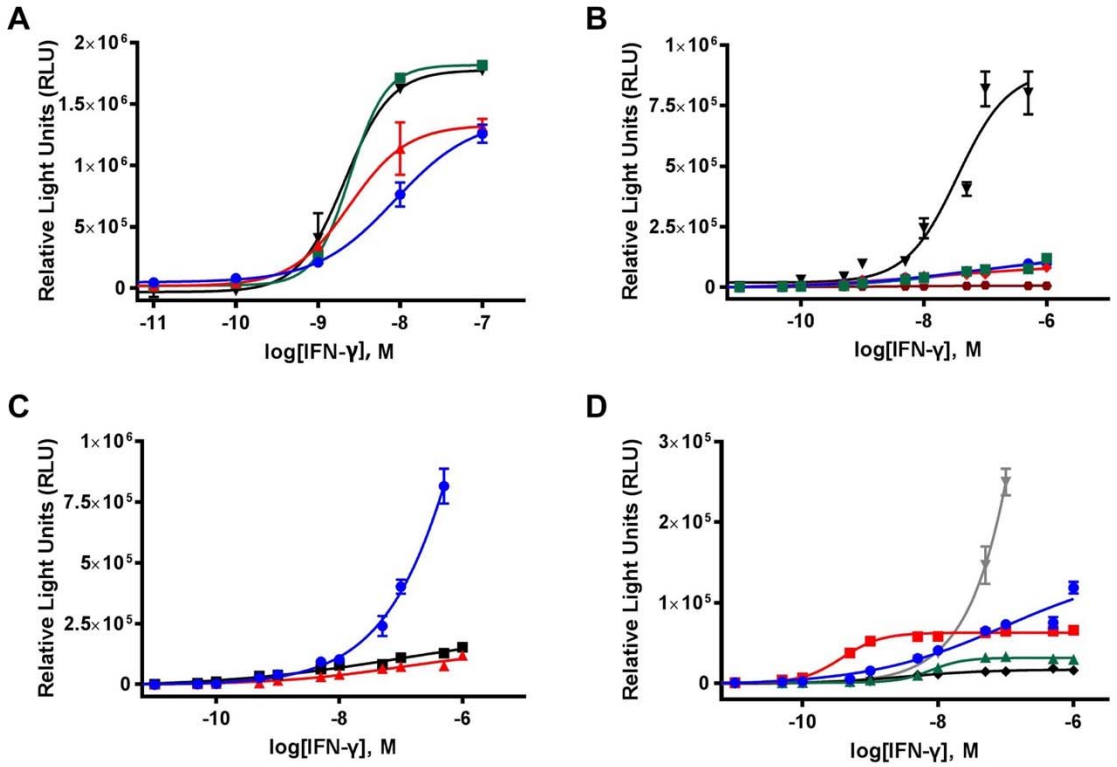

Figure 2.6. Optimization parameters of the immunoassay. A) Concentration of capture antibody ●0.5 µg/mL, ▲1.0 µg/mL, ■5.0 µg/mL, and ▼10.0 µg/mL B) Incubation time of detection antibody ■45 min, ◆ 90 min, ● 1 hour, ▲ 2 hours, ▼ 3 hours, and ●overnight C) Incubation time of IFN-γ ●1 hour, ▲2 hours, and ■3 hours D) Different commercial blocking buffers ●Starting blocking buffer, ■BLOTTO blocking buffer, ▲Sea Block buffer, ◆SuperBlock blocking buffer and ▼Protein-Free blocking buffer. All points are the mean of three measurements ± one standard deviation. Error bars that are not visible are obstructed by the data point.

The details of each optimization step are discussed in the materials and methods. The following time points were selected because they generated the lowest LOD for the assay. Also, the 2 h incubation time of IFN-γ resulted in much higher day-to-day consistency of the results. The optimization studies resulted in the following ideal immunoassay conditions. The wells of the plate were coated with the capture antibody (100 µL of 1.0

µg/mL concentration) followed by an overnight blocking step using a commercially available blocking buffer (StartingBlock™ (PBS) Blocking Buffer, Thermo Scientific Cat#37539, Waltham, MA). Next, several different dilutions of the antigen were incubated for 2 h at room temperature followed by a wash step and the incubation of the detection antibody at a concentration of 2.0 µg/mL at room temperature for 45 min. Following another wash step, the bioluminescence emission was monitored by adding 2 μg/mL of the substrate coelenterazine. Using the bioluminescence emission intensity, a calibration curve was generated and a non-linear dose-response curve was fitted to the data points using GraphPad Prism software (Figure 2.7). After these optimization parameters we concluded that the lowest limit of detection of the immunoassay was found to be $5.0X10^{-12}$ M, which is similar with the commercially available IFN-γ immunoassay (Biolegend, Cat#430104, San Diego, CA) with a detection limit of $2.4X10^{-12}$ M. The limit of detection was interpolated from the GraphPad Prism software using the formula $LOD=S_B + 3xSD_B$ where S_B and SD_B are the mean and the standard deviation of the blank signals, respectively. The range of the calibration curve is 6 orders of magnitude and the total assay time was less than 3 hours.

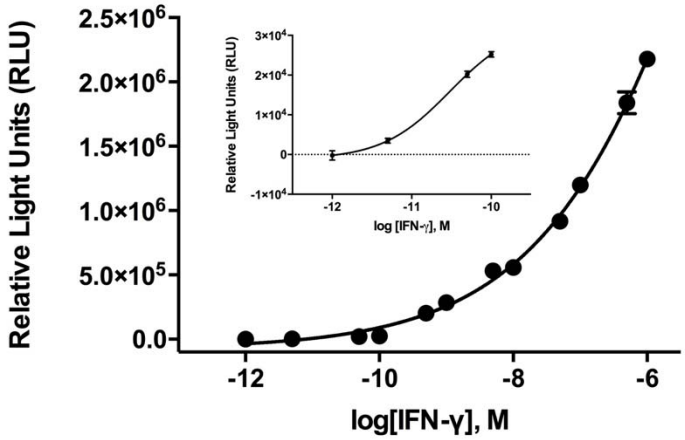

Figure 2.7. Dose response curve for IFN-γ. The insert shows the region of calibration curve near the detection limit. The data points are an average of three measurements ± 1 standard error of the mean. Some error bars are obscured by the symbols of the points.

We have also tested the accuracy of the immunoassay by running the assay against known concentrations of IFN-γ ($2.5x10^{-8}$ M) spiked into blocking buffer and measured using the calibration curve and then interpolating the signal to find the concentration. The interpolated concentration was calculated to be $2.27x10^{-8}$ M. The accuracy of the assay was calculated to be 90.8%. The precision of the assay was tested by running the assay test on different days (Figure 2.8). The results showed a coefficient of variation of less than 20% for every concentration.

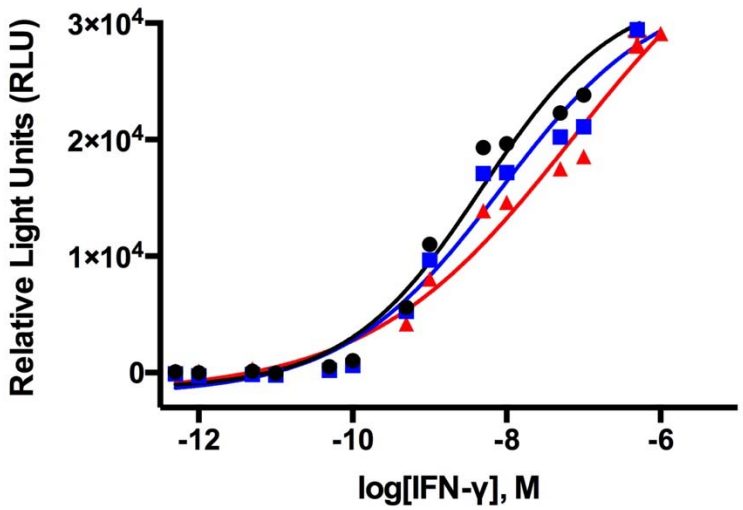

Figure 2.8. Calibration curve generated using three different plates performed to monitor precision of the assay; 1st day (●), 2nd day (■), 3rd day (▲). The data points are an average of three measurements ± 1 standard error of the mean. Some error bars are obscured by the symbols of the points.

2.2.6 Evaluation of Matrix Effects

Immunoassays are employed to detect antigens in a variety of matrices including blood, serum, saliva, and urine depending upon the type of antigen. The presence of other biologically active molecules can interfere with the assay affecting its analytical performance. For this purpose, we have evaluated the possible matrix effects for our test by running the immunoassay in undiluted and 1:10 diluted pooled human serum, which is the sample of choice for IFN-γ detection. Serum samples were spiked with different known concentrations of IFN-γ and the assay was performed. Using the same plate, we concurrently ran our immunoassay in phosphate buffered saline (PBS) as the control. By adding the substrate coelenterazine and using the bioluminescence emission data, three separate calibration curves were generated, and three non-linear response curves were fitted to the data points using GraphPad Prism software (Figure 2.9). The results show that the assay can be run in diluted or undiluted serum with similar performance characteristics as in the buffer matrix. We have performed One-way ANOVA followed by Tukey's

multiple comparisons test using GraphPad Prism software. The results showed no statistical difference at 95% confidence interval indicating that the mean of each measurement is identical. We have confirmed the lack of matrix effect by performing a recovery study in which a known amount of IFN-γ ($2.5x10^{-8}$ M) was spiked into both serum and diluted serum and the resultant signal was interpolated to the IFN-γ concentration using the calibration curve. The interpolated concentration for the serum was calculated to be $1.78x10^{-8}$ M and the percent recovery was 71.2%, and for the diluted serum was $2.84x10^{-8}$ M with the percent recovery equal to 113.6%. The observed percent recoveries are within the accepted range (±30%) for clinical samples.[148,149] Also, we tested the levels of IFN-γ in three patients with irritable bowel syndrome (IBD), who have significant bacterial infection using our immunoassay. We ran our immunoassay in 1:10 diluted serum and found levels of IFN-γ to be 4.12 nM, 9.51 nM and 3.63 nM in these samples.

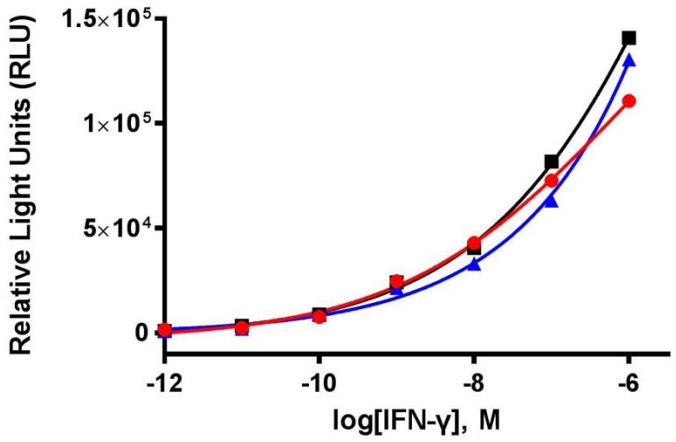

Figure 2.9. Matrix effect with human serum and diluted human serum. ● IFN-γ in blocking buffer, ▲ IFN-γ in human serum, ■IFN-γ in 1:10 diluted human serum. The data points are an average of three measurements ± 1 standard error of the mean. Some error bars are obscured by the symbols of the points.

2.3 Conclusion

In conclusion, we have developed and validated a very sensitive bioluminescence-based immunoassay for the detection of IFN-γ using a bioorthogonal conjugation strategy between the bioluminescent protein GLucY and an antibody against IFN-γ using a novel reagent FBDP as the crosslinker. Since the conjugation strategy involves the use of FBDP, the required reaction conditions are mild and, therefore, do not require pH and temperature extremes. Therefore, the antibody and the bioluminescent protein are not denatured and preserve their functionality. Since our choice of label is a bioluminescent protein attached directly to a primary antibody, we eliminate the secondary antibody incubation, as well as the incubation with the chromogenic substrate. Therefore, our assay is sensitive and requires less incubation time. Our assay demonstrated excellent performance with high precision and accuracy as well as a broad dynamic range and low limit of detection.

2.4 Materials and methods

2.4.1 Expression and Purification of Gaussia Luciferase from Escherichia coli

The expression of the protein GLucY from Origami^{TM} 2 *E.coli* was performed according to Hunt et al.[146] Briefly, the overnight cultures of *E. coli* containing the pCold-1GLucY plasmid were grown in terrific broth supplemented with 0.1 mg/mL ampicillin. These overnight cultures were then expanded into 300 mL of terrific broth supplemented with 0.1 mg/mL ampicillin. The cultures were grown to an OD_{600} of 1.6. The cells were cold-shocked in an ice bath for 1 hour and were induced with IPTG at a final concentration of 1.0 mM following an overnight induction at 15 ºC. The cells were collected by centrifugation, were resuspended in Lysis buffer of 50 mM Tris-HCl pH 8.0, 150 mM sodium chloride, 10 mM imidazole, 1% (vol.) nonyl phenoxypolyethoxylethanol (NP-40),

0.2% (vol.) polyoxyethylene (20) sorbitan monolaurate (Tween 20), and 10 mM 2-mercaptoethanol (β-ME).[150] Afterwards the 1x ProBlock™ Gold Bacterial Protease Inhibitor Cocktail (Gold Biotechnology Inc., St. Louis, MO) was added to the cell suspension followed by sonication (Model 500 Sonic Dismembrator, Fisher Scientific™, Pittsburgh, PA) with a microtip probe for 5 min with a 0.5 second on/off pulse sequence[151]. The insoluble material was removed by centrifugation at 10,000 xg at 4 ºC for 30 minutes and the supernatant was filtered through 0.22 μm filter. The filtered crude protein was then incubated with Ni-NTA agarose (Qiagen, Valencia, CA) at 4 ºC for 45 minutes, collected on a Pierce™ Centrifuge Column (Life Technologies, Grand Island, NY) by gravity flow, washed with 10 column volumes of lysis buffer followed by 20 column volumes of a wash buffer of 50 mM Tris-HCl pH 8.0, 150 mM sodium chloride, and 20 mM imidazole. The protein was then eluted with an elution buffer of 50 mM Tris-HCl pH 8.0, 150 mM sodium chloride, and 150 mM imidazole in 1 column volume to each of six elutions. The purity of the protein in each elution fraction was confirmed by SDS-PAGE using a 4-20% Tris-Glycine gel according to manufacturer's instructions.

The elution fractions containing pure protein were pooled and then dialyzed into a phosphate buffered saline (PBS) of 100 mM sodium phosphate pH 7.2 and 150 mM sodium chloride. Slide-A-Lyzer™ Dialysis Cassettes (Life Technologies, Grand Island, NY) with a molecular weight cutoff (MWCO) of 10 kDa were used. Protein concentration was determined using the Bicinchoninic Acid (BCA) Protein Assay Kit (Pierce Biotechnology, Rockford, IL) and a SpectraMax 190 Microplate Reader (Molecular Devices, Sunnyvale, CA) for absorbance measurements. The concentration of the purified protein was measured using BCA assay according to manufacturer's instructions.

2.4.2 Synthesis of the Formylbenzene Diazonium Hexafluorophosphate (FBDP)

Formylbenzene diazonium hexafluorophosphate (FBDP) was synthesized according to the protocol described by Gavrilyuk et al.[37] Briefly, the 4-aminobenzaldehyde polymer was suspended in 12 N HCl solution at a concentration of 0.5 M at -15 ºC and the cold aqueous solution $NaNO_2$ (0.7 M) was added dropwise to the mixture. The resulting solution was stirred for 1.5 h. Then, the aqueous 60% HPF_6 (1.70 eq) was added to the orange-brown solution and the reaction mixture was left to stir for 30 min at -15 ºC and for 30 min at room temperature. The white-yellow solid was collected by vacuum filtration and was washed with cold water and ethyl acetate. The yield of the reaction was 40%. The solid was stored in the freezer and under Ar atmosphere. ^{1}H NMR (400 MHz, DMSO-d6) δ 8.39 (d, J = 9.2 Hz, 2H), 8.85 (d, J = 8.4 Hz, 2H), 10.17 (s, 1 H).

A stock solution of 0.01 M FBDP was prepared in PBS. With a total reaction volume of 1 mL reaction, one equivalent FBDP was added to $5.8x10^{-6}$ moles of GLucY and incubated at room temperature (~20 °C) for 2 h. The modified variants were then buffer exchanged by dialysis (10 kDa MWCO) into 100 mM sodium citrate pH 6.0 and 150 mM sodium chloride to remove excess FBDP and prepare the modified variants for subsequent reaction with the hydrazine-modified antibody. Specific modification was confirmed by mass spectrometry performed by the Laboratory for Biological Mass Spectrometry at Indiana University (Bloomington, IN). The introduction of an aldehyde functionality by FBDP was also confirmed using an Aldehyde Quantification Assay Kit (Abcam, Cambridge, MA), and by colorimetric reaction with 2,4-dinitrophenylhydrazine.

2.4.3 Concentration of the Purified Anti-human IFN-γ Antibody

The purified anti-human IFN-γ antibody (BioLegend, Cat#502502, San Diego, CA) was concentrated using 100K MWCO Amicon Ultra 0.5 mL Centrifugal filters [Millipore, Cat#UFC510024, Billerica, MA] according to the user's manual to achieve a final concentration of ~2-3 mg/mL. Briefly, the antibody was washed with 500 μL PBS (100 mM sodium phosphate, 150 mM NaCl, pH=7.4) by centrifuging the unit at 14,000 xg for 5 min for a total of four times. The absorbance of each wash was measured using UV-Vis spectroscopy at 280 nm (Spectramax 190, Molecular Devices, Sunnyvale, CA) to confirm that there was no loss of the antibody. After collecting the concentrated purified anti-human IFN-γ antibody, the final concentration of the antibody was measured with UV-Vis spectroscopy at 280 nm.

2.4.4 Bioconjugation of the Antibody with the GLucYFBDP

A 1.0 mg sulfo-succinimidyl-6-hydrazino-nicotinamide (sulfo-S-Hynic) [Solulink, Cat#S-1011-105, San Diego, CA] was dissolved in 100 μL PBS. An aliquot of this solution that corresponds to 20.0 eq was added to the solution of anti-IFN-γ antibody and the mixture was incubated for 2 h at room temperature (~20 °C). Then the unreacted sulfo-S-Hynic was removed from the reaction mixture using microdialysis tubes (MWCO 4K, 20-150 μL). The buffer was also exchanged to the conjugation buffer (100 mM sodium citrate, 150 mM sodium chloride, pH 6.0) and the concentration of purified antibody was measured with UV-Vis spectroscopy at 280 nm. After dialysis the extent of hydrazine modification was determined using UV-Vis spectroscopy and measuring the absorbance values at 380 nm. *p*-Nitrobenzaldehyde was used as the standard, which forms a chromogenic product with sulfo-S-Hynic and has absorbance at 380 nm.

Depending on the number of sulfo-S-Hynic molecules on the antibody, an excess of the modified protein was added to the modified antibody solution and incubated overnight at 4 ºC.

2.4.5 Bioconjugation of the Antibody via Glutaraldehyde

The GLucY solution was added to 7.5 equivalent excess of antibody solution. In a fume hood 10 μL of 25% glutaraldehyde (Sigma, Cat#G7526, St. Louis, MO) was added per mL antibody/protein. The reaction was left for 2 h at 4 °C. The resultant Schiff bases was reduced using sodium cyanoborohydride at a final concentration of 10 mg/mL and the reduction was performed for 1 h at 4 °C.[134]

2.4.6 Purification of both Conjugated Antibodies

The unreacted protein from the antibody mixture was removed using 100K MWCO Amicon Ultra 0.5 mL Centrifugal filters [Millipore, Cat#UFC510024, Billerica, MA] according to the user's manual. The concentration of the labeled antibody was measured with UV-Vis spectroscopy at 280 nm and the conjugation of the antibody to GLuc was confirmed using Western blot analysis.

2.4.7 Western Blot Analysis

A SDS polyacrylamide gel electrophoresis was performed using a 4-20% Tris-Glycine gel as described previously using 1 μg purified antibody GLuc conjugate in duplicate. The proteins then were transferred onto a polyvinylidene fluoride (PVDF) membrane using a Bio-Rad semi dry blotting instrument according to the manufacturer's instructions. After the transfer was complete, the membrane was blocked with Odyssey Blocking Buffer (PBS) [LI-COR, Cat#927-40000) for 2 hours at room temperature. Then one of the

membranes was incubated with a monoclonal mouse anti-Gaussia luciferase antibody (Nanolight Technology, Cat#401M, Pinetop, AZ) whereas the other membrane was incubated with an anti-mouse secondary antibody labeled with proprietary infrared dye (binds to Fc portion of mouse antibody), overnight at 4 ºC. The membranes were washed three times with phosphate buffered saline containing 0.05% Tween-20 (PBST) buffer and three times with phosphate buffered saline (PBS). The first membrane was incubated with an anti-mouse secondary antibody labeled with proprietary infrared dye for 2 h at room temperature. The membrane was washed three times with PBST buffer and three times with PBS. Both membranes were scanned in a LI-COR Odyssey infrared scanner.

2.4.8 Immunoassay Parameter Optimization Studies

In order to optimize the immunoassay, the concentration of cAb, the incubation time of dAb and of the antigen and the commercial blocking buffers were tested for a better detection limit. A MaxiSorp 96-well microtiter plate [ThermoFisher Cat#437111] was coated with anti-human IFN-γ cAb [BD Pharmingen Cat#551221]. The capture antibody solution (0.5 μg/mL, 1.0 μg/mL, 5.0 μg/mL, 10.0 μg/mL,) was prepared in 100 mM $NaHCO_3$, pH 9.6, and an aliquot of 100 μL were dispensed into each well of the plate using a multichannel pipettor. The plate was shaken overnight at room temperature. The next day, capture antibody solution was removed by using the plate washer (MultiWash+, Molecular Devices, Sunnyvale, CA) using Wash Buffer (100 mM sodium phosphate, 150 mM sodium chloride pH 7.2, 0.05% Tween-20, 1% Blocking buffer). The plate was blocked with 200 μL blocking buffer (Starting Block T20 PBS [Thermo Scientific Cat#37539], Blocker™ BLOTTO in TBS [Thermo Scientific Cat#37530], SEA BLOCK Blocking Buffer [Thermo Scientific Cat#37527], SuperBlock™ (PBS) Blocking Buffer

[Thermo Scientific Cat#37515] and Pierce™ Protein-Free (PBS) Blocking Buffer [Thermo Scientific Cat#37572] while shaking at 500 rpm overnight at 4 °C. After the overnight blocking was complete, the blocking buffer was removed. Several dilutions of IFN-γ [BioLegend Cat#570206] in blocking buffer were prepared. 100 μL aliquots of the IFN-γ at the various concentrations were placed in each well and incubated for different times (1, 2, 3 hours) at room temperature. After the incubation, the antigen was removed by using the plate washer with the same settings. Then, 100 μL aliquots of the dAb at a concentration of 2 μg/mL was added into each well, and incubated for different times (45 min, 90 min, 1 hour, 2 hours, 3 hours overnight) at room temperature. After the incubation, the dAb was removed, and the wells were washed with the plate washer. Finally, the bioluminescence intensity of each well was measured in the CLARIOSTAR OPTIMA by injecting 100 μL of native coelenterazine at a final concentration of 2.0 μg/mL.

2.4.9 Immunoassay

In order to optimize the time of incubation with antigen for a better detection limit, a MaxiSorp 96-well microtiter plate [ThermoFisher Cat#437111, Waltham, MA] was coated with anti-human IFN-γ capture antibody [BD Pharmingen Cat#551221, San Diego, CA]. The capture antibody solution (1.0 μg/mL) was prepared in 100 mM $NaHCO_3$, pH 9.6, and an aliquot of 100 μL was dispensed into each well of the plate using a multichannel pipettor. The plate was shaken overnight at room temperature. The next day, capture antibody solution was removed by using the plate washer (MultiWash+, Molecular Devices, Sunnyvale, CA) using Wash Buffer (100 mM sodium phosphate, 150 mM sodium chloride pH 7.2, 0.05% Tween-20, 1% Starting Block buffer). The plate was blocked with 200 μL Starting Block T20 PBS [Thermo Scientific Cat#37539, Waltham, MA] while shaking at

500 rpm overnight at 4 °C. After the overnight blocking was complete, the blocking buffer was removed. Several dilutions of IFN-γ [BioLegend Cat#570206, San Diego, CA] in blocking buffer were prepared. 100 μL aliquots of the IFN-γ at the various concentrations was placed in each well and incubated for 2 h at room temperature. After the incubation, the antigen was removed by using the plate washer with the same settings. Then, 100 μL aliquots of the GLuc conjugated detection antibody at a concentration of 2 μg/mL was added into each well and incubated for 45 minutes at room temperature. After the incubation, the excess detection Ab was removed, and the wells were washed with the plate washer. Finally, the bioluminescence intensity of each well was measured in the CLARIOSTAR OPTIMA (BMG Labtech, Ortenberg, Germany) by injecting 100 μL of native coelenterazine at a final concentration of 2.0 μg/mL.

Chapter 3

Bioluminescent Protein-Inhibitor Pair in the Design of a Molecular Aptamer Beacon Biosensor

Overview

Quenching of the fluorophores on the molecular beacon is broadly studied and has been applied to many detection systems. Bioluminescent molecular beacons with quenchers have been proven to have higher signal-to-noise ratio and thus more sensitivity. However, this system still suffers from challenges of inefficient quenching. Another, more elegant, solution to inefficient quenching can be realized by capitalizing on the unique enzyme/substrate relationship of a specific bioluminescent protein. By designing a competitive inhibitor that is structurally very similar to the native substrate, essentially complete substrate exclusion can be realized. In this work, we designed a conjugated molecular aptamer beacon (MAB) attached to a bioluminescent protein, *Gaussia* luciferase (GLuc) and an inhibitor molecule with similar structure as the native the inhibitor molecule can be bound. To prove that MAB is more sensitive and has better signal-to-noise ratio, a bioluminescent assay was developed against interferon-γ (IFN-γ) and the detection limit was calculated to be 20 pM. We believe that this inhibitor approach may improve the sensitivity of the molecular beacon detection systems.

3.1 Preface

Nucleic acids provide a highly relevant biomarker in the diagnosis of infectious diseases,[152] identification of genetic alterations[153] and in the case of aptamers, the detection of clinically-relevant non-nucleic acid molecules.[154] Nucleic acids have recently increased in popularity due to their ability to merge highly sensitive and selective detection with modern point-of-care demands such as simplistic assay interfaces and rapid generation of results.[155] Of particular importance to assay design, nucleic acid probes are easily synthesized, highly selective, and are useful for the detection of DNA, RNA, and proteins.[156]

The single-step nucleic acid detection system relies on probe hybridization with a complementary target. Single-step detection is typically a rapid technique, frequently utilizing resonance energy-transfer (RET) conditions, in which the presence of target is indicated by a wavelength shift or loss of fluorescence as a reporter-conjugated nucleic acid probe becomes displaced from its target-specific, acceptor-conjugated complementary strand.[157-160] Our laboratory has expanded this type of system by substituting a bioluminescent protein in a BRET-based competitive assay that was able to detect target DNA by evaluating a dose-dependent loss of BRET signal from displacement of a quantum dot-labeled complementary strand.[161] Moreover, we improved the speed and sensitivity of this system by including head-to-head orientation of the RET probes such that hybridization of both probes was required to identify the target and served to minimize the donor/acceptor distance for enhanced BRET efficiency.[162]

Molecular beacon (MB) technology, first developed by Tyagi and Kramer in 1996, is a variant of the traditional single-step detection platform in which independent

donor/acceptor energy transfer probes were replaced with a single-stranded oligonucleotide that self-hybridizes in a stem-loop configuration.[63] Upon hybridization of a complimentary target to the single-stranded loop region, the double-stranded stem is forced apart. By conjugating a fluorophore/quencher pair to the stem termini, target-induced opening of the stem removes the quencher from close proximity of the fluorophore, leading to a dose-dependent increase in fluorescence. This type of fluorescent MB has been used in many applications besides nucleic acid detection, including real-time hybridization in living cells,[163,164] DNA-protein interactions,[165] as well as monitoring enzymatic cleavage[166] and real time polymerase chain reactions (qPCR).[167,168] However, they can suffer from severe sensitivity issues mainly due to background fluorescence from the excitation source.[156] In order to address these shortcomings, our group was the first to report a bioluminescent stem-loop probe (BSLP).[116,117] For this, a bioluminescent luciferase (Rluc8) replaced the traditional fluorophore and demonstrated a significant improvement in sensitivity. Modulation of the bioluminescent signal was essentially identical to a standard MB and was applied to the detection of miR-21, a commonly dysregulated biomarker. Although a drastic improvement in the signal amplitude was demonstrated when compared to fluorescence-based stem loop probes, the system suffered from similar drawbacks such as inefficient quenching of the bioluminescent signal, resulting in a signal-to-noise ratio that was still open to improvement.

Another, more elegant, solution to inefficient quenching can be realized by capitalizing on the unique enzyme/substrate relationship of a specific bioluminescent protein. By designing a competitive inhibitor that is structurally very similar to the native substrate, essentially complete substrate exclusion can be realized. We hypothesized that a significant

improvement in MB sensitivity can be achieved by eliminating unintended triggering of the bioluminescent reaction altogether. A couple of detection systems have already employed inhibitors capable of interacting with the luciferase active site with varying degrees of affinity.[169] Poutiainen et al.[170] developed a peptide-based sensor conjugated with a luciferase inhibitor, and Shimada et al.[171] designed a weakly inhibiting aptamer system for thrombin detection. To the best of our knowledge, however, there are no inhibitor-based MBs that combine a bioluminescent protein with a substrate analog. Importantly, it has been shown elsewhere that the effective concentration of an inhibitor dramatically increases upon local tethering to a target enzyme, thereby achieving inhibition at lower concentrations than a free inhibitor.[172]

The system developed here combines an inhibition-based MB with an aptamer-based loop domain in order to detect the immune-stimulating cytokine, interferon-γ (IFN-γ) (Figure 3.1). Aptamers are single-stranded oligonucleotides with binding properties similar to antibody-antigen interactions.[69,70] They are selected by a method called Systematic Evolution of Ligands by EXponential enrichment (SELEX) that identifies specific targets such as proteins, small molecules and even whole cells.[173,174] The advantages of using aptamers over antibodies include simple synthesis, easy labeling with fluorophore dyes or enzymes, and greater stability in non-physiological conditions.[72]

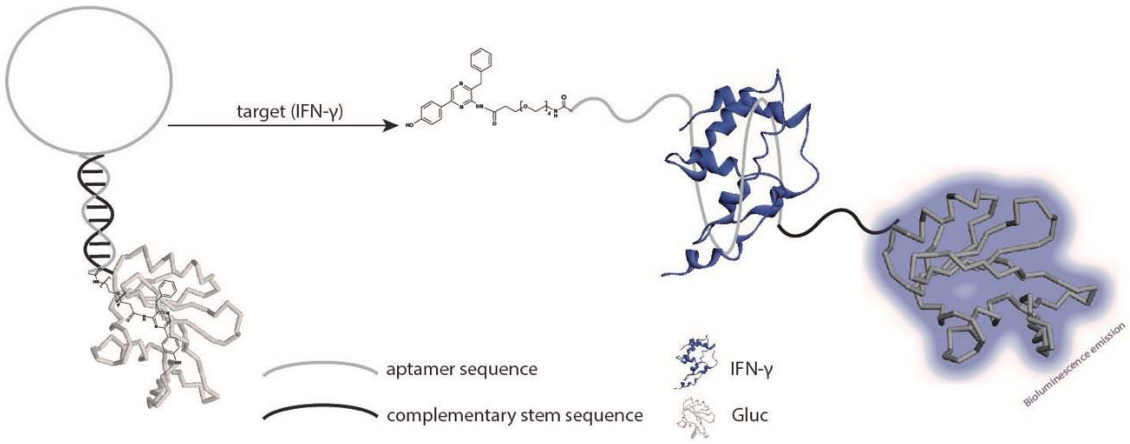

Figure 3.1. General principle with the molecular aptamer beacon assay. The IFN-γ crystal structure is from protein databank: 1HIG and an example of protein structure represents the GLuc since the crystal structure is not resolved yet.

The insertion of an aptamer sequence in the MB creates a molecular aptamer beacon (MAB), combining advantages of both such as binding specificity and switchable reporter signaling. MABs have been developed in the recent past for real-time detection,[175,176] imaging,[177] and other applications.[81] However, this is the first demonstration, to our knowledge, of a bioluminescent aptamer-based MB and the use of an inhibitor rather than a quencher. This strategy opens up another way to improve the toolkit of highly sensitive mix and measure detection of nucleic acid and other biomolecules using MBs and MABs. In this work, the inhibitor molecule coelenteramine was chosen for the bioluminescent protein *Gaussia* luciferase (GLuc) due to the structural similarity to its native substrate, coelenterazine.

3.2 Discussion

3.2.1 Development of Molecular Aptamer Beacon

The sequence of the MAB against IFN-γ is underlined and was found to be 5’GGGGTTGGTTGTGTTGGGTGTTGTGTCCAACCCC3’ according to the literature.[178] The stem part of the MAB was created by adding complementary nucleotides

at the 3' end. The commercially available oligonucleotide sequence had a 5'-carboxylic acid end and a 3'-azide end for the bioconjugation of the MAB with coelenteramine-inhibitor and GLuc, respectively. Coelenteramine-inhibitor was synthesized in two-step reaction, including a polyethylene glycol (PEG) linker attachment on the coelenteramine molecule and the deprotection of the primary amine moiety (Figure 3.2A). The PEG linker introduced flexibility to the inhibitor facilitating its binding to the enzymatic pocket of GLuc. We decided to use two different PEG linkers with two and four ethylene oxide monomers to compare the inhibition efficiency. Both products were characterized with NMR spectroscopy as well as high resolution mass spectrometry (Materials and Methods).

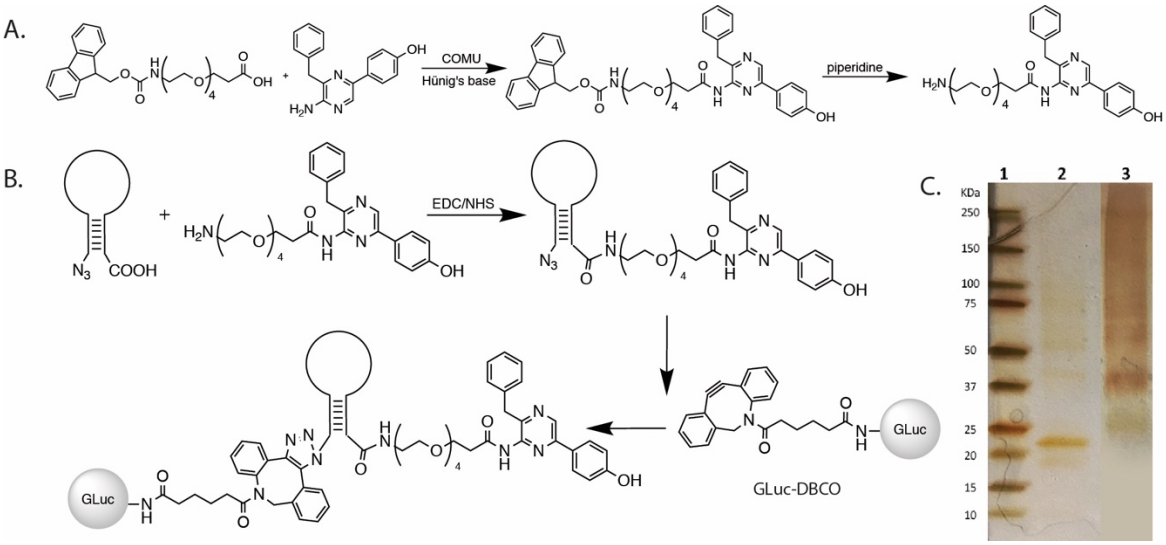

Figure 3.2. A. Two-step reaction of the coelenteramine inhibitor synthesis B. Bioconjugation scheme of the bioluminescent molecular aptamer beacon C. SDS-PAGE gel stained with silver staining; Lanes 1: Protein Ladder, 2: purified GLuc, and 3: conjugated molecular aptamer beacon with GLuc and coelenteramine-inhibitor.

The general bioconjugation scheme for the bioluminescent MAB is shown in Figure 3.2B. The GLuc was modified through the lysine amines with Dibenzocyclooctyne-*N*-hydroxysuccinimidyl ester (NHS-DBCO) according to manufacturer's instructions (Lumiprobe, Hunt Valley, Maryland) which introduces a cyclo-alkyne molecule on the protein. The formation of the product, GLuc-DBCO was confirmed by UV-visible

spectroscopy. For this purpose, an azide-fluorophore 545 (Sigma, St. Louis, Missouri) was attached to the GLuc-DBCO and the absorption spectrum between 350-650 nm showed the two characteristic peaks around 520 nm and 550 nm. (Figure 3.3).

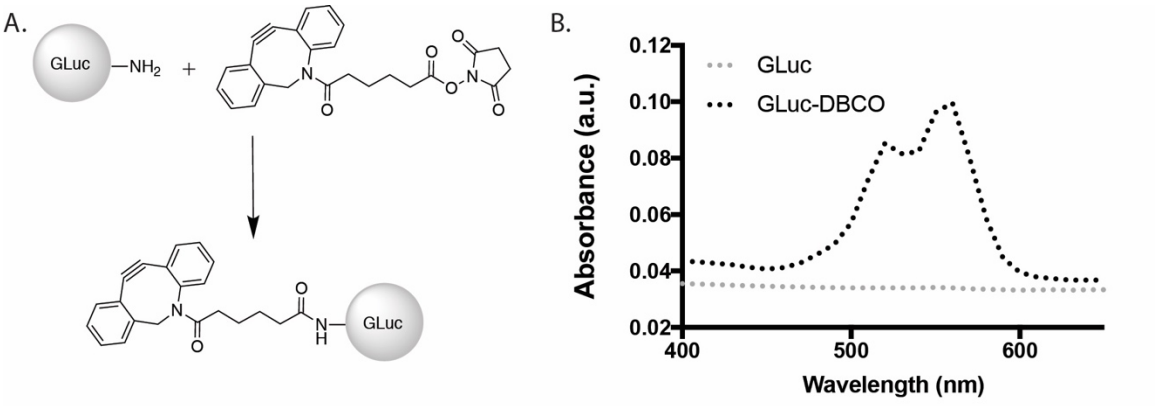

Figure 3.3. A. Reaction scheme of GLuc-DBCO and B. characterization of GLuc-DBCO with UV-vis spectroscopy.

Furthermore, the MAB was conjugated with coelenteramine-inhibitor at the 5'-carboxylic acid end. The amine group of coelenteramine-inhibitor reacts with the carboxylic acid through the reagents 1-Ethyl-3-(3-dimethylaminopropyl)carbodiimide (EDC) and hydroxysulfosuccinimide (sulfo-NHS). Because coelenteramine-inhibitor is an electroactive species, the modification of the MAB with the coelenteramine-inhibitor was monitored with differential pulse voltammetry based on the appearance and shift of the peak (Figure 3.4).

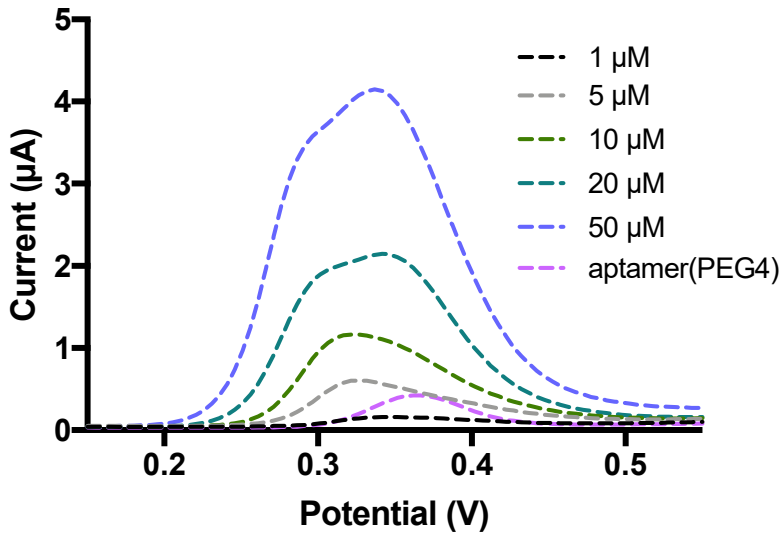

Figure 3.4. The characterization of the conjugate molecular aptamer beacon with coelenteramine-inhibitor(PEG4) using pulse voltammetry. We checked a range of concentrations of inhibitor(PEG4) (1-50 μM) and there was a characteristic peak at the conjugate around 0.35 V.

The 3'-azide end of the stem was labeled with the GLuc-DBCO through copper-free click chemistry. We decided to use a copper-free click chemistry since it was demonstrated that the copper ions affect detrimentally the biomolecules[179] and the proteins.[180] The final bioconjugation reaction was performed on a streptavidin-biotin column. We used a biotinylated complementary oligonucleotide to the aptamer sequence for the attachment of the probe on a streptavidin resin. This allows for the MAB to be in the open form for further reaction with GLuc to avoid the steric hindrance between the protein and the stem of the MAB. The formation of the product, conjugated MAB, was confirmed using SDS-PAGE analysis (Figure 3.2C). The gel was stained with the silver stain kit (Thermofischer, Weston, Florida) according to manufacturer's instructions. In Figure 3.2C, the bands of the solutions of GLuc and conjugated MAB are shown. The characteristic band of GLuc is around at 22 kDa as its molecular weight. On the other hand, after the two-step conjugation steps, the conjugated MAB showed two bands. The 37 kDa and bands above 60 kDa correspond to a GLuc molecule with one MAB and with several MABs, respectively. For

convenience, the products with different PEG linkers will be referred as aptamer(PEG2)-GLuc and aptamer(PEG4)-GLuc in this manuscript (Figure 3.5)

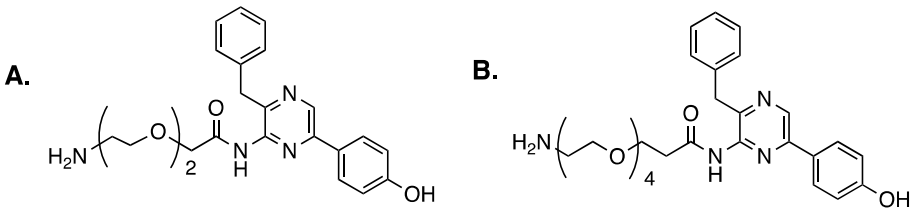

Figure 3.5. Chemical structure of A. inhibitor(PEG2) and B. inhibitor(PEG4).

3.2.2 Optimization and development of the MAB bioluminescent assay

The next step was to develop a bioluminescent assay for the detection of IFN-γ. In order to achieve the best experimental performance of our bioluminescent assay, the temperature and the incubation time were evaluated. For the temperature optimization, the assay was performed at 4 °C and compared to the room temperature, the sensitivity of the system is worse at 4 °C (Figure 3.6). Moreover, three different incubation times were investigated. For this optimization study, the conjugated MAB solution was mixed with the varying concentrations of IFN-γ and the mixtures were incubated for 0.5, 1.0 and 2.0 h and the signal-to-noise ratio (S/N) was calculated. The 1.0 h incubation time resulted in better S/N when compared to the 0.5 min but comparable S/N to 2.0 h incubation time. We selected 1.0 h as the optimal time for incubation since it is shorter incubation time than the 2.0 h.

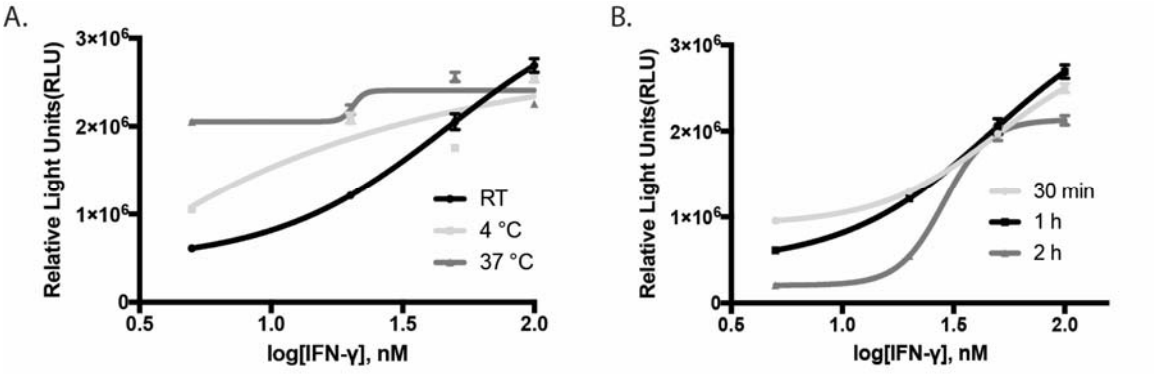

Figure 3.6. Optimization of the assay of the aptamer(PEG4)-GLuc in different A. temperature and B. incubation time.

Also, both aptamer(PEG2)-GLuc and aptamer(PEG4)-GLuc were compared according to each dose-response curve and we concluded that the aptamer(PEG4)-GLuc has better signal-to-noise ratio (Figure3.7) and hence was chosen for further studies.

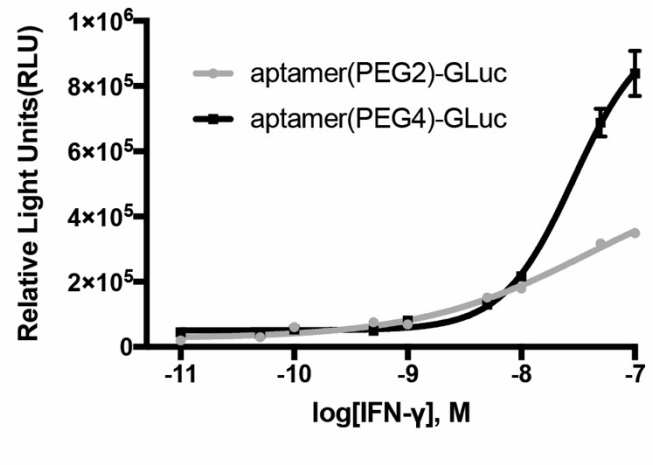

Figure 3.7. Comparison of the bioluminescence response of the two inhibitors.

Also, to demonstrate that the inhibition-based MAB gives better S/N ratio when compared to the quenching-based method, we developed an assay with the same oligonucleotide sequence attached to a quencher molecule, DABCYL. Using the same plate, both MABs were mixed with the same IFN-γ concentrations, and the bioluminescence responses were recorded. The data indicated that the signal-to-noise ratio is 2 times higher when using an inhibitor vs a quencher (Figure 3.8).

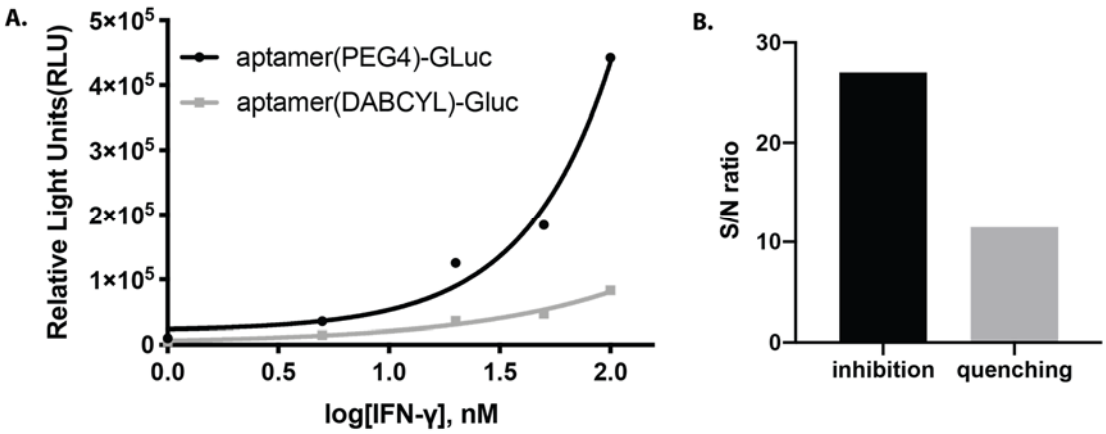

Figure 3.8. Comparison of the A. dose response curves and B. signal-to-noise ratio between inhibition and quenching. The data points are an average of three measurements ± 1 standard error of the mean. The error bars are obscured by the symbols of the points.

After the optimization studies, the bioluminescent signal was examined at different concentrations of IFN-γ. Different solutions of the target from 5 $X10^{-12}$ to 1 $X10^{-6}$ M were mixed with 15 nM of bioluminescent MAB and were incubated at room temperature for 1 h and the measured data was plotted to calculate the linear range of the bioluminescent assay. The bioluminescence emission was monitored by adding 1 μg/mL of the substrate, coelenterazine. Using the bioluminescence emission intensity, a calibration curve was generated, and a non-linear dose-response curve was fitted to the data points using GraphPad Prism software (Figure 3.9).

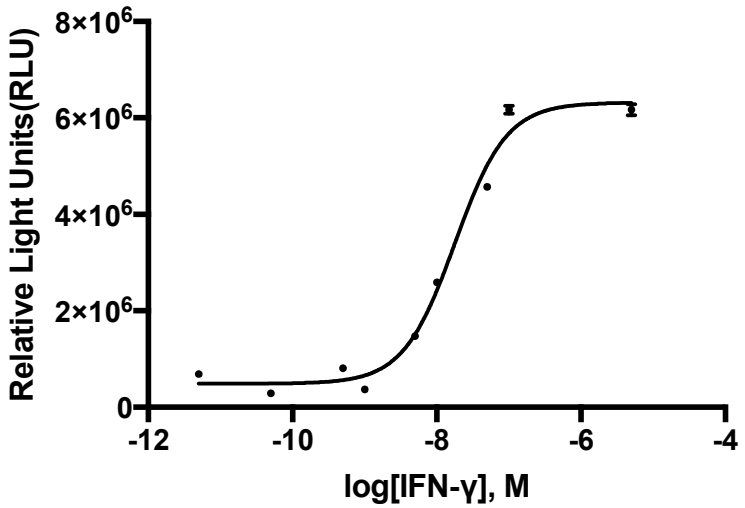

Figure 3.9. Dose response curve for IFN-γ. The data points are an average of three measurements ± 1 standard error of the mean. Some error bars are obscured by the symbols of the points.

After these optimization parameters, we concluded that the lowest limit of detection of the bioluminescent assay was found to be $2X10^{-11}$ M for aptamer(PEG4)-GLuc. The limit of detection was interpolated from the GraphPad Prism software using the formula $LOD=S_B + 3xSD_B$ where S_B and SD_B are the mean and the standard deviation of the blank signals, respectively.

3.2.3 Selectivity test and Matrix effect

Also, the selectivity of the assay was studied against other proteins. Two cytokines, the inteleukin-6 (IL-6) and tumor necrosis factor alpha (TNF-α) were chosen to check the bioluminescence response of the aptamer(PEG4)-GLuc. Both proteins belong to the family of proinflammatory cytokines as the IFN-γ and are produced from several cells of the immune system as biological responses against diseases.[181] The test showed that the aptamer(PEG4)-GLuc is selective against IFN-γ as there was no bioluminescence response according to the Figure 3.10A.

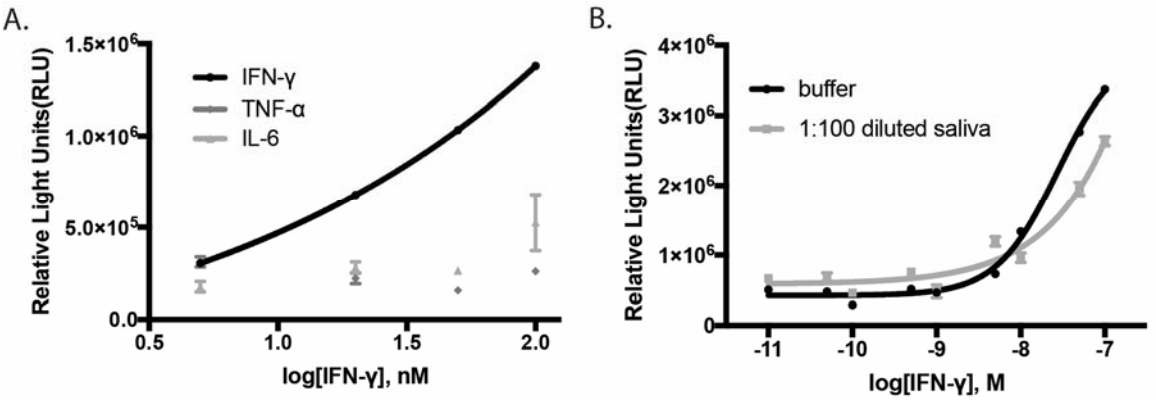

Figure 3.10. A. Selectivity test against two different cytokines B. Matrix effect with diluted saliva. The data points are an average of three measurements ± 1 standard error of the mean. Some error bars are obscured by the symbols of the points.

Any assay that is developed is usually tested for the matrix effect in a biological fluid. The presence of other components such as enzymes, oligonucleotides can affect the analytical performance of the assay. We have selected saliva as the biological fluid of our choice because IFN-γ can be detected in saliva for several diseases[182-184] and it is considered a non-invasive fluid collection. Therefore, we have evaluated the possible matrix effects for our test by running the assay in 1:100 diluted human saliva. Saliva samples were spiked with different known concentrations of IFN-γ and the assay was performed. Using the same plate, we concurrently ran our assay in 10 mM Tris base, 150 mM NaCl, pH 7.4 as the control. We have confirmed the minimum matrix effect by performing a recovery study in which a known amount of IFN-γ ($3.0x10^{-7}$ M) was spiked in 1:100 diluted saliva and the resultant signal was interpolated to the IFN-γ concentration using the calibration curve (Figure 3.10B). The interpolated concentration for the diluted saliva was calculated to be $2.21x10^{-7}$ M and the percent recovery was 74%. The observed percent recoveries are within the accepted range (±30%) for clinical samples.[148,149]

3.3 Conclusion

In summary, we conjugated the MAB with the coelenteramine-inhibitor, that inhibits GLuc bioluminescence though EDC/NHS chemistry and with GLuc though azide/alkyne copper-free click chemistry. We first synthesized an inhibitor-based bioluminescent MAB and validated a solution assay against the target, IFN-γ. Since the coelenterazine-inhibitor binds to the enzymatic pocket due to hydrophobic interactions, the bioluminescent assay showed a better performance and better signal-to-noise ratio compared to the DABCYL-based MAB. Besides the sensitivity, the MAB is selective and didn't show any bioluminescence response against other cytokines. Therefore, this is the first demonstration, to our knowledge, of a successful design of bioluminescent MAB that uses an inhibitor rather than a quencher in the assay development yielding a superior sensitivity.

3.4 Materials and methods

3.4.1 Expression and Purification of *Gaussia* Luciferase from Escherichia coli

The expression of the protein GLuc from Origami™ 2 *E.coli* was performed according to the below protocol. Briefly, the overnight cultures of *E. coli* containing the pCold-1GLuc plasmid were grown in luria broth supplemented with 0.1 mg/mL ampicillin. These overnight cultures were then expanded into 300 mL of luria broth supplemented with 0.1 mg/mL ampicillin. The cultures were grown to an OD_{600} of 0.6. The cells were cold-shocked in an ice bath for 1 hour and were induced with IPTG at a final concentration of 0.1 mM following an overnight induction at 15 ºC. The cells were collected by centrifugation, were resuspended in Lysis buffer of 50 mM Tris-HCl pH 8.0, 150 mM sodium chloride, 10 mM imidazole, 1% (vol.) nonyl phenoxypolyethoxylethanol (NP-40), 0.2% (vol.) polyoxyethylene (20) sorbitan monolaurate (Tween 20), and 10 mM 2-

mercaptoethanol (β-ME). Afterwards the 1x ProBlock™ Gold Bacterial Protease Inhibitor Cocktail (Gold Biotechnology Inc., St. Louis, MO) was added to the cell suspension followed by sonication (Model 500 Sonic Dismembrator, Fisher Scientific™, Pittsburgh, PA) with a microtip probe for 20 min with a 0.5 second on/off pulse sequence. The insoluble material was removed by centrifugation at 19,000 rpm at 4 ºC for 30 minutes and the supernatant was filtered through 0.45 μm and 0.22 μm filter. The filtered crude protein was then incubated with Ni-NTA agarose (Qiagen, Valencia, CA) at 4 ºC for 45 minutes, collected on a Pierce™ Centrifuge Column (Life Technologies, Grand Island, NY) by gravity flow, washed with 10 column volumes of lysis buffer followed by 20 column volumes of a wash buffer of 50 mM Tris-HCl pH 8.0, 150 mM sodium chloride, and 20 mM imidazole. The protein was then eluted with an elution buffer of 50 mM Tris-HCl pH 8.0, 150 mM sodium chloride, and 150 mM imidazole in 1 column volume to each of six elutions. The purity of the protein in each elution fraction was confirmed by SDS-PAGE using a 4-20% Tris-Glycine gel according to manufacturer's instructions.

The elution fractions containing pure protein were pooled and then dialyzed into a phosphate buffered saline (PBS) of 100 mM sodium phosphate pH 8.45 and 150 mM sodium chloride. Slide-A-Lyzer™ Dialysis Cassettes (Life Technologies, Grand Island, NY) with a molecular weight cutoff (MWCO) of 10 kDa were used. Protein concentration was determined using the Bicinchoninic Acid (BCA) Protein Assay Kit (Pierce Biotechnology, Rockford, IL) and a SpectraMax 190 Microplate Reader (Molecular Devices, Sunnyvale, CA) for absorbance measurements. The concentration of the purified protein was measured using BCA assay according to manufacturer's instructions.

3.4.2 Synthesis of inhibitor(PEG2)

A 5 mL conical vial equipped with magnetic stirrer was charged with {2-[2-(9H-Fluore-9-ylmethoxycarbonylamino)-ethoxy]-ethoxy}-acetic acid (BioBlocks, CAS: 166108-71-0) (1.00 eq), coelenteramine (NanoLight, Cat.#300-250) (1.10 eq), *N*,*N*-Diisopropylethylamine (Sigma-Aldrich, #387649) and 0.5 M DMF at 0 ºC. The (1-Cyano-2-ethoxy-2-oxoethylidenaminooxy)dimethylamino-morpholino-carbenium hexafluorophosphate (2.00 eq), COMU (CHEM-IMPEX INT'L INC, Cat.#26427) was added to the yellow solution and the reaction mixture was cooled at 0 ºC for 1 hour. The reaction mixture was allowed to come to room temperature and stirred overnight. The reaction was monitored by thin layer chromatography on precoated silica gel TLC plates (1:1 EtOAc:Hexane, R_f 0.14). The aqueous layer was extracted with ethyl acetate (25 mL), 1 N HCl (2x5 mL), 1N $NaHCO_3$ and saturated NaCl (2x5 mL) and dried over $MgSO_4$, filtered, and concentrated on a rotary evaporator. The crude mixture was purified by column chromatography over silica gel using hexane and ethyl acetate as eluents to obtain the pure product. The product was purified through a gradient elution from 0% to 100% EtOAc. The product was isolated in 51% yield as a yellow oil and characterized with ^{1}H-NMR. ^{1}H NMR (400 MHz, $CDCl_3$) δ 3.23 (t, J = 4.8 Hz, 2H), 3.32 (t, J = 5.4 Hz, 2H), 3.49 (t, J = 5.6 Hz, 2H), 3.69 (t, J = 4.8 Hz, 2H), 4.17 (s, 2H), 7.29-7.81 (m, aromatic H).

The deprotection reaction happened with 20% piperidine in DMF overnight and was monitored with TLC. The final product was purified with liquid column chromatography and silica as a stationary phase and was concentrated in a rotary evaporator. The final product was characterized with ^{1}H-NMR. ^{1}H NMR (400 MHz, $CDCl_3$) δ 1.54 (b, 2H), 3.24 (t, J = 5.0 Hz, 2H), 3.31 (t, J = 5.4 Hz, 2H), 3.49 (t, J = 5.6 Hz, 2H), 3.69 (t, J = 5.0 Hz,

2H), 4.18 (s, 2H), 6.92 (d, J = 6.5 Hz, 2H), 7.32 (m, 3H), 7.52 (s, 1H), 7.84 (d, J = 6.8 Hz, 2H).

3.4.3 Synthesis of inhibitor(PEG4)

A 10 mL two neck round bottom vial equipped with magnetic stirrer and Ar was charged with 1-(9H-Fluore-9-yl)-3-oxo-2,7,10,13,16-pentaoxa-4-azaoctadecan-18-oic acid (Ark Pharm, Number: AK601801) (1.00 eq), coelenteramine (NanoLight, Cat.#300-250) (1.10 eq), *N*,*N*-Diisopropylethylamine (Sigma-Aldrich, #387649) and 2.5 mL DMF at 0 ºC. The (1-Cyano-2-ethoxy-2-oxoethylidenaminooxy)dimethylamino-morpholino-carbenium hexafluorophosphate (2.00 eq), COMU (CHEM-IMPEX INT'L INC, Cat.#26427) was added to the yellow solution and the reaction mixture was cooled at 0 ºC for 1 hour. The reaction mixture was allowed to come to room temperature and stirred overnight. Next day, the reaction was monitored with thin layer chromatography (TLC) in 1:1 EtOAc/Hex. The protected product was extracted with 1 N HCl (2 x 5 mL), 1 N $NaHCO_3$ (2 x 5 mL) and Brine (2 x 5 mL). The product was purified in liquid column chromatography through a gradient elution from 0% to 100% EtOAc and concentrated on a rotary evaporator.

^{1}H NMR (400 MHz, Acetone-d_6) δ 8.44 (s, 1H), 8.05 – 8.00 (m, 2H), 7.86 (d, J = 7.5 Hz, 2H), 7.68 (d, J = 7.5 Hz, 2H), 7.44 – 7.26 (m, 9H), 7.21 (dd, J = 7.8, 5.1 Hz, 3H), 6.58 (t, J = 6.0 Hz, 1H), 5.69 (s, 2H), 4.48 (s, 2H), 4.36 (d, J = 7.1 Hz, 2H), 4.24 (t, J = 7.0 Hz, 1H), 4.18 (s, 2H), 3.81 (dd, J = 5.8, 3.4 Hz, 2H), 3.68 (dd, J = 5.8, 3.5 Hz, 2H), 3.54 (t, J = 5.5 Hz, 2H), 3.32 (q, J = 5.6 Hz, 2H), 3.15 – 3.10 (m, 1H), 2.88 (s, 3H), 2.79 (s, 1H), 2.09 (s, 1H), 1.29 (s, 2H), 1.21 (s, 1H).

^{13}C NMR (101 MHz, Acetone-d_6) δ 169.55, 156.95, 152.73, 150.07, 144.21, 141.22, 140.31, 139.65, 137.79, 137.12, 135.48, 128.88, 128.40, 127.66, 127.07, 126.40, 126.17,

125.21, 121.77, 119.95, 70.37 (d, J = 13.7 Hz), 69.97, 67.96, 66.20 (d, J = 5.0 Hz), 47.23 (d, J = 17.5 Hz), 40.60, 39.54, 37.59.

The deprotection reaction happened with 20% piperidine in DMF overnight and was monitored with TLC. The final product was purified with liquid column chromatography and silica as a stationary phase and was concentrated in a rotary evaporator.

^{1}H NMR (400 MHz, Chloroform-*d*) δ 8.33 (s, 1H), 8.02 (s, 1H), 7.86 – 7.81 (m, 2H), 7.36 – 7.28 (m, 4H), 6.98 – 6.91 (m, 2H), 4.37 (s, 2H), 4.19 (s, 2H), 3.55 – 3.46 (m, 2H), 3.36 – 3.29 (m, 2H), 1.69 (q, J = 5.8 Hz, 3H), 1.65 – 1.53 (m, 5H).

ESI-MS Calculated for $C_{28}H_{36}N_4O_6$ ($M+NH_4^+$): 542.66, found 542.28.

3.4.4 Synthesis of GLuc-DBCO

The molecular aptamer beacon was bought commercially from Integrated DNA Technologies 5'-Carboxy/GGGGTTGGTTGTGTTGGGTGTTGTGTCAACCCC/AzideN-3' with two chemical modifications in each stem end; a carboxylic acid and an azide. To conjugate the molecular aptamer beacon with the bioluminescent protein, GLuc, we introduced an cyclic alkyne group for a further click chemistry reaction. 8 equivalents of dibenzocyclooctyne (DBCO) NHS ester were mixed with 1 equivalent GLuc in 100 mM phosphate-buffered saline (PBS), 150 mM NaCl, pH 8.45. The reaction was 4 h at room temperature and the product, GLuc-DBCO was purified with Slide-A-Lyzer™ Dialysis Cassettes MWCO 10,000. 10 µL of GLuc-DBCO reacted with 1 µL of azide-fluorophore 545 and the next day, the conjugate was checked with an absorbance spectrum using UV-vis spectroscopy (Figure 3.3). Protein concentration was determined using the Bicinchoninic Acid (BCA) Protein Assay Kit (Pierce Biotechnology, Rockford, IL) and a SpectraMax 190 Microplate Reader for absorbance measurements. The concentration of

the purified protein was measured using BCA assay according to manufacturer's instructions.

3.4.5 Synthesis of the conjugate molecular aptamer beacon with inhibitor

20 equivalents EDC, 50 equivalents sulfo-NHS and 50 equivalents coelenterazine inhibitor were added to the 100 µM of molecular aptamer beacon solution. The reaction was left at room temperature overnight under Ar atmosphere. The product was purified with microtube dialysis (Tube-O-DIALYZER, GBiosciences, Cat#786-611) with MWCO 4,000 and characterized with differential pulse voltammetry. Standard dilutions with known concentrations (1, 5, 10, 20, 50 µM) of coelenterazine inhibitor were made and from the standard curve, the 10 times diluted the aptamer-inhibitor was interpolated (Figure 3.4). Comparing the concentration of the conjugate and the total concentration that was measured with Spectramax 190 Microplate Reader, the yield of the reaction was calculated to be 90%.

3.4.6 Bioconjugation of molecular aptamer beacons with GLuc-DBCO

The reaction happened in a biotin-streptavidin column overnight at room temperature. The inhibitor modified molecular aptamer beacon was mixed with equal moles of biotin-complementary sequence (ACACAACACCCAACACAACCAACCCC, Sigma) in 80 °C for 5 min and 37 °C for 1 h. Afterwards, the appropriate amount of streptavidin was added according to manufacturer's instructions and mixed with 1.5 equivalents of GLuc-DBCO. The next day, the bioluminescent molecular aptamer beacon was washed with 100 µL PBS (100 mM sodium phosphate, 150 mM NaCl, pH 7.4) and eluted with 50 µL nuclease-free water at 80 °C. The concentration of the elutions was measured with Spectramax 190

Microplate Reader. After the concentration of the elutions with high-speed vacuum, the product was characterized with SDS-PAGE gel stained with silver stain.

3.4.7 Development of the bioluminescent assay

The bioluminescent molecular aptamer beacon was diluted to concentration 30 nM and was placed on a hot plate for 5 min at 80 °C. In the meantime, different dilutions of IFN-γ were prepared (10^{-11} M- 10^{-7} M) in protein LoBind tubes (Eppendorf, Cat#80077-232, Hauppauge, NY). After the 5 min, the dilution of the bioluminescent molecular beacon was left at RT for 15 min and it was added to the IFN-γ solutions to the final concentration of 15 nM. The tubes were left on an orbital shaker at room temperature for 1 h. 50 µL of each dilution in triplicates were loaded on a 96-well non-binding black plate. The bioluminescence response was measured in Clariostar by adding 100 µL of 1 µg/mL coelenterazine in each well.

Chapter 4

Prospective Research

4.1 Perspective work

The overall aim of the research discussed in the previous chapters, was the synthesis of novel biomolecules attached with reporters, specifically bioluminescent protein, luciferases that can be applied in different detection systems. The developed detection techniques introduced different approaches in molecular diagnostic with reduced assay times and faster results.

One of the approaches discussed, the molecular aptamer beacon approach has many challenges. One of the major difficulties is the availability of bioconjugation methods to link biomolecules. Recent advances made in the field of bioorthogonal chemistry can potentially offer improvements to simplify bioconjugation. In addition, different variants of bioluminescent protein, luciferases have been since developed with distinct bioluminescent properties and sizes which can offer novel properties such as increase in bioluminescent intensity, red-shift in emission and glow-type kinetics.[146] Therefore, by combining new bioconjugations techniques and employing novel reporters, biosensors with unique advantages can be developed.

Last but not least, it is necessary, for the developed biosensors, besides being sensitive, accurate and selective, to be simple and portable. In this regard, diagnostic tools that are suitable to be used in developed countries are often incompatible for underdeveloped

countries due to lack of resources. For example, there are no trained people to use the instruments or even power to plug these instruments. Therefore, the medical care in these countries is even more challenging.

This chapter, titled Prospective Research, is inspired from the projects that have already been discussed in this dissertation. The future aspect of this work may affect the bioanalytical research to develop new diagnostic tools with lower sensitivity which will enable investigators diagnose potential diseases earlier than currently possible therefore increasing the effectiveness of the therapeutic interventions. The following sections are short discussions of individual projects which will improve the work already presented in this dissertation.

4.2 Different protein bioorthogonal conjugation with the molecular aptamer beacon

The method used to attach the linker NHS-DBCO on the bioluminescent protein, GLuc, is through the amines of the lysines residues. As it has been discussed in the first chapter, the succinimidyl ester chemistry cannot be controlled easily due to the abundance of lysine residues on proteins. Moreover, the crystal structure of GLuc is not known which complicates the conjugation problem even further. To avoid this drawback, a new bioorthogonal technique needs to be introduced which will modify the protein in a stoichiometric manner.

In the Chapter 2, FBDP, first synthesized by Barba's group, was introduced.[37] From our experience, the reaction between FBDP and the ortho position of the tyrosine residue happens in high yields under physiological conditions. Therefore, we can introduce another

diazonium reagent with an alkyne modification in the *para* position of the diazonium salt. The reagent, 4-Ethynylaniline is available commercially and performing the reaction of the synthesis of FBDP, a new diazonium reagent may be synthesized (Figure 4.1). This reagent provides bioorthogonal alkyne functionality which can further react with the azide end of the molecular aptamer beacon with copper-catalyzed click chemistry.

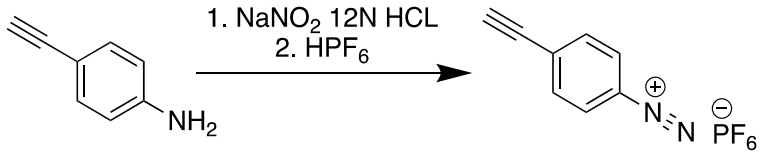

Figure 4.1. Synthesis of the alkyne diazonium salt.

Briefly, the reaction steps might proceed as follow (Figure 4.2):

1. Synthesis of the alkyne diazonium salt according to the protocol by Gravilyuk et al.[37]
2. Copper-catalyzed click chemistry between the azide end of the molecular aptamer beacon and the alkyne diazonium salt.
3. Conjugation of the alkyne diazonium salt end with the tyrosine GLuc (GLucY) under physiological conditions.

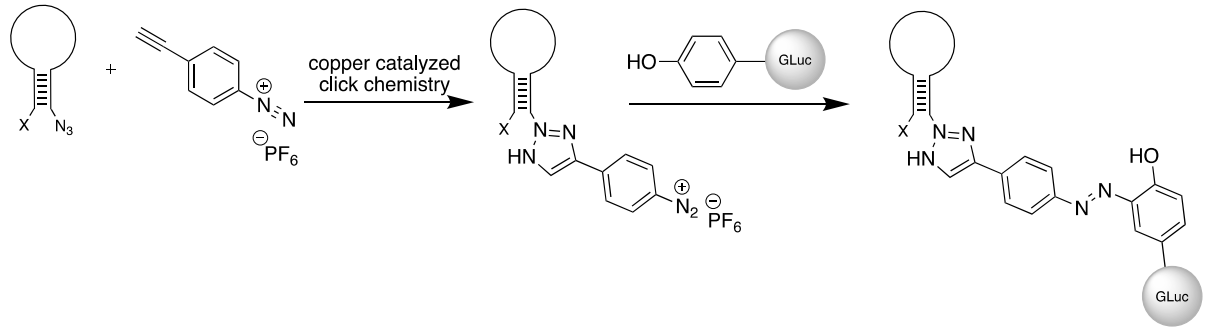

Figure 4.2. Conjugation scheme of the synthesis of the molecular aptamer beacon with GLuc using the reagent alkyne diazonium salt.

4.3 Modification of the bioluminescent molecular aptamer beacon

While the molecular aptamer beacon shown in Chapter 3 is a new approach and there is no precedence in the literature yet, the synthesis of the inhibitor and its conjugation on the beacon can be challenging. The synthesis of the inhibitor does not give a high yield product and the reagents EDC/NHS are hydrolyzed fast. The use of other inhibitors or different quenchers besides the dark-quenchers could potentially give faster synthetic results and improve the sensitivity.

As it was mentioned in Chapter 1, there are different energy acceptors except for quenchers such as gold nanoparticles and graphene oxide. It has been shown that both of them quench the fluorescence ~99% which make them good candidate for the OFF-ON signal that is necessary for the molecular aptamer beacons. However, it has not been proven that these energy acceptors can quench the bioluminescence signal that comes from the proteins.

Some preliminary data that we have performed, have shown the efficient quenching (~90%) of the bioluminescence signal from the graphene oxide (Figure 4.3). Briefly, the commercially available molecular aptamer beacon was conjugated with the bioluminescent protein GLuc according to Chapter 3 and it was mixed with an optimized concentration of graphene oxide. Upon target binding the bioluminescence was recovered almost 90%. More optimization studies need to be performed, but it may be a potential biosensor which is synthesized with relative ease when compared to the current inhibitor-based probe.

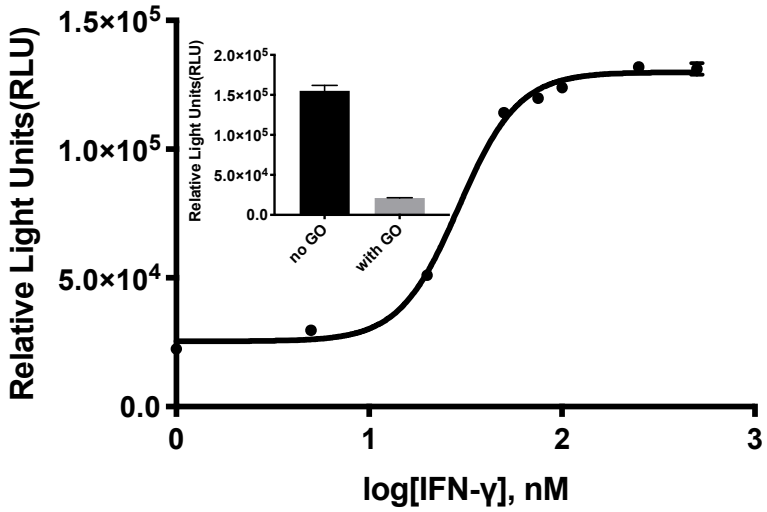

Figure 4.3. Dose response curve of the bioluminescent molecular aptamer beacon with graphene oxide (GO) and the inset shows the quenching efficiency of GO.

While there is no doubt that GLuc is an excellent bioluminescent reporter for bioanalytical and clinical research applications with many advantages such as its size or its independence to ATP or Ca^{2+} for the bioluminescent reaction to occur, there has been a number of publications introducing several mutations on GLuc in order to improve its bioluminescent properties[145,185]. Moreover, although GLuc is one of the smallest of the bioluminescent proteins we have successfully truncated GLucY previously[146] while preserving its bioluminescent properties. This truncated version of the GLucY also contained the beneficial mutations that has been described by other groups.[145,185] The reduction in size while preserving its bioluminescent properties would be very beneficial in biosensor design because transport into the cells can be facilitated with relative ease, for further studies. Therefore, the truncated GLuc variants can be introduced on the design of the inhibitor-molecular aptamer beacon, providing lower steric hindrance which in turn, expedite the inhibitor binding to the enzymatic pocket.

4.4 Assay based on electrochemistry

As it was described in Chapter 3, the characterization of the conjugation between the coelenteramine-inhibitor with the carboxylic end of the molecular aptamer beacon was performed using cyclic voltammetry. The coelenteramine-inhibitor was shown to be an electrochemically active compound since a peak was observed using differential pulse voltammetry. By taking advantage of this characteristic peak, another detection approach with an electrochemical aptamer-based biosensor can be developed.

The conventional biosensors that are based on the optical detection may have excellent performance, with good sensitivity and selectivity. On the other hand, optical-based conventional biosensors require expensive reagents such as antibodies, are insensitive in high concentration of the analyte because of the inner filter effect (linearity deviation) and the sample needs to be diluted and aren't easy to use in portable devices.

The electrochemical assays have high sensitivity, specificity, are simple, the electrodes are inexpensive and can be modified to be used with a portable instrument. There are even some cell phone based electrochemical instruments in development.[186] The main advantage of the electrochemical detection is that the electrodes can be screen-printed which are disposable, portable, and have lower cost when compared to the conventional electrodes.[187] There are several approaches of developing electrochemical assays for biological applications with screen-printed electrodes.[188] The screen-printed electrodes are similar with the conventional electrodes, and consist of working, reference, and counter electrodes and are printed using various types of materials. The inks used for printing the working electrode are mainly on carbon based and sometimes gold. Electrodes that are based on

gold nanoparticles take advantage of the high affinity between Au-S which immobilizes different thiolated molecules (DNA, antibody) covalently.

Cyclic voltammetry (CV) and electrochemical impedance spectroscopy (EIS) are two of the main methods for developing electrochemical assays. Electrochemical impedance spectroscopy is more sensitive, and it operates by measuring the charge transfer resistance (R_{ct}) on the electrode, the modification of the electrode with the probe and the analyte. Therefore, R_{ct} increases with the binding of a substance because the resistance is affected.[189] On the other hand, CV measures the oxidation/reduction potential of an electrochemically active tag. So, the oxidation peak increases with the deposition of the modified probe with tag and decreases with the increase of the concentration of the analyte. As it is aforementioned, the coelenteramine-inhibitor is a possible electrochemically active tag which can be applied and developed an aptamer-based electrochemical assay. So, it can be conjugated to a molecular aptamer beacon through EDC/NHS chemistry and afterwards this probe can be attached for example on a gold-modified surface of an electrode (Figure 4.4). The inhibitor-modified aptamer will increase the oxidation peak in a CV graph or the resistance in an EIS graph. Different amounts of the analyte can be introduced, and the electrochemical signal will be measured either with CV (decrease of the oxidation peak) or EIS (signal increase). Moreover, this electrochemical biosensor can be evaluated in biological fluids because it is easier to wash off other components such as oligonucleotides, lipids that increase the matrix effect.

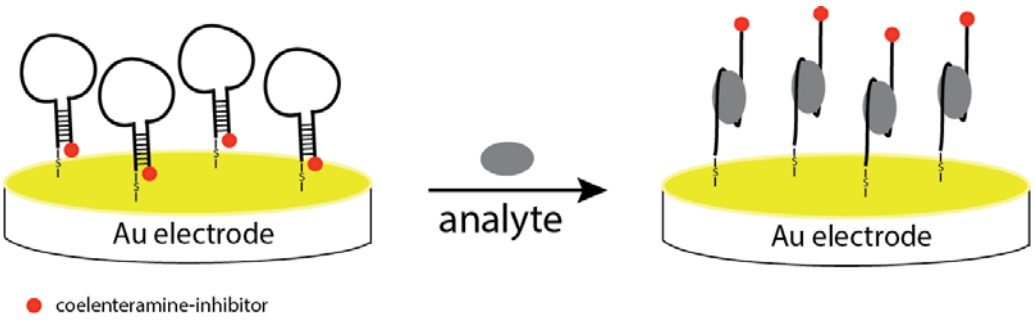

Figure 4.4. Schematic illustration of the electrochemical biosensor

4.5 Final Remarks

The research presented in this dissertation has highlighted the importance of novel, diagnostic and detection systems in biomedicine. We have demonstrated that novel sensing systems based on biomolecules such as DNA, protein and aptamers can be very selective and sensitive. One of the main areas that that need improvement in sensing system development is method of conjugation of a reporter on the biomolecule. The more control one has over the stoichiometry and the regioselectivity of a bioconjugation the better is performance of the biomolecule employed in the sensing system. Another crucial, part of the sensing system development is the improvement of sensitivity. Herein, we have demonstrated that bioluminescent proteins offer higher sensitivity and the bioluminescent signal does not suffer from the matrix effect issues. We have demonstrated that our bioluminescent immunoassay that was discussed in Chapter 2, reduced the overall processing time when comparing with the commercially available ELISA kit with similar sensitivities. Additionally, the bioluminescent inhibitor-based molecular aptamer beacon opened a new approach in the design of assays based on molecular aptamer beacon.

References

1 Ning, X., Guo, J., Wolfert, M. A. & Boons, G. J. Visualizing metabolically labeled glycoconjugates of living cells by copper-free and fast huisgen cycloadditions. *Angew Chem Int Ed Engl* **47**, 2253-2255, doi:10.1002/anie.200705456 (2008).

2 Rup, B. & O'Hara, D. Critical ligand binding reagent preparation/selection: when specificity depends on reagents. *AAPS J* **9**, E148-155, doi:10.1208/aapsj0902016 (2007).

3 Boutureira, O. & Bernardes, G. J. Advances in chemical protein modification. *Chem Rev* **115**, 2174-2195, doi:10.1021/cr500399p (2015).

4 Spicer, C. D. & Davis, B. G. Selective chemical protein modification. *Nat Commun* **5**, 4740, doi:10.1038/ncomms5740 (2014).

5 Hermanson, G. T. *Bioconjugate techniques*. 2nd edition. edn, (Academic Press, 2008).

6 Xia, B. *et al.* Biofunctionalisation of porous silicon (PS) surfaces by using homobifunctional cross-linkers. *Journal of Materials Chemistry* **16**, 570-578, doi:10.1039/B511175G (2006).

7 Narain, R. *Chemistry of bioconjugates : synthesis, characterization, and biomedical applications*. (Wiley, 2014).

8 Bhatia, S. K. *et al.* Use of thiol-terminal silanes and heterobifunctional crosslinkers for immobilization of antibodies on silica surfaces. *Anal Biochem* **178**, 408-413 (1989).

9 Riener, C. K. *et al.* Heterobifunctional crosslinkers for tethering single ligand molecules to scanning probes. *Analytica Chimica Acta* **497**, 101-114, doi:10.1016/j.aca.2003.08.041 (2003).

10 Koniev, O. & Wagner, A. Developments and recent advancements in the field of endogenous amino acid selective bond forming reactions for bioconjugation (vol 44, pg 5495, 2015). *Chemical Society Reviews* **44**, 5743-5743, doi:10.1039/c5cs90060c (2015).

11 Ariyasu, S., Hayashi, H., Xing, B. G. & Chiba, S. Site-specific dual functionalization of cysteine residue in peptides and proteins with 2-azidoacrylates. *Bioconjugate Chem* **28**, 897-902, doi:10.1021/acs.bioconjchem.7b00024 (2017).

12 Gunnoo, S. B. & Madder, A. Chemical protein modification through cysteine. *Chembiochem* **17**, 529-553, doi:10.1002/cbic.201500667 (2016).

13 Hang, H. C., Yu, C., Kato, D. L. & Bertozzi, C. R. A metabolic labeling approach toward proteomic analysis of mucin-type O-linked glycosylation. *Proc Natl Acad Sci U S A* **100**, 14846-14851, doi:10.1073/pnas.2335201100 (2003).

14 Sletten, E. M. & Bertozzi, C. R. Bioorthogonal chemistry: fishing for selectivity in a sea of functionality. *Angew Chem Int Ed Engl* **48**, 6974-6998, doi:10.1002/anie.200900942 (2009).

15 Shih, H. W., Kamber, D. N. & Prescher, J. A. Building better bioorthogonal reactions. *Curr Opin Chem Biol* **21**, 103-111, doi:10.1016/j.cbpa.2014.07.002 (2014).

16 Lim, R. K. & Lin, Q. Bioorthogonal chemistry-a covalent strategy for the study of biological systems. *Sci China Chem* **53**, 61-70, doi:10.1007/s11426-010-0020-4 (2010).

17 Dirksen, A., Dirksen, S., Hackeng, T. M. & Dawson, P. E. Nucleophilic catalysis of hydrazone formation and transimination: implications for dynamic covalent chemistry. *J Am Chem Soc* **128**, 15602-15603, doi:10.1021/ja067189k (2006).

18 Dirksen, A., Hackeng, T. M. & Dawson, P. E. Nucleophilic catalysis of oxime ligation. *Angew Chem Int Ed Engl* **45**, 7581-7584, doi:10.1002/anie.200602877 (2006).

19 Blackman, M. L., Royzen, M. & Fox, J. M. Tetrazine ligation: fast bioconjugation based on inverse-electron-demand Diels-Alder reactivity. *J Am Chem Soc* **130**, 13518-13519, doi:10.1021/ja8053805 (2008).

20 Devaraj, N. K., Weissleder, R. & Hilderbrand, S. A. Tetrazine-based cycloadditions: application to pretargeted live cell imaging. *Bioconjug Chem* **19**, 2297-2299, doi:10.1021/bc8004446 (2008).

21 Bakthadoss, M., Devaraj, A., Madhanraj, R. & Murugavel, S. (E)-3-(1,3-Benzodioxol-5-yl)-2-{[N-(2-formylphenyl)-4-methylbenzenesulfon-amido]methyl}prop-2-enenitrile. *Acta Crystallogr Sect E Struct Rep Online* **68**, o3164-3165, doi:10.1107/S1600536812042663 (2012).

22 McKay, C. S. & Finn, M. G. Click chemistry in complex mixtures: bioorthogonal bioconjugation. *Chem Biol* **21**, 1075-1101, doi:10.1016/j.chembiol.2014.09.002 (2014).

23 Oya, T. *et al.* Methylglyoxal modification of protein. Chemical and immunochemical characterization of methylglyoxal-arginine adducts. *J Biol Chem* **274**, 18492-18502 (1999).

24 Kramer, J. R. & Deming, T. J. Preparation of multifunctional and multireactive polypeptides via methionine alkylation. *Biomacromolecules* **13**, 1719-1723, doi:10.1021/bm300807b (2012).

25 Kramer, J. R. & Deming, T. J. Reversible chemoselective tagging and functionalization of methionine containing peptides. *Chem Commun (Camb)* **49**, 5144-5146, doi:10.1039/c3cc42214c (2013).

26 Lin, S. *et al.* Redox-based reagents for chemoselective methionine bioconjugation. *Science* **355**, 597-602, doi:10.1126/science.aal3316 (2017).

27 Li, X. F., Zhang, L. S., Hall, S. E. & Tam, J. P. A new ligation method for N-terminal tryptophan-containing peptides using the Pictet-Spengler reaction. *Tetrahedron Lett* **41**, 4069-4073, doi:Doi 10.1016/S0040-4039(00)00592-X (2000).

28 Sletten, E. M. & Bertozzi, C. R. Bioorthogonal Chemistry: Fishing for selectivity in a sea of functionality. *Angew Chem Int Edit* **48**, 6974-6998, doi:10.1002/anie.200900942 (2009).

29 Tilley, S. D. & Francis, M. B. Tyrosine-selective protein alkylation using pi-allylpalladium complexes. *J Am Chem Soc* **128**, 1080-1081, doi:10.1021/ja057106k (2006).

30 Joshi, N. S., Whitaker, L. R. & Francis, M. B. A three-component Mannich-type reaction for selective tyrosine bioconjugation. *J Am Chem Soc* **126**, 15942-15943, doi:10.1021/ja0439017 (2004).

31 Mileo, E. *et al.* Enlarging the panoply of site-directed spin labeling electron paramagnetic resonance (SDSL-EPR): sensitive and selective spin-labeling of tyrosine using an isoindoline-based nitroxide. *Bioconjug Chem* **24**, 1110-1117, doi:10.1021/bc4000542 (2013).

32 Ban, H. *et al.* Facile and stabile linkages through tyrosine: bioconjugation strategies with the tyrosine-click reaction. *Bioconjug Chem* **24**, 520-532, doi:10.1021/bc300665t (2013).

33 Ban, H., Gavrilyuk, J. & Barbas, C. F., 3rd. Tyrosine bioconjugation through aqueous ene-type reactions: a click-like reaction for tyrosine. *J Am Chem Soc* **132**, 1523-1525, doi:10.1021/ja909062q (2010).

34 Schlick, T. L., Ding, Z., Kovacs, E. W. & Francis, M. B. Dual-surface modification of the tobacco mosaic virus. *J Am Chem Soc* **127**, 3718-3723, doi:10.1021/ja046239n (2005).

35 Hooker, J. M., Kovacs, E. W. & Francis, M. B. Interior surface modification of bacteriophage MS2. *J Am Chem Soc* **126**, 3718-3719, doi:10.1021/ja031790q (2004).

36 Jones, M. W. *et al.* Direct peptide bioconjugation/PEGylation at tyrosine with linear and branched polymeric diazonium salts. *J Am Chem Soc* **134**, 7406-7413, doi:10.1021/ja211855q (2012).

37 Gavrilyuk, J., Ban, H., Nagano, M., Hakamata, W. & Barbas, C. F., 3rd. Formylbenzene diazonium hexafluorophosphate reagent for tyrosine-selective modification of proteins and the introduction of a bioorthogonal aldehyde. *Bioconjug Chem* **23**, 2321-2328, doi:10.1021/bc300410p (2012).

38 Dirksen, A. & Dawson, P. E. Rapid oxime and hydrazone ligations with aromatic aldehydes for biomolecular labeling. *Bioconjug Chem* **19**, 2543-2548, doi:10.1021/bc800310p (2008).

39 Kolb, H. C., Finn, M. G. & Sharpless, K. B. Click chemistry: diverse chemical function from a few good reactions. *Angew Chem Int Ed Engl* **40**, 2004-2021 (2001).

40 Kiick, K. L., Saxon, E., Tirrell, D. A. & Bertozzi, C. R. Incorporation of azides into recombinant proteins for chemoselective modification by the Staudinger ligation. *Proc Natl Acad Sci U S A* **99**, 19-24, doi:10.1073/pnas.012583299 (2002).

41 Dube, D. H. & Bertozzi, C. R. Metabolic oligosaccharide engineering as a tool for glycobiology. *Curr Opin Chem Biol* **7**, 616-625 (2003).

42 Kho, Y. *et al.* A tagging-via-substrate technology for detection and proteomics of farnesylated proteins. *Proc Natl Acad Sci U S A* **101**, 12479-12484, doi:10.1073/pnas.0403413101 (2004).

43 Prescher, J. A., Dube, D. H. & Bertozzi, C. R. Chemical remodelling of cell surfaces in living animals. *Nature* **430**, 873-877, doi:10.1038/nature02791 (2004).

44 Huisgen, R. 1,3-Dipolar cycloadditions. past and future. *Angewandte Chemie International Edition in English* **2**, 565-598, doi:doi:10.1002/anie.196305651 (1963).

45 Tornoe, C. W., Christensen, C. & Meldal, M. Peptidotriazoles on solid phase: [1,2,3]-triazoles by regiospecific copper(i)-catalyzed 1,3-dipolar cycloadditions of terminal alkynes to azides. *J Org Chem* **67**, 3057-3064 (2002).

46 Rostovtsev, V. V., Green, L. G., Fokin, V. V. & Sharpless, K. B. A stepwise huisgen cycloaddition process: copper(I)-catalyzed regioselective "ligation" of azides and terminal alkynes. *Angew Chem Int Ed Engl* **41**, 2596-2599, doi:10.1002/1521-3773(20020715)41:14<2596::AID-ANIE2596>3.0.CO;2-4 (2002).

47 Wittig, G. & Krebs, A. Zur existenz niedergliedriger cycloalkine, I. *Chemische Berichte* **94**, 3260-3275, doi:doi:10.1002/cber.19610941213 (1961).

48 Turner, R. B. *et al.* Heats of Hydrogenation .10. Conjugative interaction in cyclic dienes and trienes. *Journal of the American Chemical Society* **95**, 8605-8610, doi:DOI 10.1021/ja00807a017 (1973).

49 Agard, N. J., Prescher, J. A. & Bertozzi, C. R. A strain-promoted [3+2] azide-alkyne cycloaddition for covalent modification of blomolecules in living systems. *Journal of the American Chemical Society* **126**, 15046-15047, doi:10.1021/ja0449981 (2004).

50 Baskin, J. M. *et al.* Copper-free click chemistry for dynamic in vivo imaging. *Proc Natl Acad Sci U S A* **104**, 16793-16797, doi:10.1073/pnas.0707090104 (2007).

51 Fischer-Durand, N., Salmain, M., Vessieres, A. & Jaouen, G. A new bioorthogonal cross-linker with alkyne and hydrazide end groups for chemoselective ligation. Application to antibody labelling. *Tetrahedron* **68**, 9638-9644, doi:10.1016/j.tet.2012.09.062 (2012).

52 Ran, B. *et al.* Bioorthogonal reaction-mediated ELISA using peroxide test strip as signal readout for point-of-care testing. *Analytical Chemistry* **89**, 6114-6120, doi:10.1021/acs.analchem.7b00831 (2017).

53 Merkel, M., Peewasan, K., Arndt, S., Ploschik, D. & Wagenknecht, H. A. Copper-free postsynthetic labeling of nucleic acids by means of bioorthogonal reactions. *Chembiochem* **16**, 1541-1553, doi:10.1002/cbic.201500199 (2015).

54 Gierlich, J., Burley, G. A., Gramlich, P. M., Hammond, D. M. & Carell, T. Click chemistry as a reliable method for the high-density postsynthetic functionalization of alkyne-modified DNA. *Org Lett* **8**, 3639-3642, doi:10.1021/ol0610946 (2006).

55 Beyer, C. & Wagenknecht, H. A. In situ azide formation and "click" reaction of nile red with DNA as an alternative postsynthetic route. *Chem Commun (Camb)* **46**, 2230-2231, doi:10.1039/b924471a (2010).

56 Seela, F., Xiong, H., Leonard, P. & Budow, S. 8-Aza-7-deazaguanine nucleosides and oligonucleotides with octadiynyl side chains: synthesis, functionalization by the azide-alkyne 'click' reaction and nucleobase specific fluorescence quenching of coumarin dye conjugates. *Org Biomol Chem* **7**, 1374-1387, doi:10.1039/b822041g (2009).

57 Singh, I., Freeman, C. & Heaney, F. Efficient synthesis of DNA conjugates by strain-promoted azide-cyclooctyne cycloaddition in the solid phase. *Eur J Org Chem*, 6739-6746, doi:10.1002/ejoc.201101045 (2011).

58 Borsenberger, V. & Howorka, S. Diene-modified nucleotides for the DielsAlder-mediated functional tagging of DNA. *Nucleic Acids Research* **37**, 1477-1485, doi:10.1093/nar/gkn1066 (2009).

59 Li, J. J., Fang, X. & Tan, W. Molecular aptamer beacons for real-time protein recognition. *Biochem Biophys Res Commun* **292**, 31-40 (2002).

60 Pysz, M. A., Gambhir, S. S. & Willmann, J. K. Molecular imaging: current status and emerging strategies. *Clin Radiol* **65**, 500-516, doi:10.1016/j.crad.2010.03.011 (2010).

61 Abbott, A. A post-genomic challenge: learning to read patterns of protein synthesis. *Nature* **402**, 715-720, doi:10.1038/45350 (1999).

62 Liang, Y. *et al.* Aptamer beacons for visualization of endogenous protein HIV-1 reverse transcriptase in living cells. *Biosens Bioelectron* **28**, 270-276, doi:10.1016/j.bios.2011.07.031 (2011).

63 Tyagi, S. & Kramer, F. R. Molecular beacons: probes that fluoresce upon hybridization. *Nat Biotechnol* **14**, 303-308, doi:10.1038/nbt0396-303 (1996).

64 Zheng, J. *et al.* Rationally designed molecular beacons for bioanalytical and biomedical applications. *Chem Soc Rev* **44**, 3036-3055, doi:10.1039/c5cs00020c (2015).

65 Lee, T. M. *et al.* Gender differences in neural correlates of recognition of happy and sad faces in humans assessed by functional magnetic resonance imaging. *Neurosci Lett* **333**, 13-16 (2002).

66 Tsourkas, A., Behlke, M. A., Rose, S. D. & Bao, G. Hybridization kinetics and thermodynamics of molecular beacons. *Nucleic Acids Res* **31**, 1319-1330 (2003).

67 Tyagi, S., Bratu, D. P. & Kramer, F. R. Multicolor molecular beacons for allele discrimination. *Nat Biotechnol* **16**, 49-53, doi:10.1038/nbt0198-49 (1998).

68 Kramer, F. R., Mills, D. R., Cole, P. E., Nishihara, T. & Spiegelman, S. Evolution in vitro: sequence and phenotype of a mutant RNA resistant to ethidium bromide. *J Mol Biol* **89**, 719-736 (1974).

69 Tuerk, C. & Gold, L. Systematic evolution of ligands by exponential enrichment: RNA ligands to bacteriophage T4 DNA polymerase. *Science* **249**, 505-510 (1990).

70 Ellington, A. D. & Szostak, J. W. In vitro selection of RNA molecules that bind specific ligands. *Nature* **346**, 818-822, doi:10.1038/346818a0 (1990).

71 Robertson, D. L. & Joyce, G. F. Selection in vitro of an RNA enzyme that specifically cleaves single-stranded DNA. *Nature* **344**, 467-468, doi:10.1038/344467a0 (1990).

72 Iliuk, A. B., Hu, L. & Tao, W. A. Aptamer in bioanalytical applications. *Anal Chem* **83**, 4440-4452, doi:10.1021/ac201057w (2011).

73 Prakash, J. S. & Rajamanickam, K. Aptamers and their significant role in cancer therapy and diagnosis. *Biomedicines* **3**, 248-269, doi:10.3390/biomedicines3030248 (2015).

74 Zhou, J. & Rossi, J. Aptamers as targeted therapeutics: current potential and challenges. *Nat Rev Drug Discov* **16**, 181-202, doi:10.1038/nrd.2016.199 (2017).

75 Han, K., Liang, Z. & Zhou, N. Design strategies for aptamer-based biosensors. *Sensors (Basel)* **10**, 4541-4557, doi:10.3390/s100504541 (2010).

76 Ku, T. H. *et al.* Nucleic Acid Aptamers: An emerging tool for biotechnology and biomedical sensing. *Sensors (Basel)* **15**, 16281-16313, doi:10.3390/s150716281 (2015).

77 Lakowicz, J. R. Principles of fluorescence spectroscopy. 2nd edn, (Kluwer Academic/Plenum, 1999).

78 Le Reste, L., Hohlbein, J., Gryte, K. & Kapanidis, A. N. Characterization of dark quencher chromophores as nonfluorescent acceptors for single-molecule FRET. *Biophys J* **102**, 2658-2668, doi:10.1016/j.bpj.2012.04.028 (2012).

79 Li, J. W. J., Perlette, J., Fang, X. H., Kelley, S. & Tan, W. H. Novel molecular beacon DNA probes for protein-nucleic acid interaction studies. *Prog Biom O* **1**, 27-33 (2000).

80 Hamaguchi, N., Ellington, A. & Stanton, M. Aptamer beacons for the direct detection of proteins. *Analytical Biochemistry* **294**, 126-131, doi:DOI 10.1006/abio.2001.5169 (2001).

81 Kim, B., Jung, I. H., Kang, M., Shim, H. K. & Woo, H. Y. Cationic conjugated polyelectrolytes-triggered conformational change of molecular beacon aptamer for highly sensitive and selective potassium ion detection. *J Am Chem Soc* **134**, 3133-3138, doi:10.1021/ja210360v (2012).

82 Li, J. W. J., Fang, X. H. & Tan, W. H. Molecular aptamer beacons for real-time protein recognition. *Biochem Bioph Res Co* **292**, 31-40, doi:10.1006/bbrc.2002.6581 (2002).

83 Tok, J., Lai, J., Leung, T. & Li, S. F. Y. Molecular aptamer beacon for myotonic dystrophy kinase-related Cdc42-binding kinase alpha. *Talanta* **81**, 732-736, doi:10.1016/j.talanta.2010.01.013 (2010).

84 Yamamoto, R. & Kumar, P. K. R. Molecular beacon aptamer fluoresces in the presence of Tat protein of HIV-1. *Genes Cells* **5**, 389-396, doi:DOI 10.1046/j.1365-2443.2000.00331.x (2000).

85 Liang, Y. *et al.* Aptamer beacons for visualization of endogenous protein HIV-1 reverse transcriptase in living cells. *Biosensors & Bioelectronics* **28**, 270-276, doi:10.1016/j.bios.2011.07.031 (2011).

86 Tuleuova, N. *et al.* Development of an aptamer beacon for detection of interferon-gamma. *Anal Chem* **82**, 1851-1857, doi:10.1021/ac9025237 (2010).

87 Wu, C. C. *et al.* Engineering of Switchable Aptamer Micelle Flares for Molecular Imaging in Living Cells. *Acs Nano* **7**, 5724-5731, doi:10.1021/nn402517v (2013).

88 Song, K. M., Lee, S. & Ban, C. Aptamers and their biological applications. *Sensors-Basel* **12**, 612-631, doi:10.3390/s120100612 (2012).

89 Shigdar, S. *et al.* Aptamers as theranostic agents: modifications, serum stability and functionalisation. *Sensors (Basel)* **13**, 13624-13637, doi:10.3390/s131013624 (2013).

90 Shi, H. *et al.* Activatable aptamer probe for contrast-enhanced in vivo cancer imaging based on cell membrane protein-triggered conformation alteration. *P Natl Acad Sci USA* **108**, 3900-3905, doi:10.1073/pnas.1016197108 (2011).

91 Chuang, E. Y. *et al.* A FRET-guided, NIR-responsive bubble-generating liposomal system for in vivo targeted therapy with spatially and temporally precise controlled release. *Biomaterials* **93**, 48-59, doi:10.1016/j.biomaterials.2016.03.040 (2016).

92 Hardman, R. A toxicologic review of quantum dots: toxicity depends on physicochemical and environmental factors. *Environ Health Perspect* **114**, 165-172, doi:10.1289/ehp.8284 (2006).

93 Bruchez, M., Jr., Moronne, M., Gin, P., Weiss, S. & Alivisatos, A. P. Semiconductor nanocrystals as fluorescent biological labels. *Science* **281**, 2013-2016 (1998).

94 Levy, M., Cater, S. F. & Ellington, A. D. Quantum-dot aptamer beacons for the detection of proteins. *Chembiochem* **6**, 2163-2166, doi:10.1002/cbic.200500218 (2005).

95 Kim, J. H., Morikis, D. & Ozkan, M. Adaptation of inorganic quantum dots for stable molecular beacons. *Sensor Actuat B-Chem* **102**, 315-319 (2004).

96 Medintz, I. L. *et al.* Self-assembled nanoscale biosensors based on quantum dot FRET donors. *Nat Mater* **2**, 630-638 (2003).

97 Ge, J. & Yin, Y. Responsive photonic crystals. *Angew Chem Int Ed Engl* **50**, 1492-1522, doi:10.1002/anie.200907091 (2011).

98 Wang, C., Lim, C. Y., Choi, E., Park, Y. & Park, J. Highly sensitive user friendly thrombin detection using emission light guidance from quantum dots-aptamer beacons in 3-dimensional photonic crystal. *Sensor Actuat B-Chem* **223**, 372-378, doi:10.1016/j.snb.2015.09.101 (2016).

99 Chi, C. W., Lao, Y. H., Li, Y. S. & Chen, L. C. A quantum dot-aptamer beacon using a DNA intercalating dye as the FRET reporter: Application to label-free thrombin detection. *Biosensors & Bioelectronics* **26**, 3346-3352, doi:10.1016/j.bios.2011.01.015 (2011).

100 Shin, S., Nam, H. Y., Lee, E. J., Jung, W. & Hah, S. S. Molecular beacon-based quantitiation of epithelial tumor marker mucin 1. *Bioorg Med Chem Lett* **22**, 6081-6084, doi:10.1016/j.bmcl.2012.08.037 (2012).

101 Lao, Y. H. *et al.* Signal-on Protein Detection via Dye Translocation between Aptamer and Quantum Dot. *Acs Appl Mater Inter* **8**, 12048-12055, doi:10.1021/acsami.6b02871 (2016).

102 Bagalkot, V. *et al.* Quantum dot - Aptamer conjugates for synchronous cancer imaging, therapy, and sensing of drug delivery based on Bi-fluorescence resonance energy transfer. *Nano Letters* **7**, 3065-3070, doi:10.1021/nl071546n (2007).

103 Dong, H., Gao, W., Yan, F., Ji, H. & Ju, H. Fluorescence resonance energy transfer between quantum dots and graphene oxide for sensing biomolecules. *Anal Chem* **82**, 5511-5517, doi:10.1021/ac100852z (2010).

104 Wang, Y. *et al.* Aptamer/graphene oxide nanocomplex for in situ molecular probing in living cells. *J Am Chem Soc* **132**, 9274-9276, doi:10.1021/ja103169v (2010).

105 Chen, L. *et al.* Nitrogen and Sulfur Codoped Reduced Graphene Oxide as a General Platform for Rapid and Sensitive Fluorescent Detection of Biological Species. *Acs Appl Mater Inter* **8**, 11255-11261, doi:10.1021/acsami.6b01030 (2016).

106 Zhen, S. J. *et al.* Carbon nanotubes as a low background signal platform for a molecular aptamer beacon on the basis of long-range resonance energy transfer. *Anal Chem* **82**, 8432-8437, doi:10.1021/ac100709s (2010).

107 He, Y., Wang, Z. G., Tang, H. W. & Pang, D. W. Low background signal platform for the detection of ATP: when a molecular aptamer beacon meets graphene oxide. *Biosens Bioelectron* **29**, 76-81, doi:10.1016/j.bios.2011.07.069 (2011).

108 Zhuang, H. L., Zhen, S. J., Wang, J. & Huang, C. Z. Sensitive detection of prion protein through long range resonance energy transfer between graphene oxide and molecular aptamer beacon. *Anal Methods-Uk* **5**, 208-212, doi:10.1039/c2ay26156a (2013).

109 Dubertret, B., Calame, M. & Libchaber, A. J. Single-mismatch detection using gold-quenched fluorescent oligonucleotides. *Nat Biotechnol* **19**, 365-370, doi:10.1038/86762 (2001).

110 Seferos, D. S., Prigodich, A. E., Giljohann, D. A., Patel, P. C. & Mirkin, C. A. Polyvalent DNA nanoparticle conjugates stabilize nucleic acids. *Nano Lett* **9**, 308-311, doi:10.1021/nl802958f (2009).

111 Zheng, D., Seferos, D. S., Giljohann, D. A., Patel, P. C. & Mirkin, C. A. Aptamer nano-flares for molecular detection in living cells. *Nano Lett* **9**, 3258-3261, doi:10.1021/nl901517b (2009).

112 Zhang, J. Q. *et al.* A gold nanoparticles-modified aptamer beacon for urinary adenosine detection based on structure-switching/fluorescence-"turning on" mechanism. *J Pharm Biomed Anal* **70**, 362-368, doi:10.1016/j.jpba.2012.05.032 (2012).

113 Armstrong, R. E. & Strouse, G. F. Rationally manipulating aptamer binding affinities in a stem-loop molecular beacon. *Bioconjug Chem* **25**, 1769-1776, doi:10.1021/bc500286r (2014).

114 Zheng, J., Nicovich, P. R. & Dickson, R. M. Highly fluorescent noble-metal quantum dots. *Annu Rev Phys Chem* **58**, 409-431, doi:10.1146/annurev.physchem.58.032806.104546 (2007).

115 Liu, G., Li, J., Feng, D. Q., Zhu, J. J. & Wang, W. Silver nanoclusters beacon as stimuli-responsive versatile platform for multiplex dnas detection and aptamer-substrate complexes sensing. *Anal Chem* **89**, 1002-1008, doi:10.1021/acs.analchem.6b04362 (2017).

116 Hunt, E. A. & Deo, S. K. Bioluminescent stem-loop probes for highly sensitive nucleic acid detection. *Chem Commun (Camb)* **47**, 9393-9395, doi:10.1039/c1cc13495g (2011).

117 Joda, H., Moutsiopoulou, A., Stone, G., Daunert, S. & Deo, S. Design of Gaussia luciferase-based bioluminescent stem-loop probe for sensitive detection of HIV-1 nucleic acids. *Analyst* **143**, 3374-3381, doi:10.1039/c8an00047f (2018).

118 Pellestor, F. & Paulasova, P. The peptide nucleic acids (PNAs), powerful tools for molecular genetics and cytogenetics. *Eur J Hum Genet* **12**, 694-700, doi:10.1038/sj.ejhg.5201226 (2004).

119 Jepsen, J. S., Sorensen, M. D. & Wengel, J. Locked nucleic acid: a potent nucleic acid analog in therapeutics and biotechnology. *Oligonucleotides* **14**, 130-146, doi:10.1089/1545457041526317 (2004).

120 Goldman, E. R. *et al.* Conjugation of luminescent quantum dots with antibodies using an engineered adaptor protein to provide new reagents for fluoroimmunoassays. *Anal Chem* **74**, 841-847 (2002).

121 Patterson, A. M., Siddall, H., Chamberlain, G., Gardner, L. & Middleton, J. Expression of the Duffy antigen/receptor for chemokines (DARC) by the inflamed synovial endothelium. *J Pathol* **197**, 108-116, doi:10.1002/path.1100 (2002).

122 Bander, N. H. Technology Insight: monoclonal antibody imaging of prostate cancer. *Nat Clin Pract Urol* **3**, 216-225, doi:10.1038/ncpuro0452 (2006).

123 El-Sayed, I. H., Huang, X. & El-Sayed, M. A. Surface plasmon resonance scattering and absorption of anti-EGFR antibody conjugated gold nanoparticles in cancer diagnostics: applications in oral cancer. *Nano Lett* **5**, 829-834, doi:10.1021/nl050074e (2005).

124 Carter, P., Smith, L. & Ryan, M. Identification and validation of cell surface antigens for antibody targeting in oncology. *Endocr-Relat Cancer* **11**, 659-687, doi:10.1677/erc.1.00766 (2004).

125 Agarwal, P. & Bertozzi, C. R. Site-specific antibody-drug conjugates: the nexus of bioorthogonal chemistry, protein engineering, and drug development. *Bioconjug Chem* **26**, 176-192, doi:10.1021/bc5004982 (2015).

126 Guo, H. L. *et al.* Kinetic analysis of a high-affinity antibody/antigen interaction performed by planar waveguide fluorescence immunosensor. *Rsc Adv* **6**, 13837-13845, doi:10.1039/c6ra01073c (2016).

127 Scouten, W. H., Luong, J. H. T. & Brown, R. S. Enzyme or Protein Immobilization Techniques for Applications in Biosensor Design. *Trends in Biotechnology* **13**, 178-185, doi:Doi 10.1016/S0167-7799(00)88935-0 (1995).

128 Tonkin, C. J. *et al.* Localization of organellar proteins in Plasmodium falciparum using a novel set of transfection vectors and a new immunofluorescence fixation method. *Mol Biochem Parasitol* **137**, 13-21, doi:10.1016/j.molbiopara.2004.05.009 (2004).

129 Rowe, L., Dikici, E. & Daunert, S. Engineering bioluminescent proteins: expanding their analytical potential. *Analytical Chemistry* **81**, 8662-8668, doi:10.1021/ac9007286 (2009).

130 Roda, A., Guardigli, M., Michelini, E. & Mirasoli, M. Bioluminescence in analytical chemistry and in vivo imaging. *TrAC Trends in Analytical Chemistry* **28**, 307-322, doi:http://dx.doi.org/10.1016/j.trac.2008.11.015 (2009).

131 Xiao, L. H. *et al.* Quantitation of RT-PCR amplified cytokine mRNA by aequorin-based bioluminescence immunoassay. *Journal of Immunological Methods* **199**, 139-147, doi:Doi 10.1016/S0022-1759(96)00174-3 (1996).

132 Scott, D., Dikici, E., Ensor, M. & Daunert, S. Bioluminescence and its impact on bioanalysis. *Annu Rev Anal Chem (Palo Alto Calif)* **4**, 297-319, doi:10.1146/annurev-anchem-061010-113855 (2011).

133 Cook, B. E. *et al.* Pretargeted PET Imaging using a site-specifically labeled immunoconjugate. *Bioconjug Chem* **27**, 1789-1795, doi:10.1021/acs.bioconjchem.6b00235 (2016).

134 Hermanson, G. T. *Bioconjugate techniques*. (Academic Press, 1996).

135 Lee, J. H. *et al.* High-yielding and photolabile approaches to the covalent attachment of biomolecules to surfaces via hydrazone chemistry. *Langmuir* **30**, 8452-8460, doi:10.1021/la500744s (2014).

136 Shrestha, S., Paeng, I. R., Deo, S. K. & Daunert, S. Cysteine-free mutant of aequorin as a photolabel in immunoassay development. *Bioconjug Chem* **13**, 269-275 (2002).

137 Lewis, J. C. & Daunert, S. Bioluminescence immunoassay for thyroxine employing genetically engineered mutant aequorins containing unique cysteine residues. *Anal Chem* **73**, 3227-3233 (2001).

138 Siti, W., Khan, A. K., de Hoog, H. P. M., Liedberg, B. & Nallani, M. Photo-induced conjugation of tetrazoles to modified and native proteins. *Organic & Biomolecular Chemistry* **13**, 3202-3206, doi:10.1039/c4ob02025a (2015).

139 Madl, C. M. & Heilshorn, S. C. Tyrosine-selective functionalization for bio-orthogonal cross-linking of engineered protein hydrogels. *Bioconjug Chem*, doi:10.1021/acs.bioconjchem.6b00720 (2017).

140 Joshi, N. S., Whitaker, L. R. & Francis, M. B. A three-component Mannich-type reaction for selective tyrosine bioconjugation. *Journal of the American Chemical Society* **126**, 15942-15943, doi:10.1021/ja0439017 (2004).

141 Venisnik, K. M., Olafsen, T., Gambhir, S. S. & Wu, A. M. Fusion of Gaussia luciferase to an engineered anti-carcinoembryonic antigen (CEA) antibody for in vivo optical imaging. *Molecular Imaging and Biology* **9**, 267-277, doi:10.1007/s11307-007-0101-8 (2007).

142 Tannous, B. A. Gaussia luciferase reporter assay for monitoring biological processes in culture and in vivo. *Nature Protocols* **4**, 582-591, doi:10.1038/nprot.2009.28 (2009).

143 Markova, S. V., Larionova, M. D., Burakova, L. P. & Vysotski, E. S. The smallest natural high-active luciferase: cloning and characterization of novel 16.5-kDa luciferase from copepod Metridia longa. *Biochem Biophys Res Commun* **457**, 77-82, doi:10.1016/j.bbrc.2014.12.082 (2015).

144 Tannous, B. A., Kim, D. E., Fernandez, J. L., Weissleder, R. & Breakefield, X. O. Codon-optimized Gaussia luciferase cDNA for mammalian gene expression in culture and in vivo. *Mol Ther* **11**, 435-443, doi:10.1016/j.ymthe.2004.10.016 (2005).

145 Inouye, S. & Sahara, Y. Identification of two catalytic domains in a luciferase secreted by the copepod Gaussia princeps. *Biochem Biophys Res Commun* **365**, 96-101, doi:10.1016/j.bbrc.2007.10.152 (2008).

146 Hunt, E. A. *et al.* Truncated variants of gaussia luciferase with tyrosine linker for site-specific bioconjugate applications. *Sci Rep* **6**, 26814, doi:10.1038/srep26814 (2016).

147 Roff, S. R., Noon-Song, E. N. & Yamamoto, J. K. The significance of interferon-gamma in hiv-1 pathogenesis, therapy, and prophylaxis. *Front Immunol* **4**, 498, doi:10.3389/fimmu.2013.00498 (2014).

148 Cox, K. L. *et al.* in *Assay Guidance Manual* (eds G. S. Sittampalam *et al.*) (2004).

149 Zhang, L., Kuhn, M., Peers, I. & Altan, S. *Nonclinical statistics for pharmaceutical and biotechnology industries*. (Springer, 2016).

150 Rathnayaka, T., Tawa, M., Sohya, S., Yohda, M. & Kuroda, Y. Biophysical characterization of highly active recombinant Gaussia luciferase expressed in Escherichia coli. *Biochim Biophys Acta* **1804**, 1902-1907, doi:10.1016/j.bbapap.2010.04.014 (2010).

151 Feliu, J. X., Cubarsi, R. & Villaverde, A. Optimized release of recombinant proteins by ultrasonication of E. coli cells. *Biotechnol Bioeng* **58**, 536-540 (1998).

152 Niemz, A., Ferguson, T. M. & Boyle, D. S. Point-of-care nucleic acid testing for infectious diseases. *Trends Biotechnol* **29**, 240-250, doi:10.1016/j.tibtech.2011.01.007 (2011).

153 Ross, P. L., Lee, K. & Belgrader, P. Discrimination of single-nucleotide polymorphisms in human DNA using peptide nucleic acid probes detected by MALDI-TOF mass spectrometry. *Anal Chem* **69**, 4197-4202 (1997).

154 Chang, Y. M., Donovan, M. J. & Tan, W. Using aptamers for cancer biomarker discovery. *J Nucleic Acids* **2013**, 817350, doi:10.1155/2013/817350 (2013).

155 LaBarre, P. *et al.* A simple, inexpensive device for nucleic acid amplification without electricity-toward instrument-free molecular diagnostics in low-resource settings. *PLoS One* **6**, e19738, doi:10.1371/journal.pone.0019738 (2011).

156 Wang, K. *et al.* Molecular engineering of DNA: molecular beacons. *Angew Chem Int Ed Engl* **48**, 856-870, doi:10.1002/anie.200800370 (2009).

157 Li, H., Zhang, Y., Wang, L., Tian, J. & Sun, X. Nucleic acid detection using carbon nanoparticles as a fluorescent sensing platform. *Chem Commun (Camb)* **47**, 961-963, doi:10.1039/c0cc04326e (2011).

158 Gootenberg, J. S. *et al.* Nucleic acid detection with CRISPR-Cas13a/C2c2. *Science* **356**, 438-442, doi:10.1126/science.aam9321 (2017).

159 Tan, L. *et al.* Molecular beacons for bioanalytical applications. *Analyst* **130**, 1002-1005, doi:10.1039/b500308n (2005).

160 Sando, S. & Kool, E. T. Imaging of RNA in bacteria with self-ligating quenched probes. *J Am Chem Soc* **124**, 9686-9687 (2002).

161 Cissell, K. A., Campbell, S. & Deo, S. K. Rapid, single-step nucleic acid detection. *Anal Bioanal Chem* **391**, 2577-2581, doi:10.1007/s00216-008-2215-5 (2008).

162 Kumar, M., Zhang, D., Broyles, D. & Deo, S. K. A rapid, sensitive, and selective bioluminescence resonance energy transfer (BRET)-based nucleic acid sensing system. *Biosens Bioelectron* **30**, 133-139, doi:10.1016/j.bios.2011.08.043 (2011).

163 Bratu, D. P., Cha, B. J., Mhlanga, M. M., Kramer, F. R. & Tyagi, S. Visualizing the distribution and transport of mRNAs in living cells. *Proc Natl Acad Sci U S A* **100**, 13308-13313, doi:10.1073/pnas.2233244100 (2003).

164 Chen, M. *et al.* A molecular beacon-based approach for live-cell imaging of RNA transcripts with minimal target engineering at the single-molecule level. *Sci Rep* **7**, 1550, doi:10.1038/s41598-017-01740-1 (2017).

165 Li, J. J., Fang, X., Schuster, S. M. & Tan, W. Molecular Beacons: A novel approach to detect protein – DNA interactions. *Angewandte Chemie International Edition* **39**, 1049-1052, doi:10.1002/(SICI)1521-3773(20000317)39:6<1049::AID-ANIE1049>3.0.CO;2-2 (2000).

166 Li, J. J., Geyer, R. & Tan, W. Using molecular beacons as a sensitive fluorescence assay for enzymatic cleavage of single-stranded DNA. *Nucleic Acids Res* **28**, E52 (2000).

167 Summerer, D. & Marx, A. A molecular beacon for quantitative monitoring of the dna polymerase reaction in real-time. *Angewandte Chemie International Edition* **41**, 3620-3622, doi:10.1002/1521-3773(20021004)41:19<3620::AID-ANIE3620>3.0.CO;2-C (2002).

168 Tyagi, S., Bratu, D. P. & Kramer, F. R. Multicolor molecular beacons for allele discrimination. *Nat Biotech* **16**, 49-53 (1998).

169 Matthews, J. C., Hori, K. & Cormier, M. J. Substrate and substrate analogue binding properties of Renilla luciferase. *Biochemistry* **16**, 5217-5220 (1977).

170 Poutiainen, P. K. *et al.* Firefly luciferase inhibitor-conjugated peptide quenches bioluminescence: a versatile tool for real time monitoring cellular uptake of biomolecules. *Bioconjug Chem* **25**, 4-10, doi:10.1021/bc4003713 (2014).

171 Shimada, J., Maruyama, T., Kitaoka, M., Kamiya, N. & Goto, M. DNA-enzyme conjugate with a weak inhibitor that can specifically detect thrombin in a homogeneous medium. *Anal Biochem* **414**, 103-108, doi:10.1016/j.ab.2011.02.035 (2011).

172 Morin, T. J. & Kobertz, W. R. Tethering chemistry and K+ channels. *J Biol Chem* **283**, 25105-25109, doi:10.1074/jbc.R800033200 (2008).

173 Ilgu, M. & Nilsen-Hamilton, M. Aptamers in analytics. *Analyst* **141**, 1551-1568, doi:10.1039/c5an01824b (2016).

174 Wilson, D. S. & Szostak, J. W. In vitro selection of functional nucleic acids. *Annu Rev Biochem* **68**, 611-647, doi:10.1146/annurev.biochem.68.1.611 (1999).

175 Guo, Y., Wang, H., Sun, Y. & Qu, B. A disulfide bound-molecular beacon as a fluorescent probe for the detection of reduced glutathione and its application in cells. *Chem Commun (Camb)* **48**, 3221-3223, doi:10.1039/c2cc17552e (2012).

176 Qiu, L. *et al.* A targeted, self-delivered, and photocontrolled molecular beacon for mRNA detection in living cells. *J Am Chem Soc* **135**, 12952-12955, doi:10.1021/ja406252w (2013).

177 Shi, H. *et al.* Activatable aptamer probe for contrast-enhanced in vivo cancer imaging based on cell membrane protein-triggered conformation alteration. *Proc Natl Acad Sci U S A* **108**, 3900-3905, doi:10.1073/pnas.1016197108 (2011).

178 Liu, Y., Tuleouva, N., Ramanculov, E. & Revzin, A. Aptamer-based electrochemical biosensor for interferon gamma detection. *Anal Chem* **82**, 8131-8136, doi:10.1021/ac101409t (2010).

179 Manova, R. K., Pujari, S. P., Weijers, C. A., Zuilhof, H. & van Beek, T. A. Copper-free click biofunctionalization of silicon nitride surfaces via strain-promoted alkyne-azide cycloaddition reactions. *Langmuir* **28**, 8651-8663, doi:10.1021/la300921e (2012).

180 Wang, Q. *et al.* Bioconjugation by copper(I)-catalyzed azide-alkyne [3 + 2] cycloaddition. *J Am Chem Soc* **125**, 3192-3193, doi:10.1021/ja021381e (2003).

181 Sanceau, J., Merlin, G. & Wietzerbin, J. Tumor necrosis factor-alpha and IL-6 up-regulate IFN-gamma receptor gene expression in human monocytic THP-1 cells by transcriptional and post-transcriptional mechanisms. *J Immunol* **149**, 1671-1675 (1992).

182 Lu, C. *et al.* Detection of AMA-M2 in human saliva: Potentials in diagnosis and monitoring of primary biliary cholangitis. *Sci Rep-Uk* **7** (2017).

183 Rathnayake, N., Gieselmann, D. R., Heikkinen, A. M., Tervahartiala, T. & Sorsa, T. Salivary Diagnostics-Point-of-Care diagnostics of MMP-8 in dentistry and medicine. *Diagnostics (Basel)* **7**, doi:10.3390/diagnostics7010007 (2017).

184 Resende, R. G. *et al.* Saliva and blood interferon gamma levels and IFNG genotypes in acute graft-versus-host disease. *Oral Dis* **18**, 816-822, doi:10.1111/j.1601-0825.2012.01955.x (2012).

185 Cox, M. A. *et al.* Short-chain fatty acids act as antiinflammatory mediators by regulating prostaglandin E(2) and cytokines. *World J Gastroenterol* **15**, 5549-5557 (2009).

186 Lillehoj, P. B., Huang, M. & Ho, C. in *2013 IEEE 26th International Conference on Micro Electro Mechanical Systems (MEMS).* 53-56.

187 Tomassetti, M. *et al.* A new surface plasmon resonance immunosensor for triazine pesticide determination in bovine milk: a comparison with conventional amperometric and screen-printed immunodevices. *Sensors (Basel)* **15**, 10255-10270, doi:10.3390/s150510255 (2015).

188 Mazloum-Ardakani, M., Hosseinzadeh, L. & Taleat, Z. Two kinds of electrochemical immunoassays for the tumor necrosis factor alpha in human serum using screen-printed graphite electrodes modified with poly(anthranilic acid). *Microchim Acta* **181**, 917-924, doi:10.1007/s00604-014-1186-9 (2014).

189 Lindholm-Sethson, B. *et al.* Electrochemical impedance spectroscopy in label-free biosensor applications: multivariate data analysis for an objective interpretation. *Analytical and Bioanalytical Chemistry* **398**, 2341-2349, doi:10.1007/s00216-010-4027-7 (2010).